NTNU
Norwegian University of
Science and Technology

Accident Frequency Analysis for the Stad Ship Tunnel

Erik Alan Ariansen

Marine Technology
Submission date: January 2018
Supervisor: Stein Haugen, IMT

Norwegian University of Science and Technology
Department of Marine Technology

Preface

This master thesis was written during the autumn semester of 2017 at the Department of Marine Technology at the Norwegian University of Science and Technology (NTNU).

Working on this thesis has been a very rewarding experience, and I have gained insight to the exciting art of extracting valuable information from a sea of data.

I would like to thank my supervisor Stein Haugen for being reachable and helpful, and for insightful advice and input. I would also like to thank my family for being a great support to me throughout the writing of this thesis.

Trondheim 14.01.2018

Erik Ariansen

Abstract

The objective of this thesis is to find a suitable method to update previous risk analyses on the projected fairways of the Stad Ship tunnel, which is planned to reduce coastal traffic exposure to severe weather in the Stad sea.

A previous analysis from 2010 carried out by the DNV utilises accident statistics and vessel exposure data to obtain a frequency of accidents for a tunnel case compared to a no tunnel case. Traffic densities are obtained from observing traffic data.

It is decided that a new frequency analysis based on a geometrical model and updated traffic data might improve on the assessment in terms of accuracy. Traffic data is obtained from the Norwegian Coastal Administration, and a program is developed to estimate traffic patterns and vessel parameters to calculate collision and grounding frequencies according to the IWRAP method. This is carried out for the current sea route and the planned tunnel route.

It is found that the collision and grounding frequencies for the tunnel route are slightly higher than found in the previous assessment, while frequencies for the sea route were significantly lower.

Sensitivity analyses show that the model is particularly sensitive to lane positioning, but also that there is a large potential for expanding the model with more accurate representations of traffic patterns off Stad, which are found to be complex.

It is concluded that the model is well suited to the enclosed waters of the Stad tunnel fairways, and that the model is useful in defining critical areas in the fairways, which is an advantage over the method utilised previously. It also allows flexibility and the opportunity to investigate scenarios for different vessels and fairway parameters Further work is suggested to improve the accuracy of the model for open seas.

To reach a sufficient level of accuracy for modelling the frequency of collisions and groundings off Stad it is suggested that further research is carried out on meteorological effects on traffic patterns and on a vessel's ability to navigate, which are important factors in quantifying the frequency of accidents for this area.

Sammendrag

Formålet med denne oppgaven er å finne en egnet metode for å oppdatere tidligere risikoanalyser Stad skipstunnel, som planlegges for å redusere kysttrafikkens eksponering for harde værforhold i Stadhavet.

En tidligere analyse utført av DNV i 2010 benytter ulykkesstatistikk og utseilt distanse i området for å oppnå frekvensen av ulykker for tunnelruten i forhold til sjøruten. Trafikktettheten i området er funnet ved å analysere trafikkdata.

Det er bestemt at en ny frekvensanalyse basert på en geometrisk risikomodell og oppdaterte trafikkdata kan forbedre denne analysen. Trafikkdata er hentet fra Kystverket, og et program er utviklet for å beregne trafikkmønstre og fartøysparametre for å beregne kollisjon og grunnstøtingsfrekvenser i henhold til IWRAP-metoden. Dette utføres for nåværende sjørute og den planlagte tunnelruten.

Det er funnet at kollisjons- og grunnstøtingsfrekvensene for tunnelruten er noe høyere enn funnet i forrige analyse, mens frekvensene for sjøruten var betydelig lavere.

Sensitivitetsanalyser viser at modellen er spesielt følsom for farveismodelleringen, men også at det er et stort potensial for å utvide modellen med mer nøyaktige representasjoner av trafikkmønstre utenfor byen, som er funnet å være komplekse.

Det konkluderes med at modellen er godt egnet til det lukkede farvannet i tunnelruten, og at modellen er svært nyttig til å definere kritiske områder farvannet, noe som er en fordel i forhold til den tidligere brukte metoden. Den er også fleksibel og gir mulighet til å undersøke forskjellige scenarier i forhold til fartøystyper og farledsparametere. Ytterligere arbeid er foreslått for å utbedre nøyaktigheten av modellen for åpent hav.

For å oppnå en tilstrekkelig grad av nøyaktighet for frekvensen av kollisjoner og grunnstøtinger utenfor Stad, foreslås det at meteorologiske effekter på trafikkmønstre og på fartøyers evne til å navigere trygt undersøkes nærmere for dette området.

Table of Contents

List of Figures

1 Introduction

1.1 Stad Ship Tunnel

Stad is a prominent headland on the Norwegian western coast which has been an obstacle and a challenge for Norwegian coastal shipping for centuries. According to the Norwegian encyclopaedia (Askheim, 2017) the name Stad is derived from the Norse *staðr*, meaning stop. The name is believed to have arisen from sailors having to wait here for better weather, and Stad is an important feature on the first sea charts of the Norwegian coast like the 1539 *Carta Marina* (Figure 1.1.)

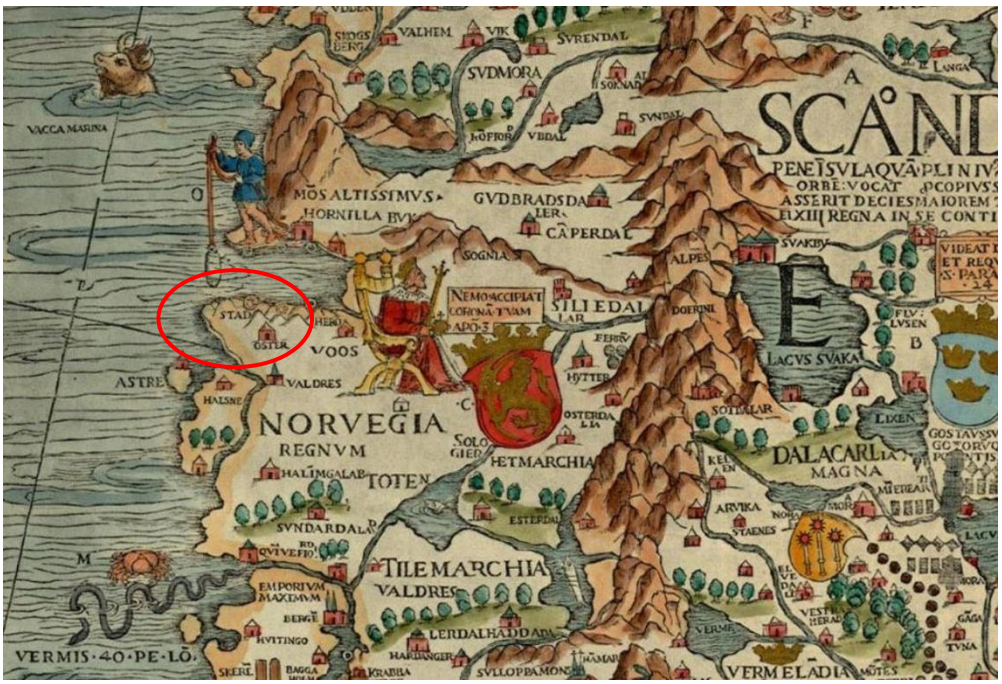

Figure 1.1 Stad marked on Olaus Magnus' Carta Marina of 1539 (University of Minnesota, 2001)

While most of the Norwegian coastline benefits from naturally sheltered fairways, the Stad headland forms a barrier which forces traffic into open seas to pass it. Additionally, the local weather is frequently severe; Kråkenes Lighthouse just south of Stad measures between 45 to 106 storm days a year. Currents, subsea topography, wind and wave conditions combine to make this section of the main coastal fairway especially demanding to navigate safely (Kystverket, 2015).

In response to this problem, a ship tunnel through the base of the headland has been proposed. The concept has been reviewed several times since the '90s and in 2014

the Norwegian Parliament approved a tunnel concept from Moldefjorden to Kjødepollen, with dimensions large enough for the coastal steamers (Hurtigruten) with a beam of 21.5m in 2014. Funding for the construction of such a channel in the was announced by the ministry of transportation in April 2017 in the national transport plan for 2018-2026 and construction is expected to commence within 2020 (Norwegian Ministry of Transportation, 2017).

1.2 Objectives

While diverting maritime traffic inshore might reduce exposure to harsh weather, it may also increase the risk of groundings or collisions. A risk assessment of the tunnel route compared to the current route was most recently carried out in 2010 by the classification society DNV, and this thesis aims to improve on the pre-existing report in establishing an updated risk picture for the tunnel and current fairways.

The objectives of the thesis are to review risk analysis tools and data sources currently available for maritime traffic risk analysis, and to apply a suitable model to the Stad ship tunnel fairways.

The ultimate objective of the thesis is to compare the results of the 2010 analysis to the results found in this analysis.

1.3 Limitations/Scope

According to (Rausand, 2011), a risk analysis is carried out to answer three questions:

1. What can go wrong?
2. What is the likelihood of that happening?
3. What are the consequences?

In response to the first question, there are only two specific hazards that will be investigated in this analysis: impact-related accidents, i.e. vessel grounding and collision. There are other hazards that a vessel might encounter in the area, such as fire outbreaks, structural or stability failure, but these events will not be considered.

The consequences of the events grounding and collision depend on many factors such as vessel speed, construction, size and cargo, as well as the nature of struck obstacles. Quantifying these factors to an accurate level is outside the scope of this thesis and the analysis will limit itself to finding the frequency of the events collision and grounding, i.e. answering question 2. Possible event consequences will however be commented and discussed throughout the analysis.

1.4 Structure

In chapter two, a previous risk assessment carried out by DNV in 2010 is analysed and possible improvements are suggested.

In chapter three, relevant methods and models for analysing the Stad tunnel fairways are discussed. Possible data sources are investigated and a methodology for the carrying out the analysis is decided.

Chapter four briefly outlines the geographical features of the planned and current Stad fairways and the hazards that are analysed in the thesis are defined.

In chapter five, traffic parameters and lane modelling is carried out, and the calculation of accident frequencies is described.

Chapter six provides the results that are obtained, along with sensitivity analyses and discussions.

Conclusions and proposed further research are found in chapters seven and eight.

2 Previous risk assessment: DNV report.

2.1 Methodology

The Norwegian Coastal Authority (NCA), Kystverket, authorised a risk assessment of a tunnel route through the Stad headland compared to the original sea route in 2010. (Det Norske Veritas, 2010). In the following section, this assessment is analysed to investigate which areas of the assessment might require updating or improvement.

The risk assessment was an updated report based on reports from 2007 and 2000, and was to include AIS (Automatic Identification System) data and an extensive range of ship types.

At the time of the DNV report's writing, two tunnel alternatives were under consideration, a 23 and a 26 m wide alternative respectively. The report makes an assessment for both alternatives, for traffic density measured in 2009 and for a traffic density prognosis for 2025. The main finding of the report is that the risk of fatalities in a 26 m wide tunnel is 5 times less than by the normal route around the Stad headland.

According to the report, historical accident data indicates that the frequency of groundings per nautical mile sailed along the Stad coast is 10 times higher than the international average, risk of collision is twice as high, and the risk of foundering is 10 times higher. Foundering is in the report defined as accidents due to weather damage or stability failure, which is interpreted as vessels broaching or being swamped by waves.

The risk calculations are based on several data sources: AIS data, historical accident data, and other traffic and vessel statistics. To estimate general accident frequencies, data from the IHS Fairplay Casualty database is utilised, in which accident frequency per year for different ship types is available. Data from IMO(International Maritime Organisation) provides an estimate for sailed distance per year for the different ship types. Together, this data provides an expected frequency of accidents per sailed distance, for each vessel type.

AIS data for traffic around Stad was collected from 2008 to 2010. Erroneous data is corrected based on DNV's vessel databases. The AIS data is used to find a value for sailed distance around Stad arranged by ship types. Accident data from the Norwegian Maritime Authority (Sjøfartsdirektoratet) provides the number of

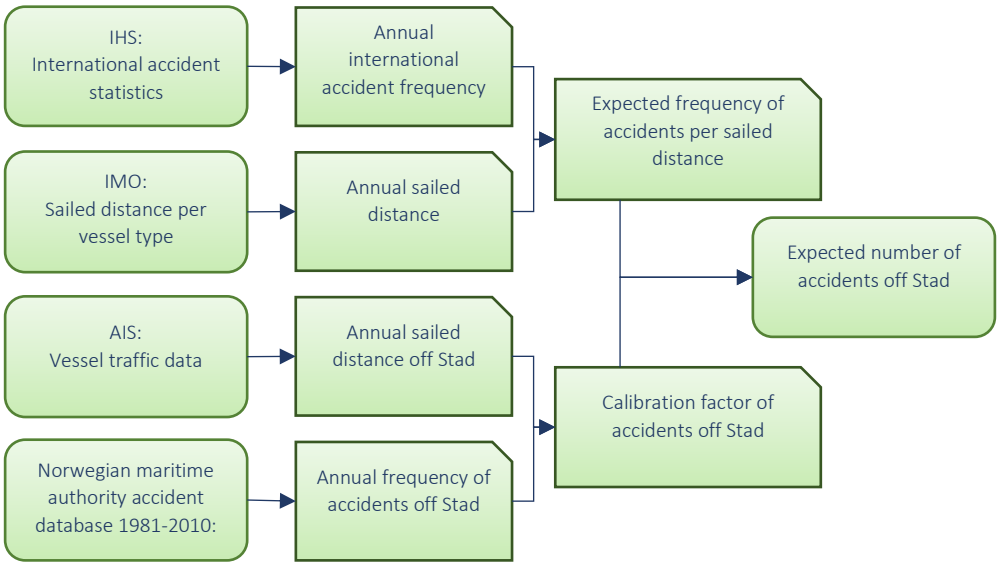

Figure 2.1 DNV methodology for calculating accident frequencies off Stad

accidents off Stad per year. Combined with the sailing distances provided by AIS data, this provides a calibration factor for accident frequencies off Stad. This is applied to the international expected frequency of accidents per sailed distance to provide an estimate of accident frequencies for different vessel types off the coast of Stad. A visualisation of this procedure is provided in Figure 2.1

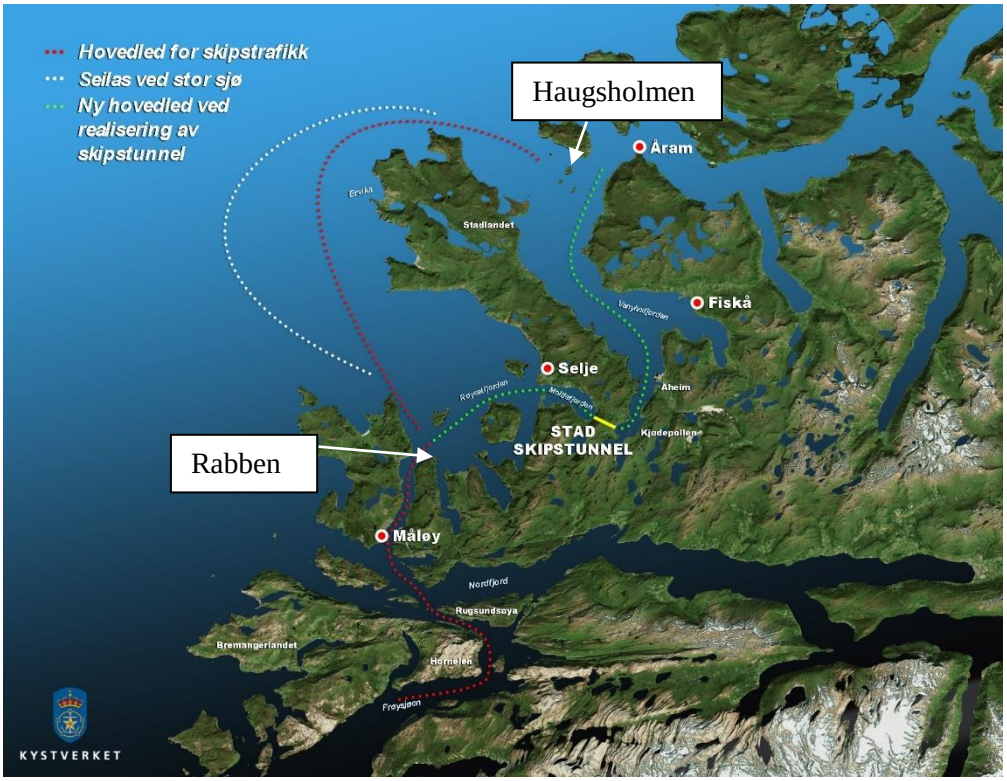

Figure 2.2 Routes analysed in the DNV report. Red: Current fairway. Green: Projected fairway. White: Sailing pattern during severe weather (Kystverket, 2017)

The analysis is restricted to the following lanes: *Rabben – Stad headland – Haugsholmen*, and *Rabben – tunnel entrance – Haugsholmen*, marked in red and green respectively in Figure 2.2.

For estimating the expected tunnel traffic, the DNV separates traffic according to whether it approaches Stad from inner or outer fairways. The process is described in the attachment to the main report: "Analyse av AIS data og beregning av ventetid" (Det Norske Veritas, 2010)**.** In addition to vessels that are too wide for the tunnel (21.5 m), it is assumed that vessels approaching from the outer fairways are not candidates for using the tunnel. Inshore and offshore traffic is distinguished according to pass lines drawn across the headland approaches, see Figure 2.3.

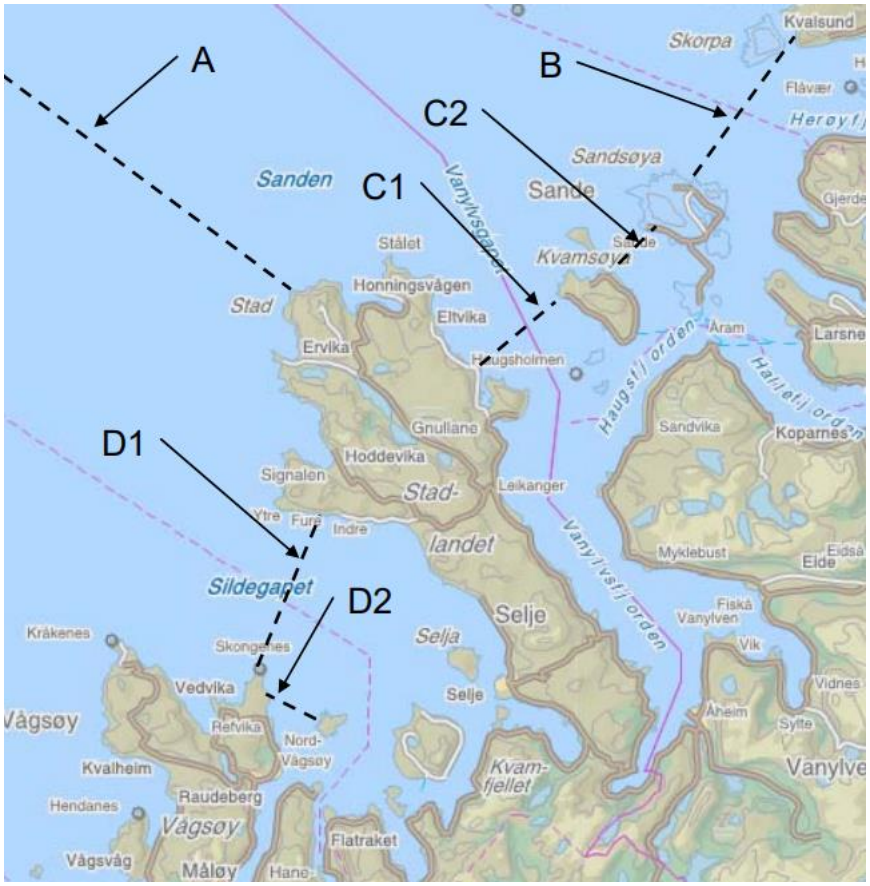

Figure 2.3 Pass lines in the DNV analysis

Vessels that pass line A as well as either of the lines D2,D1,C1,C2 or B are assumed to be tunnel candidates. For a period consisting of the years 2008 and 2009, it is found that of vessels that are narrow enough to enter the tunnel, 32206 vessels pass the Stad headland. Of these vessels, 17565 crossed at least one of the other pass lines and therefore might be expected to use the tunnel.

The 2025 traffic prognosis is carried out by the NCA and is based on national transport plans and estimated oil production plans from the Norwegian Petroleum Directorate. The estimated traffic numbers are expressed as change in yearly sailed distance per ship type, compared to the measured traffic in 2008 and 2009. According to the prognosis, the total amount of tunnel candidates in 2025 is 17523, which is slightly less than the amount found for 2008/2009.

While the risk of accidents such as foundering is expected to be high off Stad, it is also considered that there will be an increased risk of accidents in the tunnel approaches where vessels wait to enter the tunnel, due to low speeds, wind drift and

the proximity of traffic. However, the calculations of this risk increase are not included in the report. Traffic, fairway parameters and planned safety measures are considered for each part of the fairway to find a representative accident frequency per sailed distance for the accident categories fire, tunnel wall collisions, and foundering/structural failure.

2.2 Results

The results are listed in Table 2.1. It is found that the risk of foundering all but disappears with a large tunnel, and grounding risk is decreased. However, collision risk increases. The reason for the dramatic decrease in foundering accidents is that the foundering accident statistics are made up entirely of vessels of smaller beam than 21.5 m, and these vessels will no longer be forced to sail around Stad.

Table 2.1 Accident Frequencies (adapted from (Det Norske Veritas, 2010)

Accident category:	No tunnel, 2010	No tunnel, 2025	Large Tunnel, 2010	Large Tunnel, 2025
Fire	0.02	0.02	0.02	0.02
Grounding	0.20	0.22	0.17	0.19
Collision	0.05	0.05	0.06	0.07
Foundering	0.11	0.11	N/A	N/A

Additionally, a human risk analysis is carried out for three phases: Tunnel approach, tunnel passage, and for rounding the Stad headland. In short, it is found that the human risk for the narrow tunnel and no tunnel alternatives (meaning that some vessels or all vessels must sail round the headland) is high due to the high rate of fatalities in foundering accidents off the headland. This is based on historical accident data. On the other hand, the event of fire in the tunnel carries a higher human risk in the tunnel than the open sea due to the dangerous nature of tunnel fires. However, this is small compared to the human risk of foundering off the headland. The human risk for groundings in the tunnel approach is not deemed different from ordinary coastal traffic.

Furthermore, the report investigates environmental concerns and the impact of increased traffic on nature reserves and environmentally vulnerable areas close to Stad.

2.3 Discussion

It is surprising to see a calculated increase in accident frequencies for 2025, as an increase in traffic is not predicted. The reason for this might be that although traffic does not increase, the composition of traffic might be predicted to shift to vessel types that are more prone to accidents. Unfortunately, the details of the frequency analysis are not included in the report to explain the calculations.

It is noted that vessels approaching Stad from pass line B as defined above Figure 2.3 are counted as tunnel candidates. However, the route from pass line B to either Stad or the tunnel are not part of routes 1 and 2 as defined in the geographical limitations. It is therefore unclear whether the parameters of these waterways are included in the frequency analysis.

For additional details in the traffic analysis, readers are referred to the report "Analyse av fartøystrafikk, Rapportnr 2010-1639". However, the author of this project has not been able to track down the report in question, and it does not appear to exist in the NCA's archives (Andreassen, 2017).

3 Relevant Literature andTheory

3.1 Geometrical accident models

3.1.1 Accident candidates and Causation Probability

The DNV risk assessment described in the previous section is based on local historical accident data and fleet exposure. Such a statistical approach may be an inaccurate approximation regarding variations in technical standards, traffic density and local fairway parameters (Kristiansen, 2005). In the following section, alternative methods for estimating impact-type accidents (Groundings and collisions) which rely on the geometrical properties of vessels and fairways are described.

In the early '70s, the scientists Fujii and MacDuff proposed a method for estimating the amount of maritime traffic accidents (Mazaheri, 2009). They defined the idea of *accident candidates*. Accident candidates are vessels that would strike another vessel, an obstacle or the shore given that *no evasive manoeuvres* are taken.

If the amount of accidents can be described by the expression:

$$N_{Accidents} = N_{Candidates} * Causation\ Probability$$

Then the causation probability is the fraction of accident candidates that result in accident, or in other words the probability of failure to successfully carry out evasive action. The number of accident candidates can be found by geometrically calculating how many vessels would strike an obstacle, channel edges or other vessels.

According to Mazaheri's review of grounding models (Mazaheri, 2009), most recent risk models on ship grounding build on the work of MacDuff and Fujii, and relevant models to the risk assessment will be examined in the following sections.

3.1.2 Estimating the Causation Probability

There are several methods available for finding Causation probabilities for accidents. A method often employed is statistical studies. If the amount of accident candidates can be calculated for a specific area for a certain time period, finding the amount of actual accidents will allow the causation probability to be estimated.

Another approach is to use analytical methods. This approach is based on creating a mathematical model for calculating the probability of events that will lead to failure in the ability to avoid accidents. Using an analytical method is particularly useful for quantifying the effect of risk reduction measures (Pedersen, 2010).

However, in an analytical approach to finding a causation probability it is very difficult to properly account for all relevant aspects that might lead to the event of evasion failure, and extensive data for technical failure and human error is required. Examples of analytical approaches are fault and event tree analysis. Fault trees and event trees may tend to become too large for calculating the probability of evasion failure, and dependencies between events are hard to model (IWRAP, 2014). Therefore, a useful approach is a Bayesian Network (Pedersen, 2010).

Bayesian networks are graphical models that illustrate causal relationships between factors and events. Directional arcs link nodes which represent random variables and decisions. Arcs illustrate the dependencies between the nodes, such as for weather conditions to visibility. By introducing probabilities to the model, the probability of different outcomes can be calculated. This allows for compact diagrams that represent complete probabilistic descriptions of problems (Rausand, 2011).

To reach a satisfactory level of detail, environmental, technical and human errors should be accounted for. Local navigational circumstances and aids should also be included in a model. (IWRAP, 2014)

3.1.3 Kristiansen's Traffic based models, 2005

An example of a geometric collision and grounding model can be found in Traffic Based Models (Kristiansen, 2005). The model is defined for specific fairways, and the Basis of the theory is the equation:

$$C = \lambda * N$$

Where:

- C = Expected number of accidents in seaway per time-unit
- λ = Number of accidents per vessel-passage of seaway
- N = number of passages per time unit.

To increase computational efficiency this equation can be applied to sections of fairway, the total number of accidents being the sum of accidents per section. This allows connecting sections of for example crossing traffic, sections containing obstacles, and sections of one-way or head on-traffic to illustrate a single fairway which contains all these elements in the course of its length. The complexity of the sectional model must be a compromise between computational efficiency and accuracy. Sections carry various situational risks depending on their character, and Kristiansen develops several risk models for selected accident situations.

The general risk model for impact accidents is given as

$$P_a = P_c * P_i$$

Where:

- P_a = Probability of an impact accident per passage
- P_c= Probability of losing vessel control per passage
- P_i = Conditional probability of an accident given loss of vessel control

Grounding is here defined as hitting an obstacle in the fairway, and the following equation describes the probability of an accident given loss of vessel control:

$$P_i = \frac{B + d}{W}$$

W being the average width of the fairway, d being the cross-section width of the obstacle and B being the beam of the vessel. The model may be suitably modified for overlapping obstacles and the obstacles, if numerous, may also be modelled as a function of obstacle density ρ.

Further, Kristiansen describes the probability of stranding, which is here defined as impacting on the shoreline rather than obstacles in the fairway. It is assumed that a vessel losing control will continue straight ahead. The probability of stranding will then become a function of the heading at time of control loss α, see Figure 3.1:

$$P_i = \frac{\alpha}{\frac{\pi}{2}} = \frac{tan^{-1}\left(\frac{\frac{D}{2}}{\frac{W}{2}}\right)}{\frac{\pi}{2}}$$

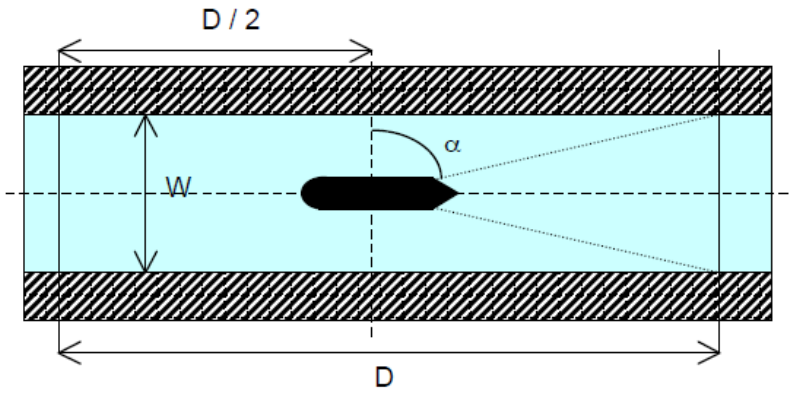

Figure 3.1 Stranding model (Kristiansen, 2005)

Replacing the arctan term with a Taylor series expansion, the simplified expression for the stranding probability is

$$P_i \approx 1 - \frac{2}{\pi} * \frac{W}{D}$$

For finding the number of head-on collisions, several vessel and fairway parameters need to be defined (Figure 3.2):

- B_1 = Mean beam of meeting ships [m]
- v_1 = Mean speed of meeting ships [knots]
- B_2 = Beam of subject ship
- v_2 = Speed of subject ship
- N_{m1} = Arrival frequency of vessels [vessels/time unit]
- D' = Relative sailing distance [nm]
- D = sailing distance [nm]

The traffic density ρ_s is found by the following equation

$$\rho_s = \frac{N_{m1} * T}{(v1 * T) * W} = \frac{N_{m1}}{v1 * W}$$

Where:

- T = an arbitrary amount of time (hrs)
- W = fairway width

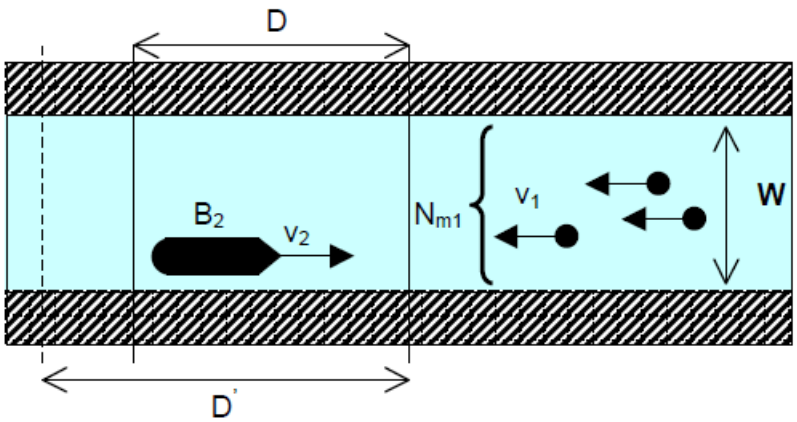

Figure 3.2 Head-on collision model (Kristiansen, 2005)

An area A where the subject ship is exposed to danger can be described as

$$A = (B_1 + B_2) * (v_1 + v_2) * \frac{D}{v_2} = B * D'$$

Thus, the expected number of collisions per passage of fairway, given loss of control, is given by the product of area A and traffic density ρ_s. This can be simplified to the expression:

$$N_i = \frac{B_1 + B_2}{W} * \frac{v_1 + v_2}{v_1 * v_2} * D * N_{m1}$$

For overtaking collisions, the principle is the same, but relative speed is expressed as the difference in speeds rather than the sum.

It is probable that there will be more than two different speeds for vessels in a uni-directional traffic flow. In these cases, a speed distribution can be included in the expression:

$$N_i = \frac{B_1 + B_2}{W} * D * N_{m1} * \sum f_x * f_y (\frac{1}{v_x - v_y})$$

Where f_x and f_y are the fractions of the traffic flow with speed v_x and v_y respectively. Every overtaking speed combination is taken under the summation.

Crossing collisions are complicated as traffic in either flow may have the role of striking or struck ship. Kristiansen's solution is to calculate the number of stricken ships in either direction, and superposing the results (Figure 3.3).

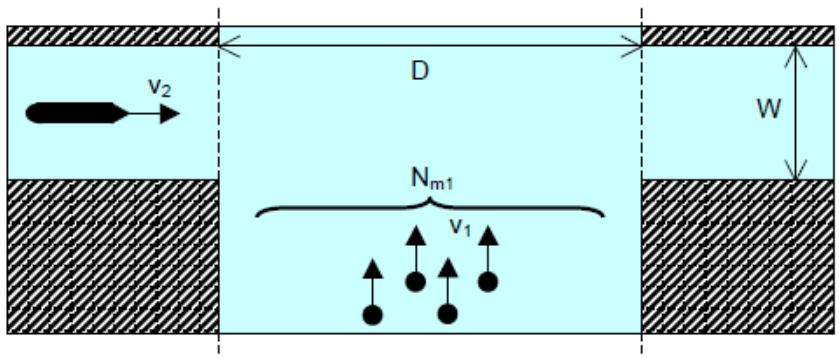

Figure 3.3 Crossing collision model (Kristiansen, 2005)

Assuming the density of crossing traffic ρ_s is expressed as before, and the relative speed is described by vector summation of both vessels velocities, the subject ship is exposed to crossing traffic in the time $T_2 = D/v_2$. The sailing distance of the crossing ship while the subject ship is exposed is $D_1 = v_1 * \frac{D}{v_2}$. The area A_1 in which a collision might happen is a product of the combined length and beam of the

exposed and crossing ship, Q_1 and the distance D_1. The expected number of collisions is the given by the product of the area A_1 and the crossing traffic density. Similar calculations are carried out for traffic on the adjacent heading, and when superposed, the number of collisions in a crossing point of two waterways can be expressed by the equation:

$$P_i = P_{i1} + P_{i2} = (B_1 + L_2) * \frac{N_{m1}}{v_2} + (L_1 + B_2) * \frac{N_{m1}}{v_1}$$

$$= \frac{N_{m1}}{v_1 * v_2}[(B_1 + L_2 * v_1 + (L_1 + B_2) * v_2]$$

To find the causation probability P_c of loss of control, Kristiansen uses historical traffic studies by Fujii, amongst others, to empirically estimate conditional probabilities, as described in section 3.1.2. Waterways and port areas in Japan, the USA and the English Channel are among the examined areas. A mean of the calculations provides the following causation probabilities:

Table 3.1 Causation Probabilities

Encounter situation	[Failures/nm]
Overtaking vessels	$1.5E10^{-5}$
Crossing traffic	$1.5E10^{-5}$
Head-on traffic	$3.0E10^{-5}$
Stranding/Grounding	$2.0E10^{-5}$ - $2.8E10^{-5}$

3.1.4 Pedersen's accident model, 1995

According to Mazaheri, (Mazaheri, 2009) Pedersen's grounding model is the most used in recent years, with many recent risk analyses and calculations being based on his work.

Grounding accidents can be divided into four categories:

- Category I: Grounding on an obstacle while following an ordinary route at normal speed
- Category II: Grounding while failing to change course at a given waypoint
- Category III: Grounding while taking evasive manoeuvres
- Category IV: All other track patterns, e.g. off-course or drifting ships.

The first two accident categories are illustrated in Figure 3.4. The number of accidents in each case can be calculated by the equations below.

$$F_{Cat.1} = \sum_{ship\ class}^{n\ class} \sum_{i=1} P_{Ci} Q_i \int_L f_i B_i ds$$

$$F_{Cat.2} = \sum_{ship\ class}^{n\ class} \sum_{i=1} P_{Ci} Q_i P_0^{(d-a_i)/a_i} \int_L f_i B_i ds$$

Where B_i is the collision indication function: 1 for striking the obstacle and 0 otherwise. P_0 is the probability of omission to check vessel position, d is the distance from turning point to obstacle, relative to the vessels lateral position on the route. a_i is the average length between navigator's position check. f is the function describing the lateral distribution of traffic across the fairway.

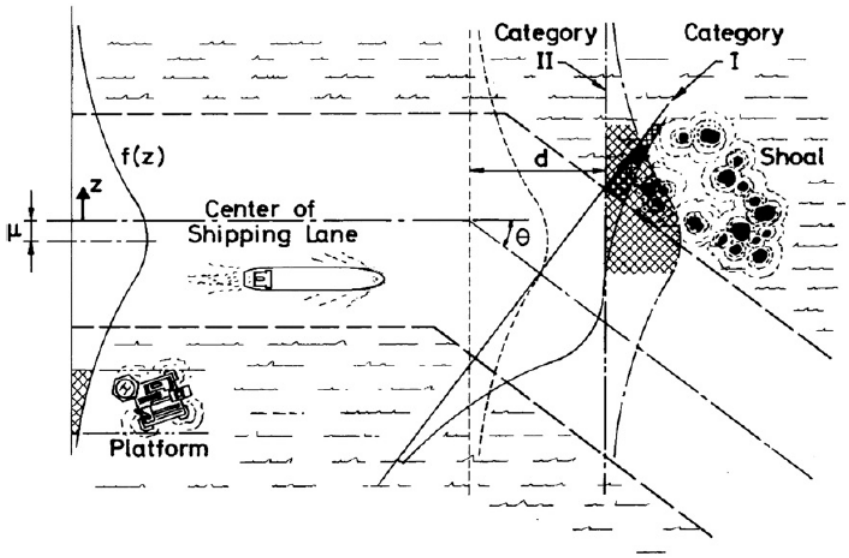

Figure 3.4 Grounding categories at route bend (Pedersen, 2010)

Similarly, geometrical calculations are used to find the number of ship-ship collisions $N_{ship-ship}$. The equation used is:

$$N_{ship-ship} = P_c N_a$$

Finding accident candidates N_a can be done geometrically. Pedersen develops the following model for calculating the number N_a for crossing fairways overlapping the area Ω, see Figure 3.5.

$$N_a = \sum_i \sum_j \int \int_{\Omega(z_i z_j)} \frac{Q_i^{(1)} Q_j^{(2)}}{V_i^{(1)} V_j^{(2)}} f_i^{(1)}(z_i) f_j^{(2)}(z_j) V_{ij} D_{ij} dA \Delta t$$

Q_j^1 denotes the traffic flow of a ship class i in waterway 1, and Q_j^2 is the traffic flow of ships class j in waterway 2. $V_{i,j}^{1,2}$ is the relative speed of respective ship classes in respective waterways. $f_{i,j}^{(1,2)}$ represents the lateral traffic density. D_{ij} is the geometrical collision diameter, defined according to Figure 3.6. V_{ij} is relative speed.

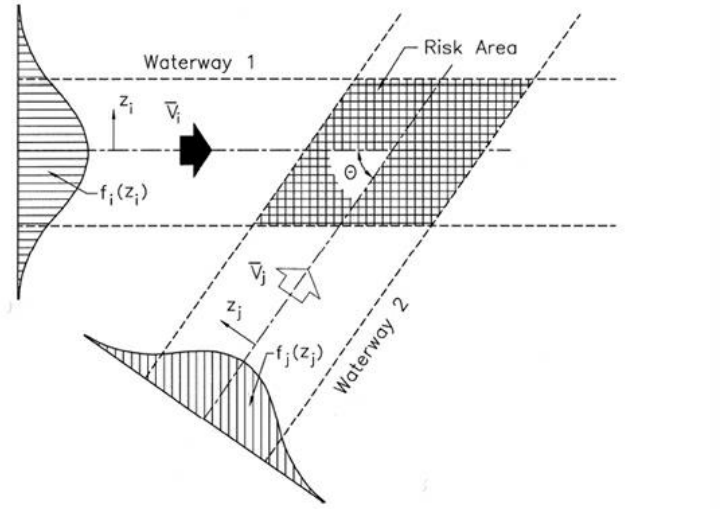

Figure 3.5 Crossing waterways (Pedersen, 2010)

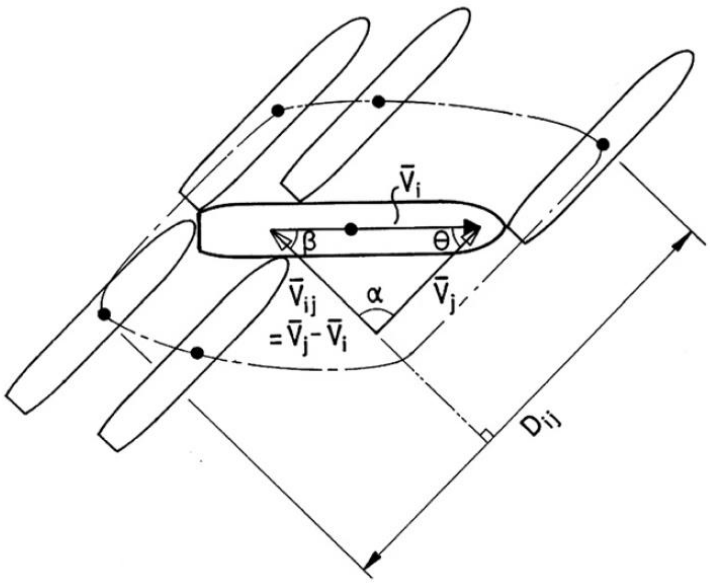

Figure 3.6 Collision Diameter (Pedersen, 2010)

3.1.5 IWRAP

IWRAP is a maritime traffic risk analysis tool developed by the IALA association (IWRAP, 2014). IWRAP implements Pedersen's method of calculating accident candidates for specific waterways.

For the number of head-on collision candidates, the model is expressed in the following equation:

$$N_g^{head-on} = L_w \sum_{i,j} P_{G\,i,j}^{head-on} \frac{V_{ij}}{V_i^{(1)} V_j^{(2)}} \left(Q_i^{(1)} Q_j^{(2)} \right)$$

Where L_w is the length of the particular waterway and $P_{G\,i,j}^{head-on}$ is the geometrical probability of head-on collision, expressed in terms of ship widths and lateral traffic distribution (Friis-Hansen, 2008).

$P_{G\,i,j}^{head-on}$ can be calculated from the following expression, when the traffic distributions in both directions are described by a normal distribution with distribution parameters μ_i, σ_i and μ_j, σ_j respectively.

$$P_{G\,i,j}^{head-on} = \Phi\left(\frac{B_{ij} - \mu_{ij}}{\sigma_{ij}}\right) - \Phi\left(-\frac{B_{ij} + \mu_{ij}}{\sigma_{ij}}\right)$$

$$\sigma_{ij} = \sqrt{(\sigma_i^2 + \sigma_j^2)}$$

B_{ij} is the average width of vessels, and μ_{ij} the distance between the mean positions of traffic in oncoming directions. Overtaking collisions are calculated in the same manner, while considering the sign of vessel speeds in uni-directional traffic.

Grounding accident candidates are divided up into categories according to Pedersen's models Figure 3.5. For the first two categories the expressions for accident candidates are:

$$N_I = \sum_{ship\ class}^{n\ class} \sum_{i=1} P_{Ci} Q_i \int_{z_{min}}^{z_{max}} f_i(z) dz$$

$$N_{II} = \sum_{ship\ class}^{n\ class} \sum_{i=1} P_{Ci} Q_i * e^{-\frac{d}{a_i}} \int_{z_{min}}^{z_{max}} f_i(z) dz$$

They differ slightly from Pedersen's models in not utilising the collision indication function B_i, the definition of which is somewhat unclear (Mazaheri, 2009). Instead, the limits z_{max} and z_{min} define the geometrical span of the obstacle. This modification to Pedersen's model was implemented by Simonsen (Simonsen, 1997).

Another modification introduced by Simonsen is on the probability of a navigator to fail to check his position. In the IWRAP formulation, the expression e^{-d/a_i} represents the probability of the navigator not checking the position of the vessel from turning point to obstacle. It is assumed that the average time between position checks is a Poisson process with expected value λ, so that distance sailed between navigational a_i checks becomes a function of vessel speed and λ. IWRAP utilises λ of 180 seconds, based on observations by Fujii and Mizuki. Simonsen notes that the resulting model is very sensitive to both conditional probability P_c and the time between position checks a_i.

IWRAP also takes into account that an obstacle at the end of the bend may not be aligned orthogonally to the route, but slanted at a line which can be expressed as $d = az + b$.

Thus, for normal traffic distributions, the expression for N_{II} is:

$$N_{II} = \sum_{ship\ class}^{n\ class} \sum_{i=1} P_{Ci} Q_i * [\frac{1}{2} \exp(\frac{a^2\sigma^2 - 2b\lambda V}{2\lambda^2 V^2}) \left\{ 2\Phi \left(\frac{z\lambda V + a\sigma^2}{\sigma\lambda V} \right) - 1 \right\}]_{z_{min}}^{z_{max}}$$

Drift grounding is also considered. The primary causes for a vessel to drift while not under command are identified as stuck rudders or main engine blackouts. Stuck rudders ae not dealt with due to lack of data, but engine blackouts are assumed to follow a Poisson process. Wind data is necessary to evaluate the probability of grounding.

Where possible, AIS data is used to decide the lateral traffic distribution. Otherwise, a normal distribution with standard deviation $\sigma = 3.65 * B$ where B is the average width of ships is suggested. Alternatively, the standard deviation can be expressed in terms of channel width rather than vessel width, a suggested value being at 40% of the channel width. There are no suggested positions of means μ in either direction relative to the channel centre.

Default causation probabilities in IWRAP are based on work by Fujii and Mizuki, and are listed in Table 3.2.

Table 3.2 IWRAP default causation probabilities

Situation	Causation factor
Head-on	$0.5E10^{-4}$
Overtaking	$1.1E10^{-4}$
Crossing collision	$1.3E10^{-4}$
Grounding – forget to turn	$1.6E10^{-4}$

3.2 Data Sources for Geometrical accident models

3.2.1 AIS data

AIS (Automatic Identification System) data forms the basis of many marine traffic risk analyses. In DNV risk assessment for the Stad Tunnel AIS is utilised to estimate traffic density and traffic patterns, and the IWRAP method suggests use of AIS to estimate lateral traffic distributions across channels and fairways.

AIS data is a navigational aid which displays a vessel's position and other information to other vessels or receiving stations. Data is broadcast over VHF frequency by all vessels larger than 300 GT, and passenger vessels. It includes dynamic vessel data such as position, speed and course over ground as well as voyage specific data such as cargo and crew aboard, and static vessel data such as

the vessel's identity number (MMSI number), size and type. Coastal authorities like the NCA can receive and store the broadcasted data using vessel tracking stations, of which there are several along the Norwegian coast. This is useful for studying historical data.

AIS messages are broadcast as strings of ASCII characters, which includes a data payload encoded according to NVMEA or AIVDM/AIVDO protocols. To decode the encoded data, the characters must be converted to six-bit. According to the correct protocol, specific parts of the resulting bit strings provide each piece of information.

There are 27 different message types defined by the International Telecommunication Union, and two types of broadcasting equipment: A, used mainly by commercial vessels and B, used mostly by fishing vessels and pleasure craft (Silveira, et al., 2013). The message types of most interest to a risk analyst might be type 1,2,3,5, 18,19 and 24. 1,2,3 are A-class position reports, and type 5 are A-class static and voyage related information messages. Type 18 and 19 are B-class position reports and 24 is B-class static data.

In order to use raw AIS signals as data, it is therefore necessary to develop a program which will decode the messages and sort them according to message type. According to Ladan & Hänninen, raw AIS data has been found to have a questionable accuracy as errors and missing data may occur (Ladan & Hänninen, 2012). Therefore, it is also important to be able to check for inconsistencies or ambiguity.

3.2.2 AIS Traffic modelling in practice

Practical aspects of a traffic analysis based on AIS data can be found in the article "Comparison study on AIS data of ship traffic behavior" (Xiao, et al., 2015).

In this analysis, AIS data is used to examine and compare the traffic behaviour in two different waterways. The purpose of the analysis is to lay the foundation for international traffic behaviour simulations. Information about ship behaviour is derived from mean values and statistical distributions of lateral position, speed, heading for various ship types and sizes.

The waterways chosen are a channel in the Port of Rotterdam in the Netherlands, and a section of the Yangtze river in China. The navigable channel in the Rotterdam case is 290 m and 2.8 km long, and has traffic in both directions. Traffic behaviour is examined at 9 cross-sections evenly spaced out along the channel. It is found that the characteristics of ship behaviour, such as lateral positions and speed distributions were similar over the length of the channel. It is found that a normal distribution can

be fitted to the lateral distribution of traffic, as seen in Figure 3.7. It is concluded that the characteristics of this distribution can be applied to a future traffic simulation model.

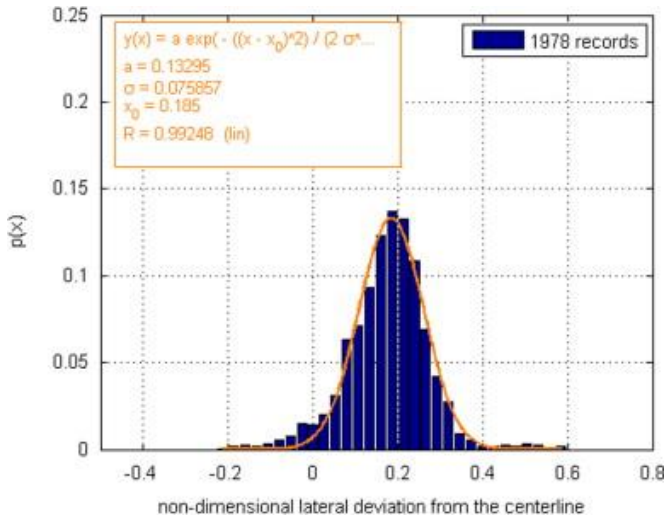

Figure 3.7 Lateral traffic distribution across Rotterdam channel (Xiao, et al., 2015)

Speed and course distributions are also extracted from the AIS data, and it is found that normal distributions fit this data as well. Ship speeds vary from 5 to 15 knots with a mean of 10.7 knots. It is commented that ship speeds varies with many factors such as the characteristics of the officer on watch and the vessel, and weather, traffic and navigational situations. Therefore, the variation in speed should be expected to be high. Course deviations are small, which is not surprising as the case in question is a straight, narrow channel.

Average speeds for each ship type are calculated for each crossing line, and it is found that the average speed varies for different sections of the channel, and in general is lower for larger vessels.

The distribution of time intervals between passages is useful for calculating the traffic density. Two years of AIS data, (January 2009 to January 2011) is examined. It is found that there is an increasing trend in traffic density for the examined time period. This is attributed to the increasingly widespread installation of AIS equipment rather than increase in traffic.

For the Yangtze river case, similar calculations are carried out. The Chinese waterway is 890 m wide, and the navigable channel consists of four traffic lanes divided by a separation zone. It is therefore a distinctly different case from the single-lane Rotterdam channel. It is found that for both cases, lateral positions,

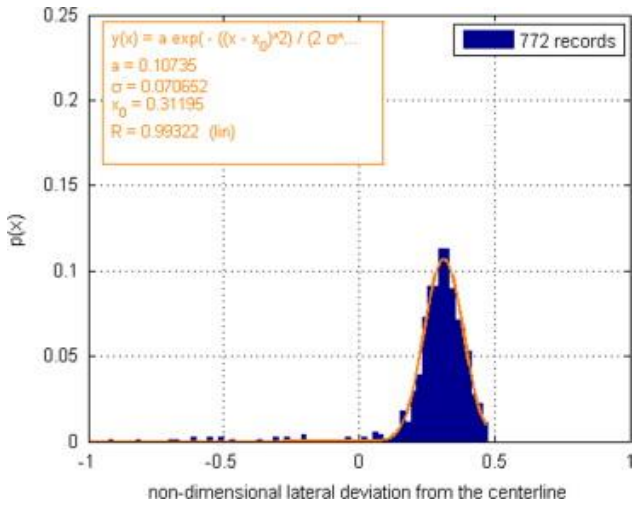

Figure 3.8 Lateral traffic distribution across the Yangtze (Xiao, et al., 2015)

speeds, courses and arrival time intervals conform to the same distributions. The differences in the waterway characteristics can be observed due to the fact that in the Yangtze, traffic does not cross onto the opposite side of the channel due to separation zones, and as local regulations prohibit overtaking manoeuvres, speeds are generally lower. Peak hours in the Yangtze are 1200 and 2400, and course variation is larger due to more navigational space. The traffic distribution is shown in Figure 3.8.

It is concluded that it is reasonable to use statistical methods to illustrate the traffic behaviour in both cases, and that the distributions that were revealed form a sound basis for simulation of traffic.

3.3 Appropriate methods for Stad tunnel fairways

The implementation of a collision and grounding frequency analysis in the Stad tunnel fairways is interesting from a data-acquisitional perspective as the route is not currently trafficked, so that predictions and assumptions must be made to model the future traffic pattern in this area.

The previous risk analysis was carried out on the basis of accident and exposure data rather than a geometrical accident model. Therefore, it might be of interest to investigate how a geometrical model compares to the results found in the previous

analysis. It is decided to use AIS as a data source in this analysis to accurately model traffic patterns for this model.

In addition to the methods described above, several methods and their implementations in risk analyses have been examined. However, many of these approaches are not applicable to the situation in question. For example, the BE-AWARE risk assessment of the North Sea area utilises Markov network logic to map routes between destinations, and uses AIS data to quantify traffic along the defined routes (BE-AWARE, 2014). Crossing collisions happen at route nodes where vessels cross over each other's paths. This method is not ideally suited to the Stad area which presents a significantly simpler routing problem, and route nodes will be irrelevant in the context of a low number of routes.

The methods described in the previous sections (Kristiansen's and Pedersen/Simonsen's models) are both possible to apply to the Stad tunnel route. Kristiansen's model is simple to understand and visualise, and may be the easiest to implement. However, it might not be sufficiently accurate. The analyst's discretion in lane placement and obstacle modelling will greatly influence the model, and therefore expert judgement might be necessary to accurately implement such a model.

For example, if a lane passes over an obstacle, several ships might ground there according to Kristiansen's model. However, from examining AIS data density plots, it is apparent that ship lanes seldom can be described as passing over obstacles. It is also apparent to the author of this report that navigators will not plan routes over obstacles. The stranding model in which vessels that lose control are assumed to continue straight ahead or on a random heading in the general direction they were sailing appears to be somewhat arbitrary. There is only a rough estimate available for the length of sailing distance in which control might be regained.

Kristiansen himself comments that the model is not suitable for finding an accurate number of events, but that it can be used to compare different alternatives. For the purpose of this analysis, the method might therefore be useful for comparing the projected route with the current route. It would, however, be insufficient to make a qualified comparison to the previous risk assessment.

Pedersen's model is more complex and accounts for situations such as grounding due to missing turns. IWRAP is a state of the art implementation of Pedersen's and Simonsen' model, and facilitates the use of AIS data to model traffic density and lateral distributions. Additionally, the IWRAP method theory is well documented, so that it can reproduced. The IWRAP documentation also provides a range of causational probabilities for different accident cases. The probabilities used by

default are empirical probabilities based on the work of Fujii and others, but analytically calculated probabilities are also available. Therefore, it is decided that a similar approach is suitable for this analysis.

4 Hazard identification

4.1 Waterway characteristics

4.1.1 Route definitions and geographical features

The analysis is geographically limited to an area between the town of Måløy to the south and Kvalsund to the north. Two fairways are examined. The Stad sea route: *Rabben – Passage round Stad – Haugsholmen*, and the Stad tunnel route: *Rabben – Tunnel passage – Haugsholmen*. The routes are illustrated in Figure 4.1. The routes are the same as the ones defined in the DNV report examined in previous sections.

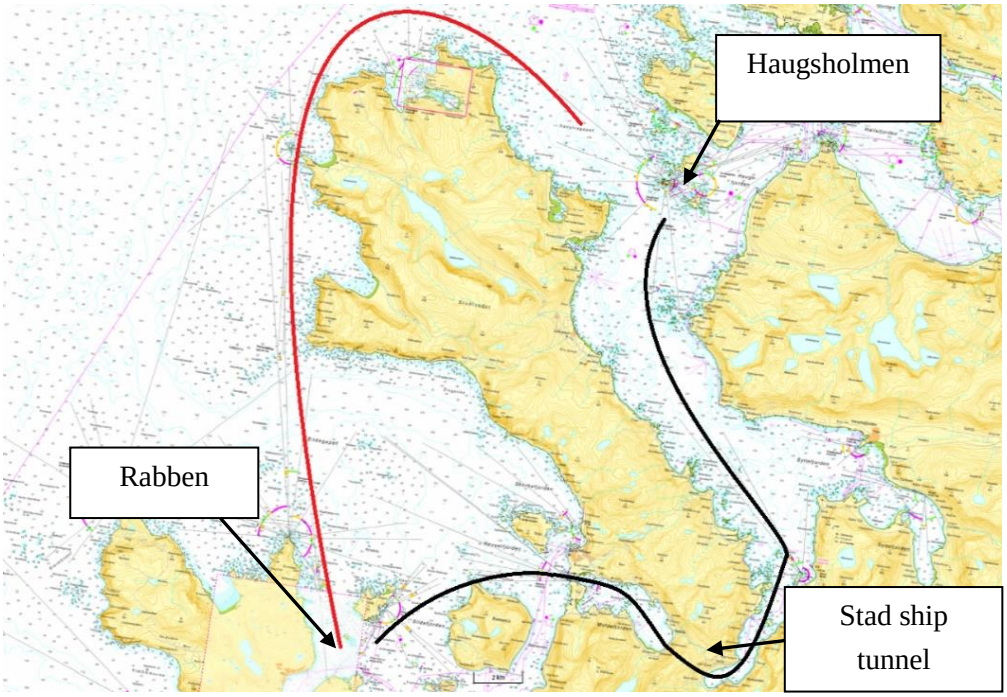

Figure 4.1 Route definitions. Red: Stad sea route. Black: Stad tunnel route

The tunnel route passes through two narrow fjords on either side of the tunnel, the Moldefjord on the west side and Kjødepollen on the east.

4.1.2 Planned safety measures

For the tunnel entrances, several safety measures to reduce risk are planned (Kystverket, 2017). Physical barriers will protrude approximately 160 m from the tunnel entrances to lead vessels towards the opening. In certain areas outside the tunnel entrances vessels will be prohibited from loitering or waiting, and some areas will be designated as "beyond the point of return" for entering vessels. Traffic will

be directed by maritime traffic centrals and signal lights. Additionally, a speed restriction of 8 knots will be implemented in the fjords on either side of the tunnel. The restrictions will apply to the entirety of the Moldefjord and Kjødspollen within the island of Børholmen (Andreassen, 2018).

4.2 Scenario definitions

4.2.1 Collision

For the purpose of the analysis specific collision events are defined. Head-on collisions happen when meeting vessels fail to evade each other. Overtaking collisions happen in situations where vessels headed in the same direction attempt to overtake each other, but fail to do so at a safe distance. Additional collision situations occur when fairways merge or cross each other. These collisions can collectively be described as crossing collisions.

In this analysis, meeting and overtaking collisions are most interesting. If traffic that currently follows the sea route is assumed to be diverted to the tunnel route, there will be no merging or crossing of major fairways. However, on the current route there may be merging encounters when inshore traffic meets traffic passing Stad from an offshore approach.

4.2.2 Grounding events

As discussed in previous sections, grounding events can be divided into several categories. In this analysis the following situations are considered:

- Striking an object in the lane.
- Striking an object or waterway edges as a result of failing to turn at bend.

Drift grounding situations, in which a vessel not under power drifts ashore or onto obstacles, may be relevant for both routes. However, a detailed model of wind and current patterns is required to accurately model drift patterns and the probability of drifting towards obstacles.

5 Frequency Analysis

5.1 Data Sources

Data has been collected from a web-based application provided by the NCA, called the Track Server, in which historical traffic data from the North Sea and Norwegian coast can be found for the past 10 years (Kystverket, n.d.). Access to this server is available by registering a user account with the NCA. The application combines visualizations of data such as density plots and coloured ship tracks with the possibility to export raw data according to geographical and ship-specific filters. Additionally, statistical analyses can be carried out directly in the web-based interface.

Carrying out analyses on the server is however time-consuming. The user is prone to be logged out for inactivity while waiting, which causes results to be lost. Therefore, it is impractical to carry out analyses or render plots of any significant size on the track server itself.

The Track Server mainly utilises AIS data received by the NCA VTS stations to map the traffic data. Data from the various sources are decoded and registered, and merged into a common track table. “Snapshots” of the track table are saved at regular intervals, making up the historical data. In this process, the data is cleared of errors and invalid messages (Åsheim, 2017). An illustration of the system architecture is provided in Figure 5.1.

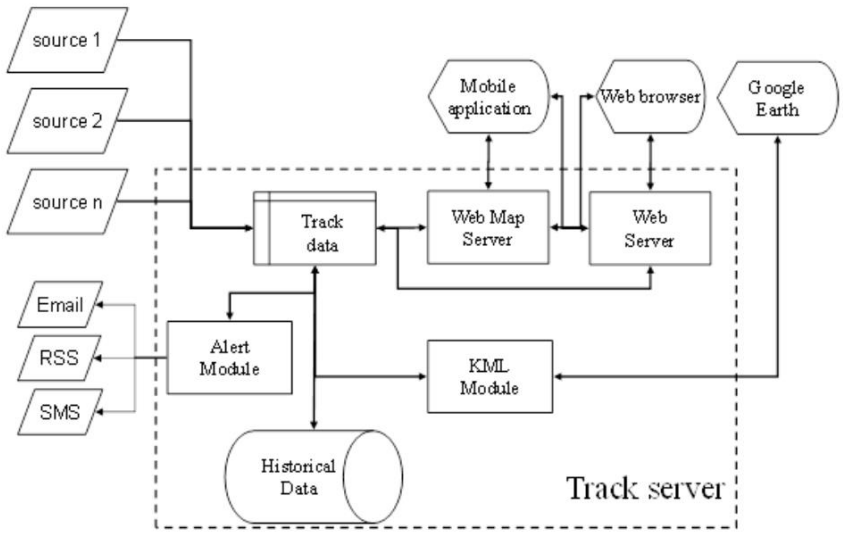

Figure 5.1 Track server system architecture (Kystverket, 2016)

When exporting data from the Track Server, there are several available options to filter the data. First, a geographical filter to limit the data to the relevant area is implemented. Using the Track Server interface, a polygon is drawn around the area in question Figure 5.2.

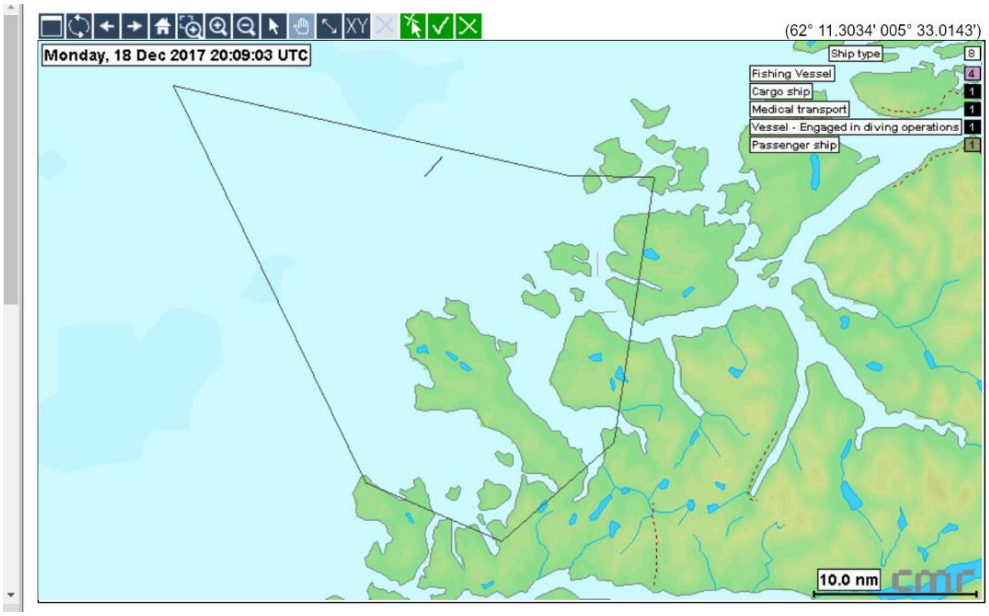

Figure 5.2 Stad sea area polygon filter drawn in the NCA's Track server (Kystverket, n.d.)

The shape of the polygon is chosen to reduce the amount of exported data, while retaining the areas important for the statistical analysis of the vessel traffic. The area is delimited by the town and narrow straits of Måløy in the South, and the town of Kvalsund in the North. Off the tip of the Stad headland, the filter extends approximately 20 nautical miles out to sea. The filter covers traffic passing in both the inland fairways and the outer fairways.

An additional filter is applied to limit the vessel beam to the maximum allowed beam in the tunnel: 21.5 m. Thus, all the vessels in the filter are nominally tunnel candidates. Vessels broadcasting with a navigational status "moored" are also filtered out to reduce the exported data amount.

5.2 Statistical Traffic Analysis

In the track server interface, relevant data fields can be selected for export Figure 5.3. For the purpose of counting the number of passing vessels and for defining lateral traffic distributions, vessel identification numbers (MMSI numbers) and decimal latitude and longitude are necessary. The selected data are downloaded in

separate fields in tab-separated format. A Matlab program is developed to read and sort the data.

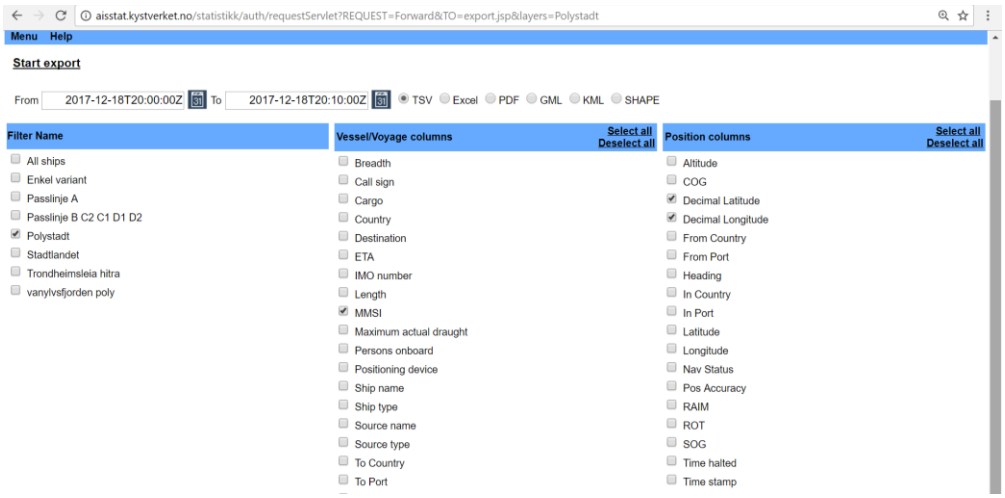

Figure 5.3 Track server data export parameters

For the Stad area, data for one year (October 2016-October 2017) is downloaded. Using the Matlab function “tdfread”, the data is read into Matlab as a struct object, from which the data can be extracted. To analyse the data, the struct arrays are catenated into large matrices containing the selected information in different columns.

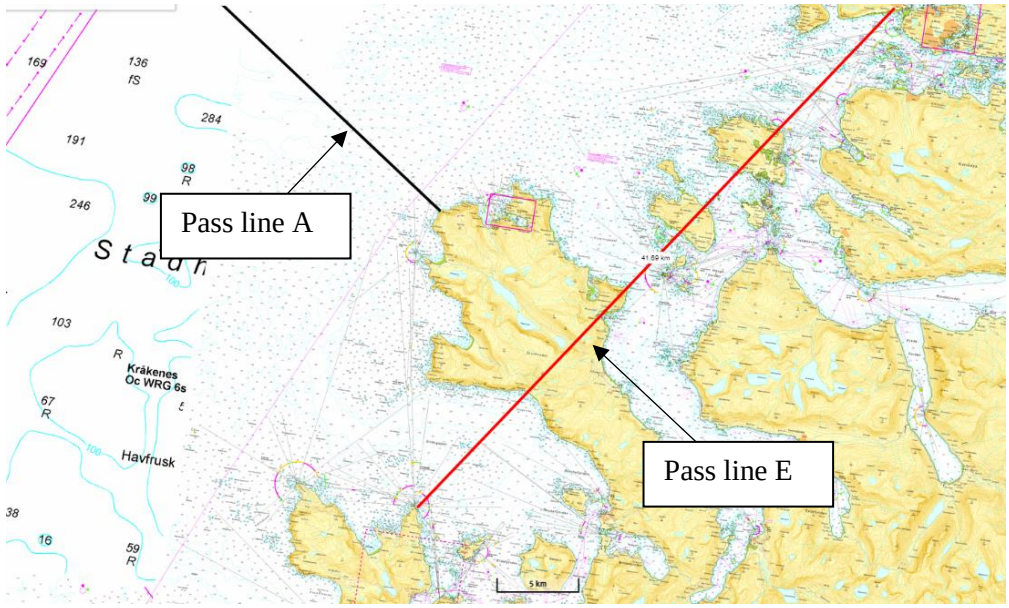

Figure 5.4 Pass lines A and E

The first task is to identify the number of vessels which can be expected to use the tunnel on a yearly basis. As in the previously discussed DNV report, it is assumed that vessels that approach the Stad headland from the inshore fairways are tunnel candidates. A pass line (A) is extended from the tip of the headland approximately 20 nautical miles out to sea, and a second line (E) orthogonally across each of the inland approaches to the headland. Vessels that pass both lines can be assumed to be tunnel candidates. The extension of the pass lines is illustrated in Figure 5.4.

To identify the crossing vessels, the AIS messages which have been exported must be rearranged. When exported from the track sever, they are arranged in the chronological order in which they were broadcast and received. A program (see Appendix G) is created to sort the data in consecutive blocks for each vessel, in order of first appearance (and in chronological order for each vessel data block). Having done this, it is possible to count passages across the lines, which are expressed in cartesian coordinates according to decimal latitude and longitude.

To find lateral distributions across the waterways, similar lines are defined across relevant cross-sections of waterway, and the crossing point on the line for each vessel is be found. Histograms of vessel crossings across the width of the cross-section can reveal the shape of the lateral traffic distributions, as visualised in Figure 5.5, showing the distribution of traffic across the entrance of the eastern tunnel approach.

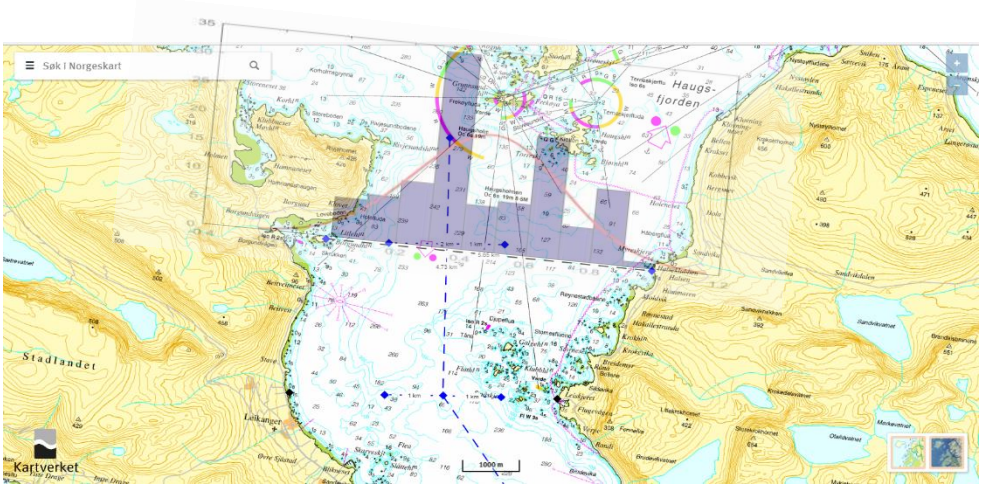

Figure 5.5 Histogram of southbound traffic distribution over a cross-section at the entrance to Vanylvsfjorden

Other data is important to increase the accuracy and detail of the risk analysis. Vessel type, length, breadth, draught and speed over ground is also exported, However, as the size of the track server exports increase rapidly for each added variable, only 1 month (March 2017) of this additional vessel data is downloaded.

Additionally, for larger data sizes, unusual or unnecessarily long vessel type descriptions cause difficulties in catenating longer fields of vessel types.

Vessels of the same type are grouped together, and then the average length, breadth and speed over ground for each vessel type can be calculated. To achieve an accurate average speed, zero speed entries are removed from the data. Vessel types that make fewer appearances than 3 within the analysed time period are grouped together in a miscellaneous category. The vessel parameters found are shown below:

Table 5.1 Vessel type distribution and parameters

Vessel type	Amount	Avg. beam	Avg. length	Avg. speed over ground
Passenger ship	18.0	15.6	96.9	13.6
Fishing vessel	108.0	9.9	43.7	9.8
Cargo ship	315.0	13.7	86.9	10.5
Dredging vessel	12.0	12.0	35.5	11.5
Tanker	65.0	16.0	99.8	12.2
High Speed Craft	13.0	9.7	30.3	27.8
Unused	9.0	14.0	67.0	11.9
Other	14.0	13.3	62.8	11.1
Tug	12.0	10.1	30.3	10.1
WIG	7.0	7.5	34.5	7.7
Miscellaneous	17.0	8.2	43.9	18.9

Table 5.1 shows that cargo ships and fishing vessels are the most numerous vessel types that might use the tunnel. There are some indeterminate vessel type classes such as ‘unused’, ‘other’ and ‘Miscellaneous’. As these classes are relatively numerous, they will be included in the analysis even though it is unclear exactly what kind of vessels they are.

5.3 Traffic density and distribution modelling

5.3.1 Traffic density

It is found that for the period October 2016-October2017 there are 14497 passages across passline A, i.e. rounding the Stad headland. Of these passages, 10162 also cross passline E, i.e. approach the headland from the inner fairways. This indicates that the tunnel will have a traffic flow of 10162 vessels per year in both directions, or approximately 28 vessels daily.

The DNV calculates 17565 crossings from the inner fairways for a two-year period in 2009 and 2010, corresponding to 25 vessels per day. The prognosis for a corresponding time period in the year 2025 estimates 17523 crossings, also corresponding to approximately 25 vessels per day. The number of crossings found in this analysis is higher than the study from 2010 and the prognosis for 2025. This might indicate an increase of traffic that the DNV did not account for in 2010, or that the use of AIS equipment has become more widespread, as suggested in the Rotterdam AIS traffic study described in section 3.2.2.

5.3.2 Lateral traffic distribution

The waterways leading to the projected tunnel entrances are not currently heavily trafficked, and it is therefore necessary to predict the future traffic lanes and the lateral traffic distributions across these lanes. As discussed in section 3.2.2, one would expect traffic to follow a normal distribution. The method used to estimate the lateral traffic distribution for the analysed waterways is described in this section.

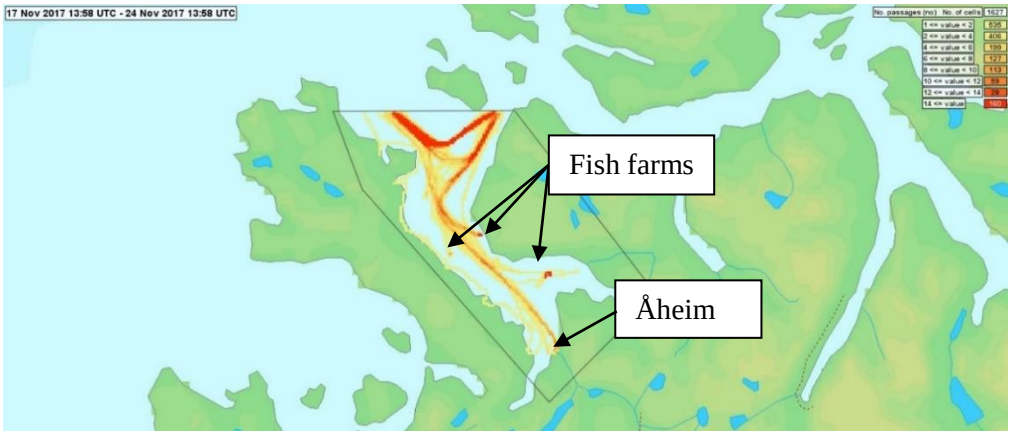

Figure 5.6 1-week density plot of Vanylvsfjorden

First, traffic patterns in the North-western approach to the Stad tunnel, Vanylvsfjorden, is examined. It appears to consist of vessels heading to the several fish farms and small ports that can be found there. A density plot of one week's traffic illustrating the traffic pattern is shown in Figure 5.6. Much of the traffic that enters the fjord sails to the small port of Åheim at the bottom of the fjord.

As Åheim is located near the entrance to the narrower part of the fjord which leads to the tunnel entrance, it might be a good assumption that future traffic will display a similar pattern.

To predict a lateral traffic distribution across Vanylvsfjorden one might therefore assume a similar distribution as the current traffic. However, the current traffic distribution across the fjord is disorganised at places by vessels peeling off the main traffic route to visit fish farms or other local destinations. This miscellaneous traffic will become much less significant compared to the main coastal traffic in transit, and their contribution to lateral distribution will cause inaccuracies in approximating the future distribution, especially for different parts of the waterway.

A simple solution might be to select the least “troubled” cross-section of the waterway and use the lateral distribution across this section to represent that of the entire waterway. The advantage of such a method would be to minimise irrelevant traffic distributions, and yet retain the actual distribution of traffic in the area, thus reflecting local navigational circumstances. A possible cross section to examine might be at the centre of the fjord, as illustrated in Figure 5.7.The lateral distribution of crossings with a fitted normal distribution is shown in Figure 5.8.

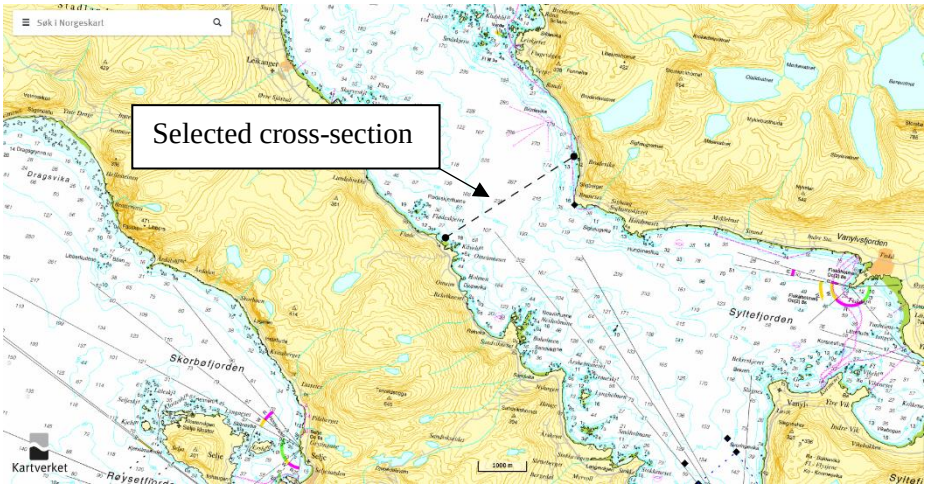

Figure 5.7 Selected cross-section for examination of lateral traffic distributions

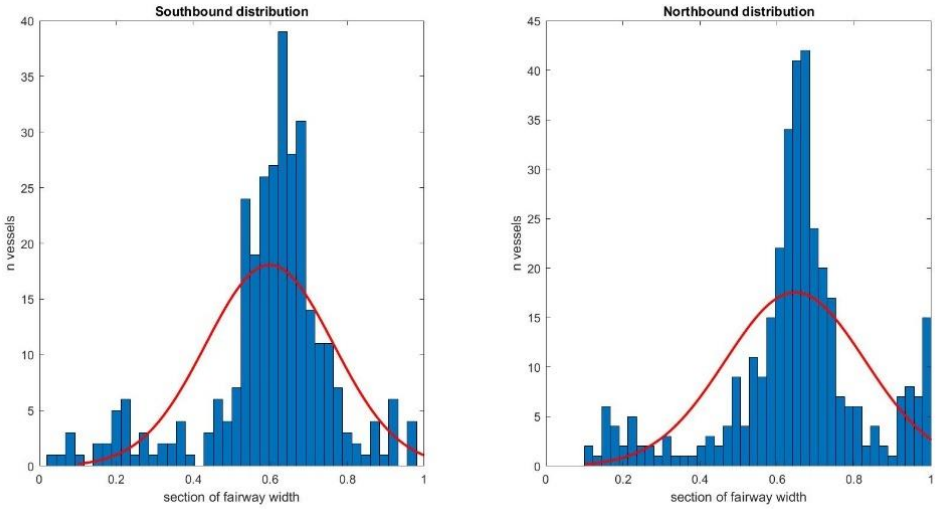

Figure 5.8 Lateral traffic distribution

It is apparent that the normal distribution does not fit very well, although there are tendencies to a normal shape.

A different approach might be to utilise the lateral distributions of nearby similar, more populated waterways. As discussed in section 3.2.2 one might expect similar distribution shapes for different waterways. Using a distribution of the current coastal traffic flow would provide a more accurate depiction of the distribution of

the future traffic. However, in this process, local navigational circumstances that might impact lateral traffic distribution will not be represented.

For the purpose of this analysis, this is selected as the best solution. It will allow a single distribution to be implemented for all sections of the analysed waterway, simplifying calculations.

The fairway between the island of Hitra and the mainland, near the entrance to the Trondheimsfjord, might be a good candidate, as it is a straight section of limited width, through which most of the coastal traffic (which should have approximately the same volume as near Stad) must pass through to stay sheltered from the open sea (Figure 5.9). Data for this area from November 2016-November 2017 is downloaded

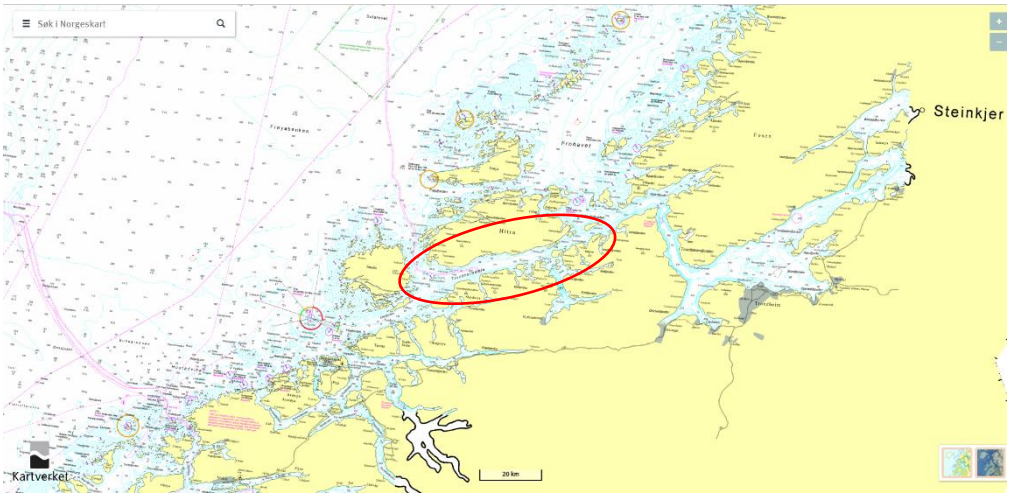

Figure 5.9 Hitra channel

The navigable areas of the waterway are identified visually from density plots of the traffic, see Figure 5.10. A cross-section of the channel approximately from the Snekkflua skerries to Eisteråa, see Figure 5.11, yields the lateral distributions shown in Figure 5.12.

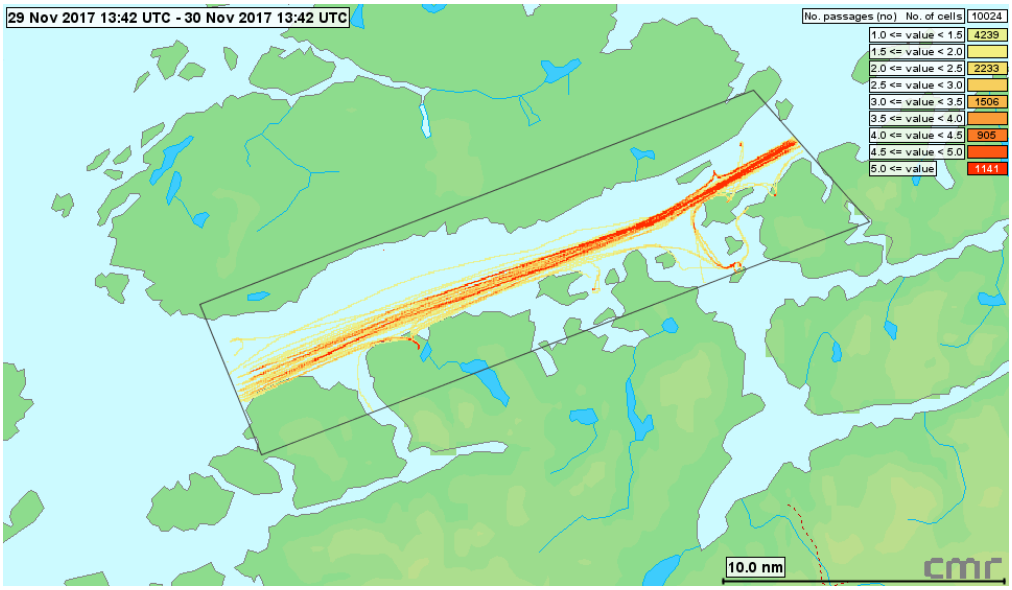

Figure 5.10 Density plot of the Hitra channel traffic

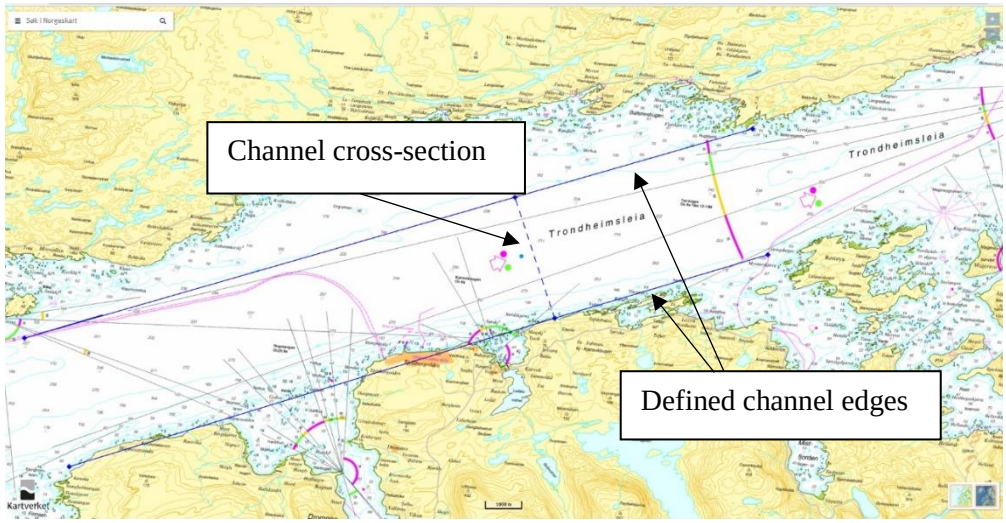

Figure 5.11 Selected cross-section and channel edges

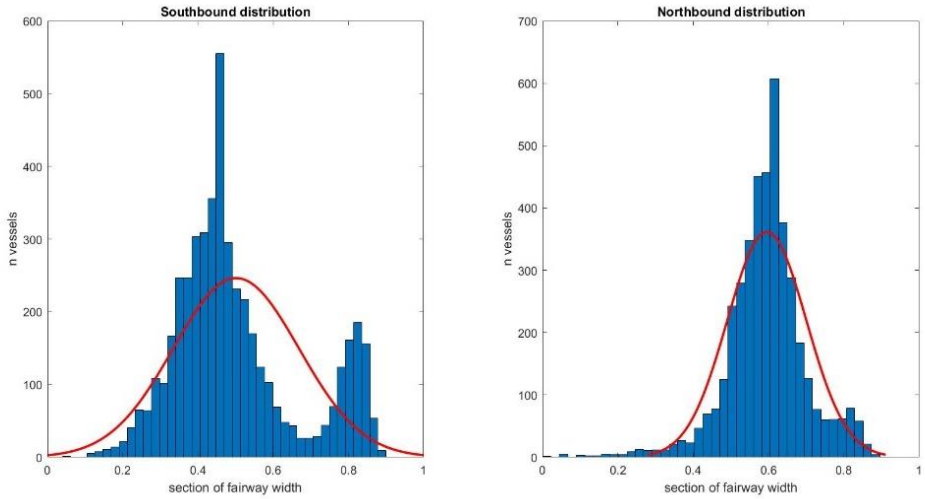

Figure 5.12 Lateral passage distribution across the Hitra channel

It is apparent that the traffic distribution is well suited to a normal fit, although the southbound distribution appears to have a secondary, independent distribution on its western side. On examining the density plot, it is likely that this traffic component derives from traffic headed to a small port on the south side of the waterway.

It is assumed that the secondary distribution is comprised of local traffic. If one is only interested in the main coastal traffic distribution, an option to filter out the local traffic is to count each passing vessel only once. Thus, local vessels that pass more often than vessels on long-haul traffic are not over-represented. The resulting distribution is shown below in Figure 5.13

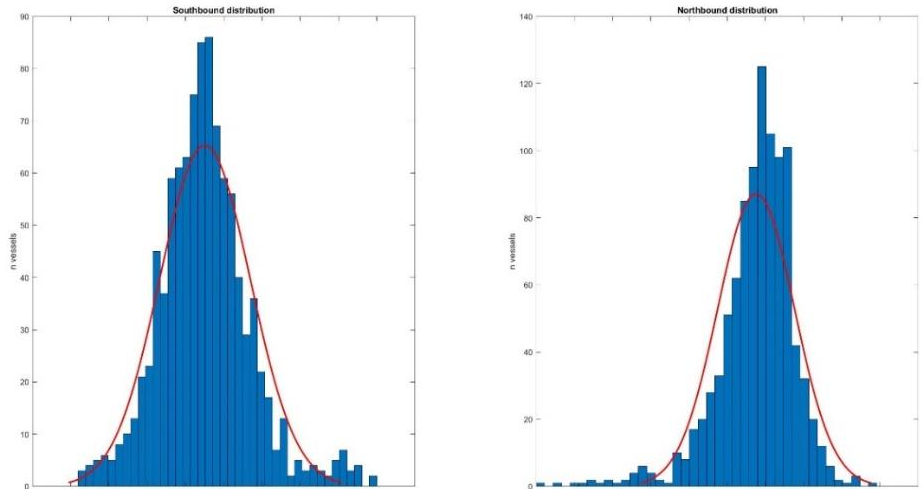

Figure 5.13 Lateral vessel distribution across Hitra channel

It is found that a clearer normal shape is revealed after filtering local traffic. The mean position of the traffic within the Hitra fairway is approximately in the centre of the navigable channel, and the traffic is shifted slightly to the starboard in either direction as one would expect.

To verify the distribution found in the Hitra channel, a cross-section of a waterway closer to the relevant area is also examined. When passing the Stad headland, most traffic passes through an approximately 800 m wide passage between the rocks at Gamla Lysbøye and Furuneset Figure 5.14. The passage distribution across the cross-section is shown in Figure 5.15.

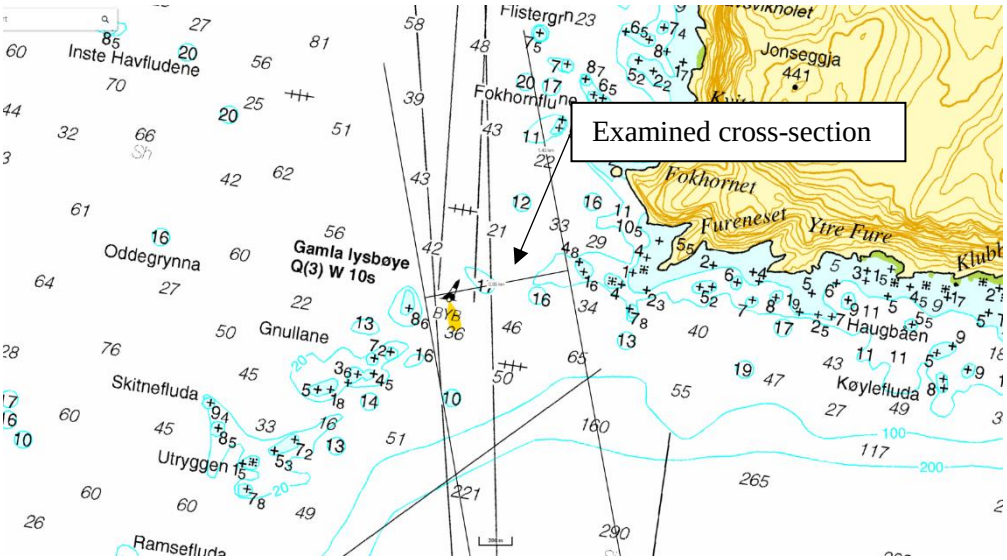

Figure 5.14 Examined cross-section between Gamla Lysbøye and Furuneset

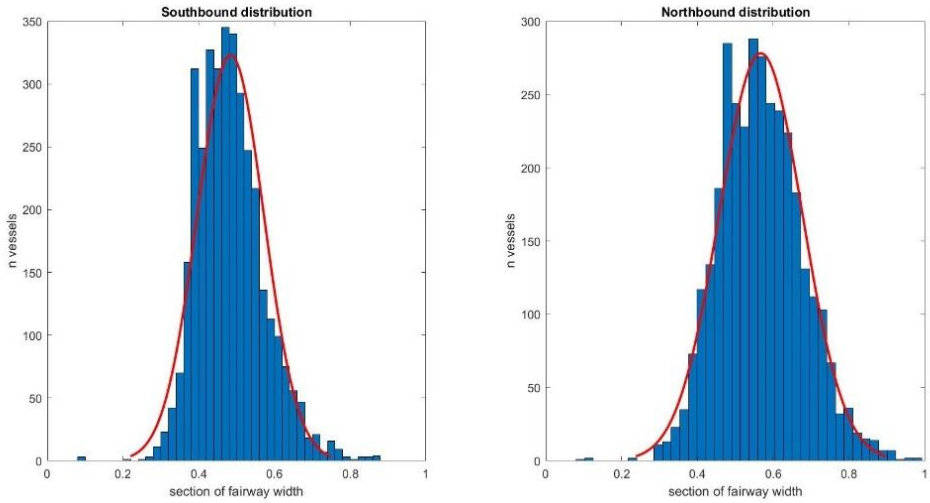

Figure 5.15 Lateral distribution of passages across Gamla Lysbøye-Furuneset cross-section

The parameters of the relevant examined cross sections are listed in Table 5.2. Values are listed in terms of lane width from 0 to 1.

Table 5.2 Lateral distribution parameters

Cross-section	**Mean μ**	**Standard deviation σ**
Hitra channel(filtered), Northbound	0.5757	0.1007
Hitra channel(filtered), Southbound	0.4509	0.1188
Gamla Lysbøye-Furuneset, Northbound	0.5582	0.1193
Gamla Lysbøye-Furuneset, Southbound	0.4626	0.0952

It is concluded that the distributions have similar shape and parameters. However, The Gamla-lysbøye – Furuneset distribution has opposing traffic slightly closer to each other. The standard deviations of this distribution are also slightly less homogenous for northbound and southbound distributions. For the purpose of the analysis the filtered Hitra channel distribution is utilised for lanes that are not currently in use.

5.4 Lane Positioning

For the purpose of calculating collision, stranding and grounding risks, the waterway is split into appropriate sections of homogenous width. Width refers to the lane width and not the physical edges of the channel. Lane placements are based as far as possible according to observed traffic patterns. Where this is not possible, lanes are defined such that there are as few bends in the waterway as possible, without the sections overlapping onto land or too far into obstacles.

5.4.1 Eastern tunnel approach model

Traffic that enters Vanylvsfjorden from the east, has Haugsholmen on its starboard side, and the skerries by Djupeflua to port. The lane width in this section is therefore

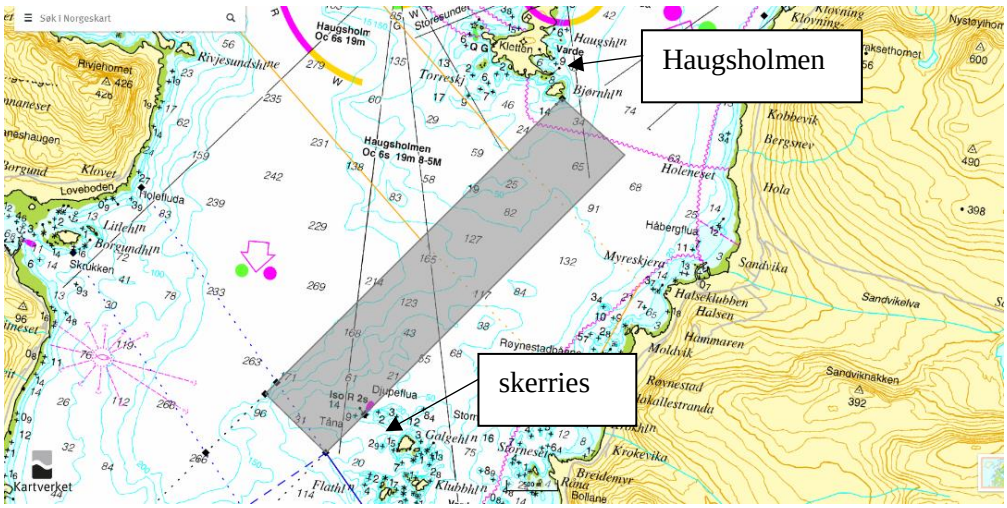

Figure 5.16 Lane Section 1, tunnel route

bounded by the edges of these obstacles, making the lane 4 km long and 0.8 km wide. It is marked in grey in Figure 5.16.

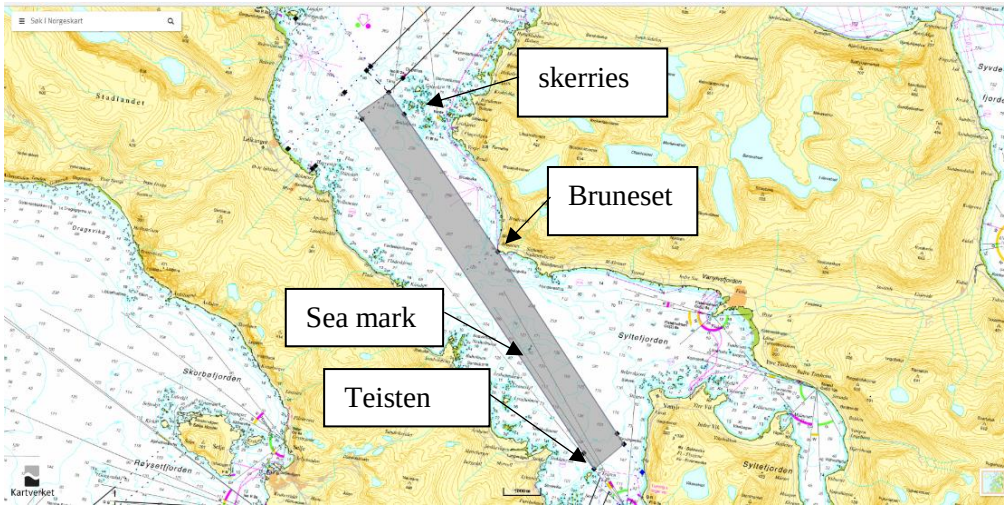

Figure 5.17 Section 2, tunnel route

After rounding the skerries, the lane is bounded by the skerry edges, the Bruneset headland on the eastern side, and the rock marked Teisten on the western side. The resulting lane is 1 km wide and 11 km long, see Figure 5.17. Near the middle of the lane, a single rock is marked by a sea mark, making it a potential obstacle for traffic to avoid**.**

After rounding Teisten, traffic will enter the smaller fjord that leads to the tunnel entrance, called Kjødspollen. The lane is significantly narrowed, but a straight lane 0.3 km wide and 4.5 km long fits between obstacles on either side. The section is

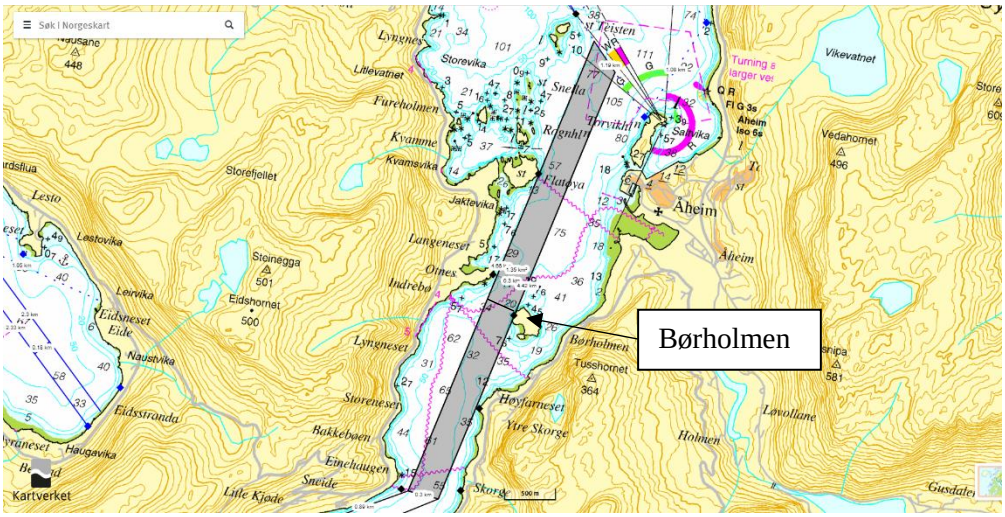

Figure 5.18 Sections 3 and 4, tunnel route

split into two at the island of Børholmen to delimit the speed restricted area. The result is two sections of 2.6 and 1.9 km length respectively, as shown in Figure 5.18

Following the bend at the end of this section, the tunnel entrance is approximately 1 km away. As discussed in section 4.1.2, safety measures such as physical barriers and traffic control will be in place near the tunnel entrances. Therefore, the number of accidents in this stretch of water are assumed to be negligible. The design of the tunnel and entrances is illustrated in Figure 5.19.

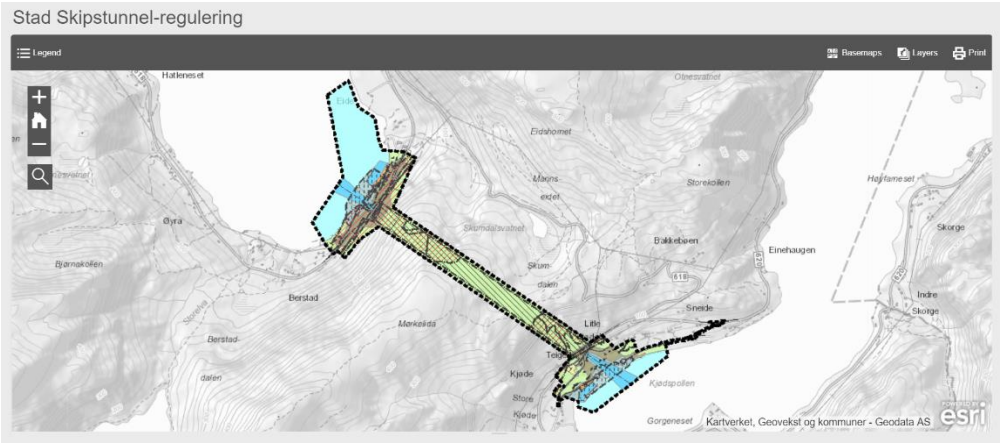

Figure 5.19 Planned tunnel design (Asplan Viak, 2017)

5.4.2 Western tunnel approach model

A density plot of current traffic in the western tunnel approaches is shown in Figure 5.20

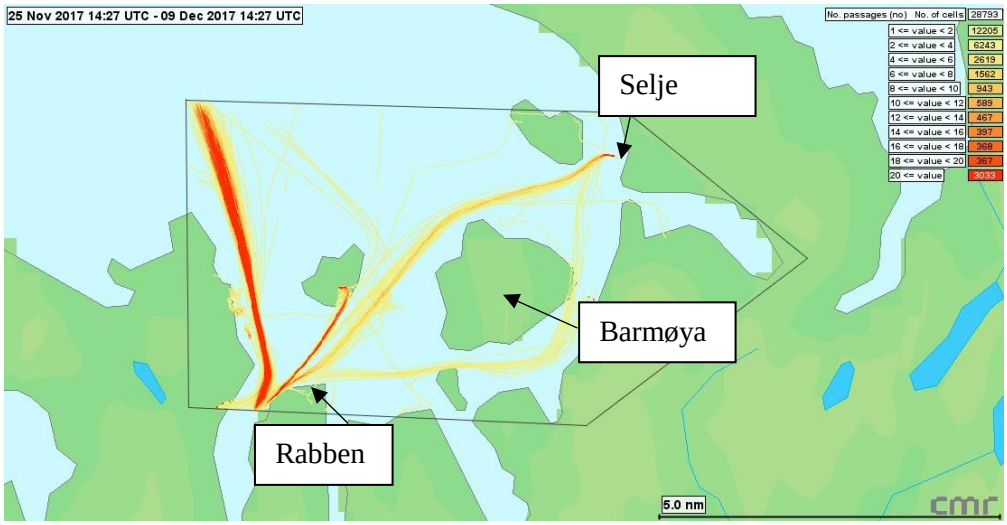

Figure 5.20 Density plot of traffic in western tunnel approaches

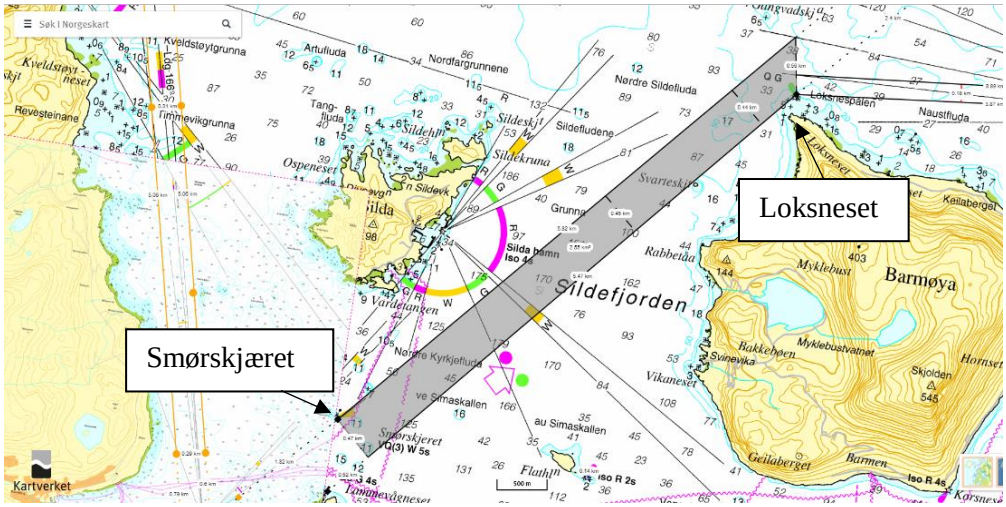

Figure 5.21 Section 10, tunnel route

According to the conceptual maps provided by the NCA (Figure 2.2), The fairway is expected to go north of Barmøya. To approximate the fairway parameters and position, the density plot of traffic headed from Rabben to the port of Selje, close to the western tunnel entrance Figure 5.20, is utilised. Using the plot as a guideline, it appears that the lane is bounded by skerries at Smørskjæret, and the sea marker off Loksneset. This results in a lane which is 0.45 km wide and 5.65 km long.

Having rounded Loksneset, traffic must now head towards the narrow sound that outlines the entrance to Moldefjorden. It is assumed that the width of the lane will narrow to fit between the lights that mark either side of the sound, as vessels rounding Loksneset set a course for the entrance, illustrated in Figure 5.22. For the

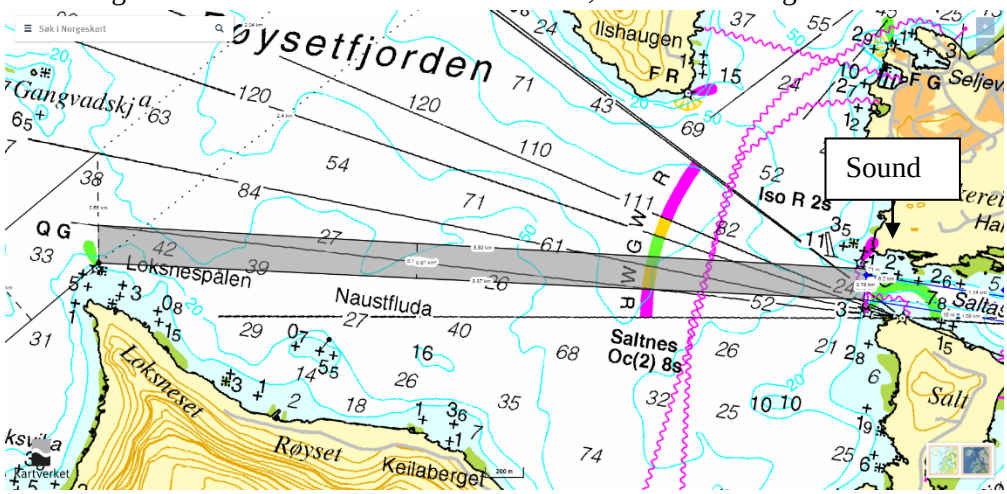

Figure 5.22 Section 9, tunnel route

sake of simplicity, this assumption is assumed to hold for traffic in the opposite direction as well. The lane section is 0.17 km wide and 8.88 km long.

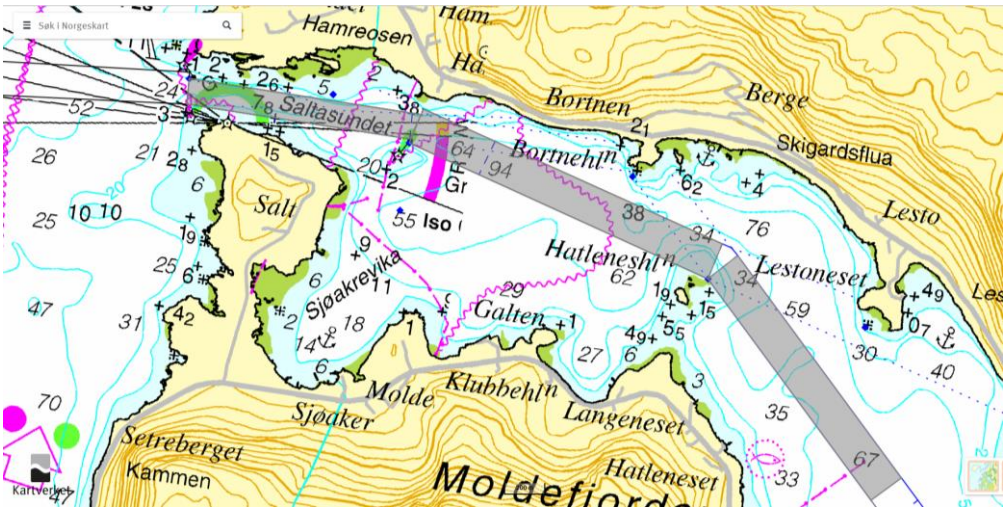

Figure 5.23 Sections 8,7 and 6 from left to right

Inside the Moldefjord, there are three sections and two bends, illustrated in Figure 5.23 The section that passes through the sound at Saltasundet is 0.12 km wide, and 1.1 km long. The next section, from the sound to Hatlenesholmen, is 1.59 km long, and 0.18 km wide. After a bend in the lane, the final section towards the tunnel

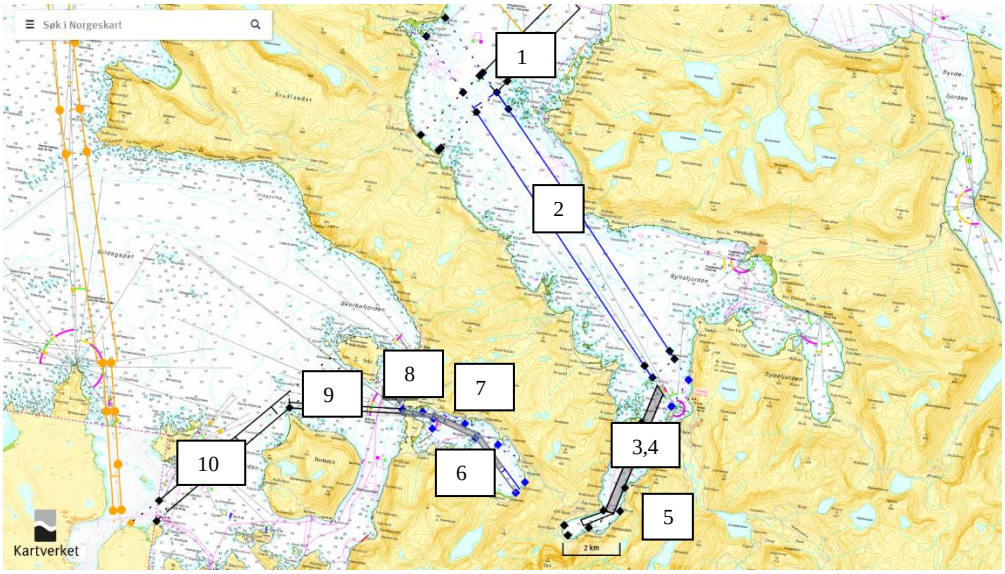

Figure 5.24 Tunnel route sections, numbered

section is 0.18 km wide and 1.33 km long. Again, the final 1 km long stretch of water near the tunnel is assumed to be a safe area due to planned safety measures.

The entire route with sections numbered from East to West, according to Figure 5.22, and the lane parameters are listed in Table 5.3.

Table 5.3 Lane parameters for the tunnel route

Section	Length [m]	Width [m]	Southbound o_{1s}, o_{2s} [m]	Northbound o_{1n}, o_{2n} [m]	Southbound obstacle span after bend	Northbound obstacle span after bend	Obstacle span in lane, X
1	4000	1000	2870,2710	N/A	0,1	0,1	0
2	11,100	1000	1200,900	2950,3100	0,1	0,1	0.38,0.4
3	4500	300	800,540	2740,2670	0,1	0,1	0
4	470	180	N/A	560,460	0	0,1	0
5	1330	180	N/A	610,490	0,1	0,1	0
6	1590	180	1650,650	690,260	0,1	0,1	0
7	1100	120	1100,960	N/A	0	0	0
8	8888	180	1660,71	N/A	0	0	0
9	5650	450	1320,520	2400,2400	0,1	0,1	0

Note that *Northbound* and *Southbound* values denote the directions of traffic within each section, rather than on a global level.

In addition to lengths and widths, the span of obstacle width in lane relative to section width *X* are defined. For sections which end in a bend at either end, the span of obstacles that lie straight ahead of the bend, z_n or z_s according to the southern or northern end of the section are also defined. The easternmost and westernmost distance from the bend to the obstacle straight ahead is needed to define the slope of the obstacle relative to the section, and thus the possibility of grounding due to forgetting to turn: $\boldsymbol{o_{1s}, o_{2s}}$ for the southern direction and $\boldsymbol{o_{1n}, o_{2n}}$ for the northern direction. Section parameter definitions are illustrated in the diagram in Figure 5.25

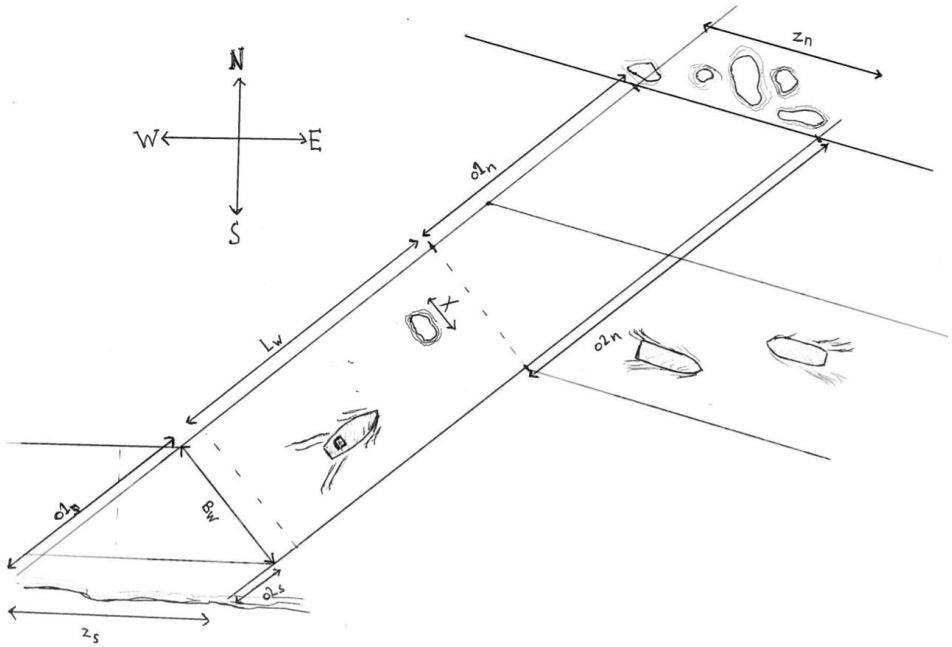

Figure 5.25 Lane parameters

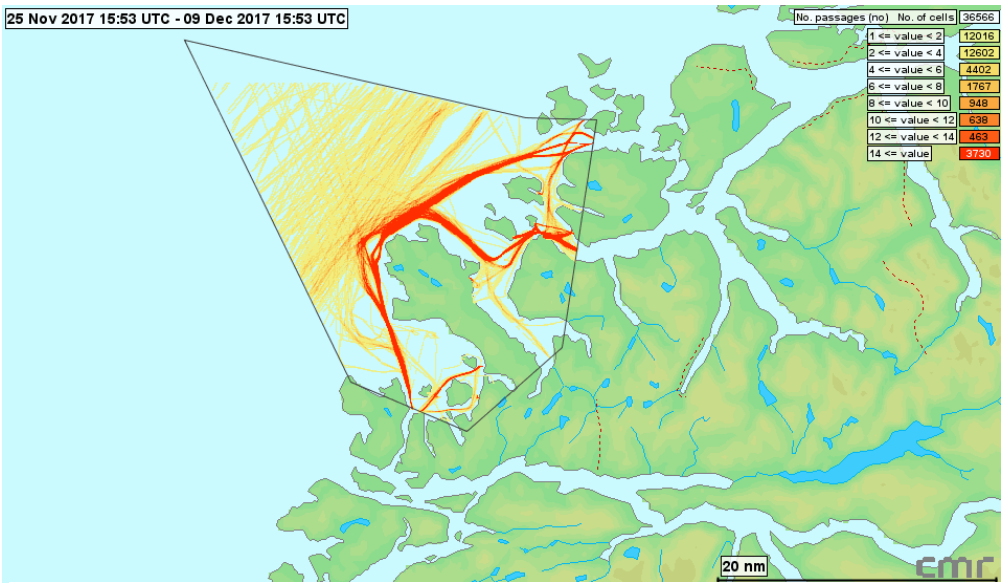

Figure 5.26 Density plot of traffic rounding Stad

5.4.3 Stad Sea Route model

The lanes round Stad are more difficult to approximate as routes vary depending on the weather (Det Norske Veritas, 2010), and are not always strictly bounded by obstacles on either side. On the other hand, the route is currently in use and AIS data can be studied to model the route. A two week-density plot exported from the NCA track server provides a visual example of the traffic pattern around Stad (Figure 5.26)

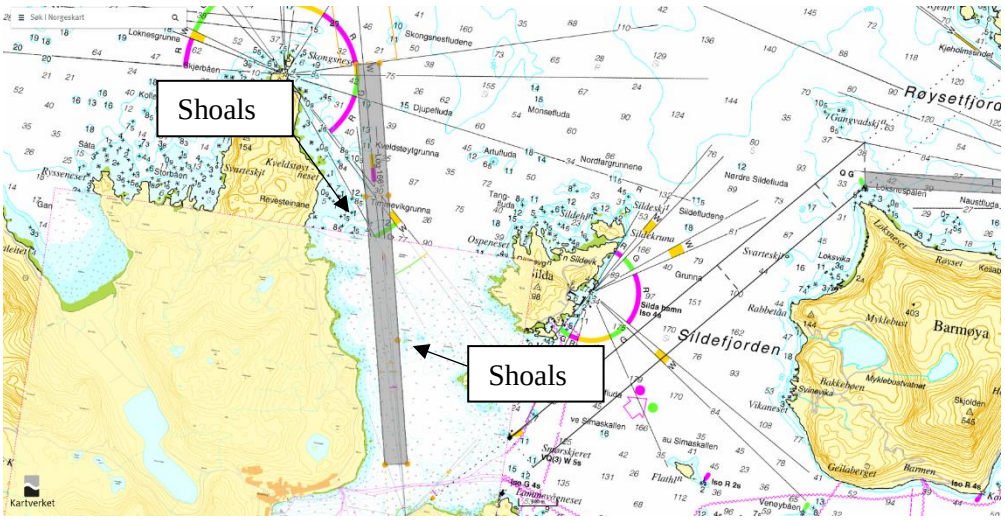

Figure 5.27 Section 1, Stad sea route

The traffic lane in the direction north from Rabben is bounded on the east side by the shoals at Halsøyr, and the shoals off the Kveldstøytneset headland on the western side. Thus, it is 0.310 km wide and 5.06 km long, see Figure 5.26

The lane over Sildegapet bay is found to be 0.710 km wide, the width being bounded by a passage through the shoals at Gamla lysbøye off the tip of Furuneset (Figure 5.28). This appears to fit well with the density plot in Figure 5.26. The section is approximately 13 km in length.

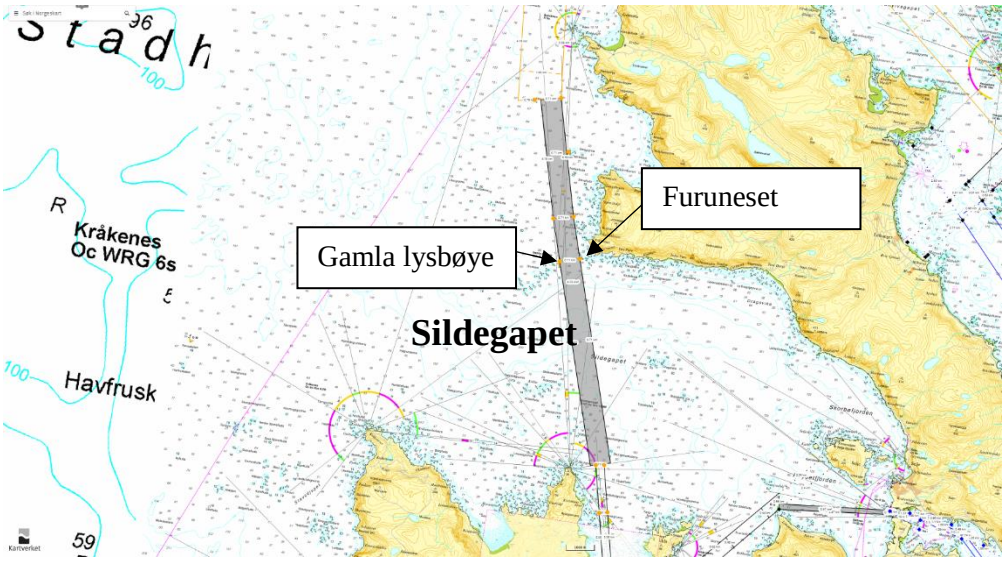

Figure 5.28 Section 2, sea route

Hereafter, the tracks become more unclear to follow, as vessels choose varying approaches to negotiate the rocks off the tip of Stad itself. Vessels pass on either side of the Vossaskallen rocks and Bukketjuvane rocks, or between them, as can be seen in the density plot in Figure 5.29. Some vessels make a course alteration long before they reach the rocks or directly in front of them, but most northbound traffic appears to alter course at a point approximately 2.2 km before reaching Bukketjuvane and 1.2 km before reaching Vossaskallen. The varying approach may be dependent on many different factors, such as weather conditions, vessel parameters or the level of navigation experience. In the opposite direction, course alterations to avoid Bukketjuvane appears to be made at approximately 1.5 km before the rocks

A solution to modelling this behaviour might be to widen the modelled lane to include the different approaches used, incorporating the rock formations Vossaskallen and Bukketjuvane as obstacles within the lane to model the fact that

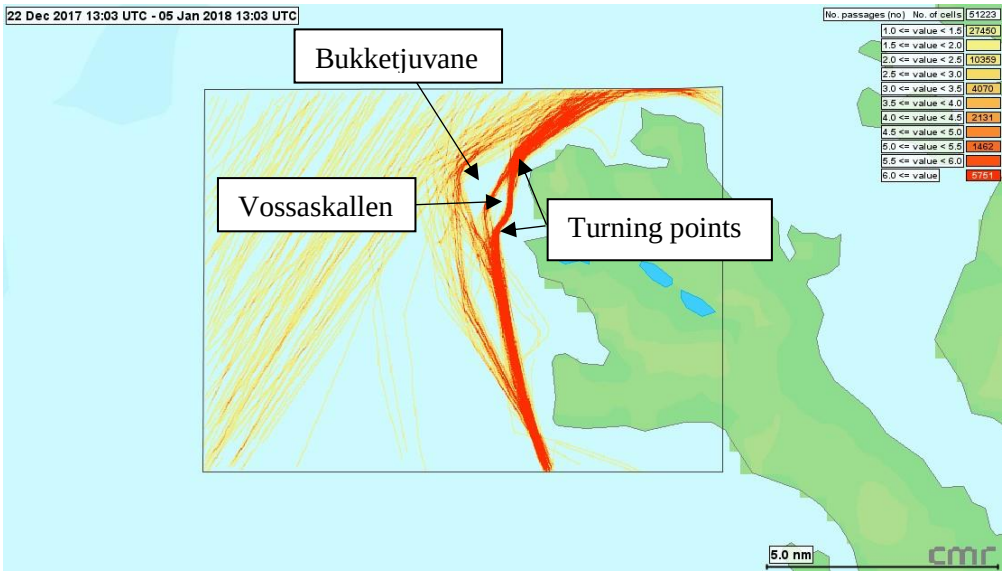

Figure 5.29 Density plot of traffic patterns around the rocks at Vossaskallen and Bukketjuvane

vessels need to actively avoid the rocks. This is a harsh interpretation of the traffic pattern, which places most of the vessels in the lane on a collision course with the obstacles. The following lane consisting of two sections is shown in

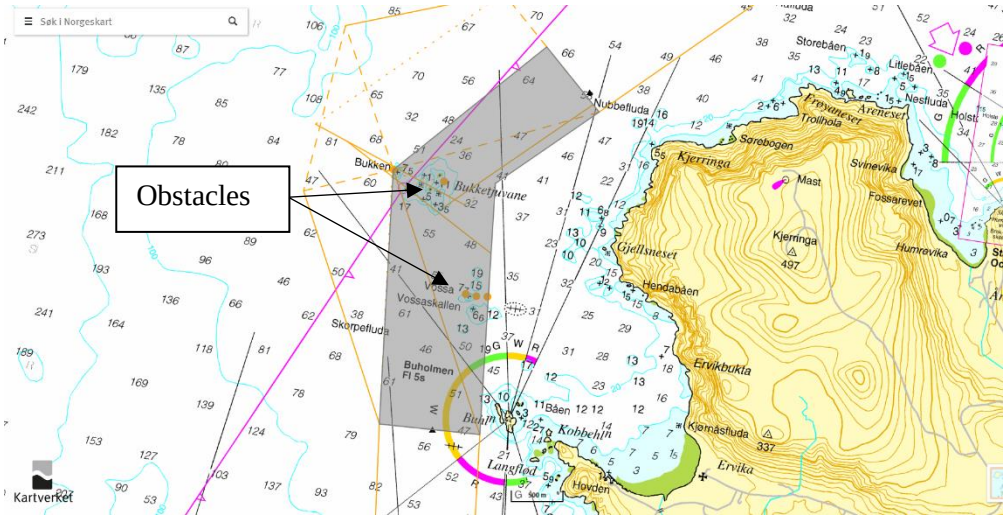

Figure 5.30 Sections modelled over obstacles off Stad

The lane is approximated from the density plot to be 950 m wide at this point, and the sections are 2.5 and 1.5 km long respectively from bottom to top. The rocks at Vossaskallen are 100 m wide, and span the width of the section from 750 to 850m. The Bukketjuvane rocks are 470 m wide, spanning the cross-section from 0 m to

470 m. For computational reasons, the section containing the obstacles is split in two, as no more than one coherent obstacle can be modelled per section in the Matlab program developed to define lane parameters.

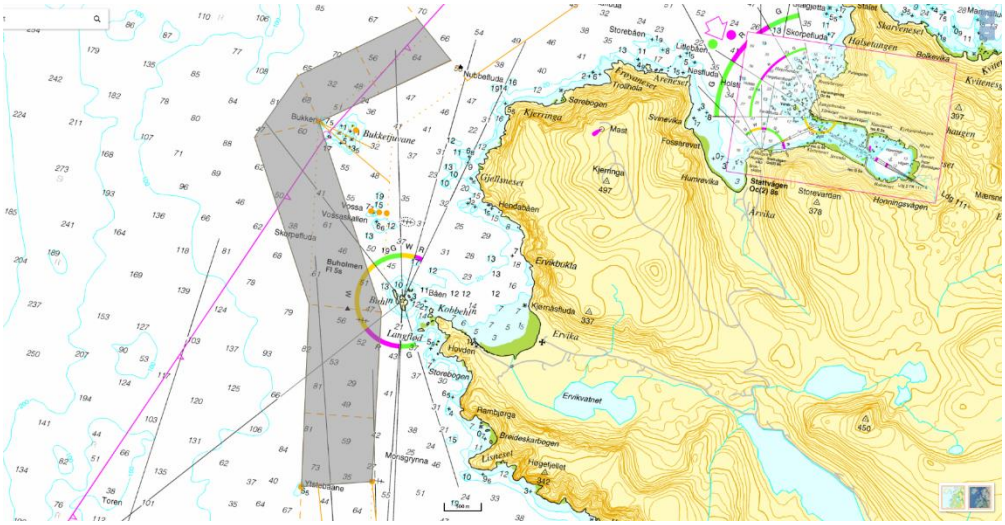

Figure 5.31 Lane sections modelled around obstacles off Stad

If, However, it is assumed that the rocks are well known-navigational features, a bend in the lane might be modelled, to illustrate that navigators in general plan to circumvent the rocks. Thus, only vessels that fail to turn as planned will strike the obstacles. In accordance with the density plot, a bend is modelled for each direction, taking the lane on the outside of the obstacles. This is a simplification of the actual traffic which in reality appears to split into three at this point. However, the model illustrates that vessels must make a manoeuvre to avoid grounding.

The lane around the obstacles is thus defined by three sections approximately 0.950 km wide, and respectively 2.3, 2.4 and 1.8 km long from south to north. A bend is modelled in at 2.3 km before the rocks for northbound traffic, and 1.7 km for the southbound traffic. The lanes positions are illustrated in Figure 5.31.

A factor which should be taken into account is the traffic passing the headland from the outer fairways, which may meet the traffic coming from the inner fairways in the area around Bukketjuvane. It will be difficult to distinguish the distribution of this traffic from the inland traffic distribution as they will be intermingled. A histogram of passages across the passline A (Figure 5.4) extended 10 km out to sea from the tip

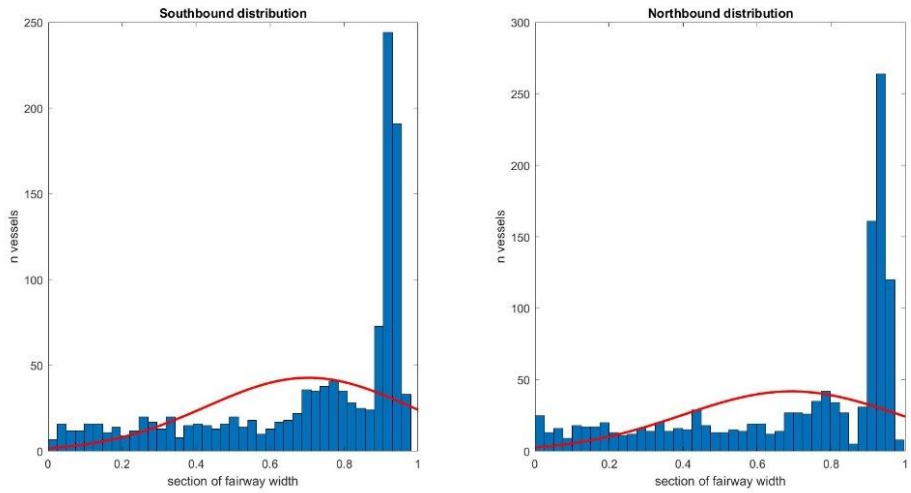

Figure 5.32 Histograms of lateral traffic distribution along passline A

of the headland shows a complex distribution of vessels, as can be seen in Figure 5.32.

After studying density plots, it appears probable that traffic distribution is made up of three independent distributions. The offshore traffic is evenly spread out across the width of the measured section, and closer to shore there are two different peaks which have a normal shape. The leftmost peak might denote inshore traffic that has rounded the rocks on the outside and the rightmost peak may be inshore traffic that has passed to the right or between the rocks. Ideally, each of these distributions should be studied more closely and properly identified, and possible lane merging situations should be investigated. For the purpose of this analysis, it will be assumed that all the inshore traffic will follow the lanes defined in this section, with distributions as defined in section 5.3.2. The offshore traffic will follow a uniform distribution spanning a width of 8 km, parallel to the inshore traffic, and merging situations will not be considered.

After negotiating the rocks off the tip of Stad, the traffic lane widens, and heads inland towards Vanylvsfjorden. The width of this part of the lane is bounded by the rocks at the entrance to the Vanylvsfjorden. At this point the lane merges with the start of the projected fairway towards the tunnel. This part of the lane is comprised of three sections:

From west to east, the sections are 1400m, 1250m and 1200m wide respectively, and correspondingly 4250 m, 3815m and 12185 m long. The sections are illustrated in Figure 5.33

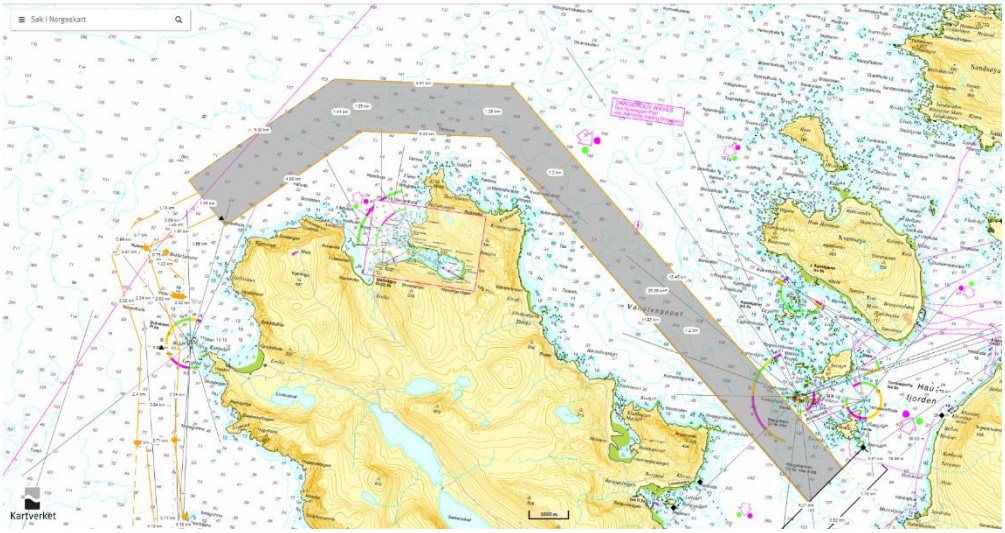

Figure 5.33 Sections 7,8,9, sea route

As can be seen in density plots (Figure 5.26), parts of the traffic diverge from the route and cross more open waters to Herøyfjorden rather than Vanylvsfjorden. This route component has not been considered by the previous risk assessment. For the sake of compatibility to the previous risk assessment, this traffic component will therefore not be analysed. The traffic is instead assumed to follow the main fairway towards Vanylvsfjorden. The section parameters for the modelled fairway round Stad, based on the fairway which incorporates the obstacles Bukketjuvane and Vossaskallen, are illustrated in Figure 5.34 and summed up in Table 5.4

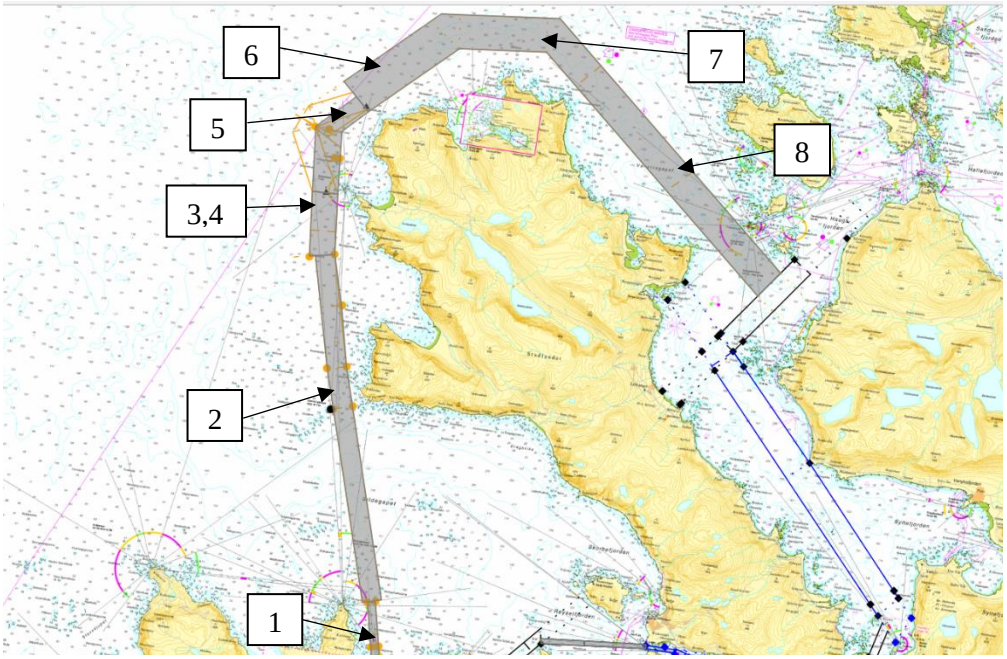

Figure 5.34 Stad sea route sections over obstacles, numbered from west to east

Table 5.4 Lane section parameters for Stad sea route over obstacles

Section	Length [m]	Width [m]	Southbound o_1, o_2 [m]	Northbound o_1, o_2 [m]	Southbound obstacle span after bend	Northbound obstacle span after bend	Obstacle span in lane, X
1	5060	300	790, 600	7260,7090	0,1	0,1	0
2	12950	710	N/A	N/A	0	0	0
3	3850	950	6500,5730	N/A	0,1	0	0.79,0.89
4	1	950	N/A	N/A	0	0	0,0.5
5	1500	950	N/A	N/A	0	0	0
6	4250	1400	N/A	N/A	0	0	0
7	3815	1250	7300,6420	N/A	0,1	0	0
8	12185	1200	2130,1780	N/A	0,1	0	0

The parameters for the lane sections of the second method, based on modelling bends around the obstacles, are summarised in Figure 5.35 and Table 5.5.

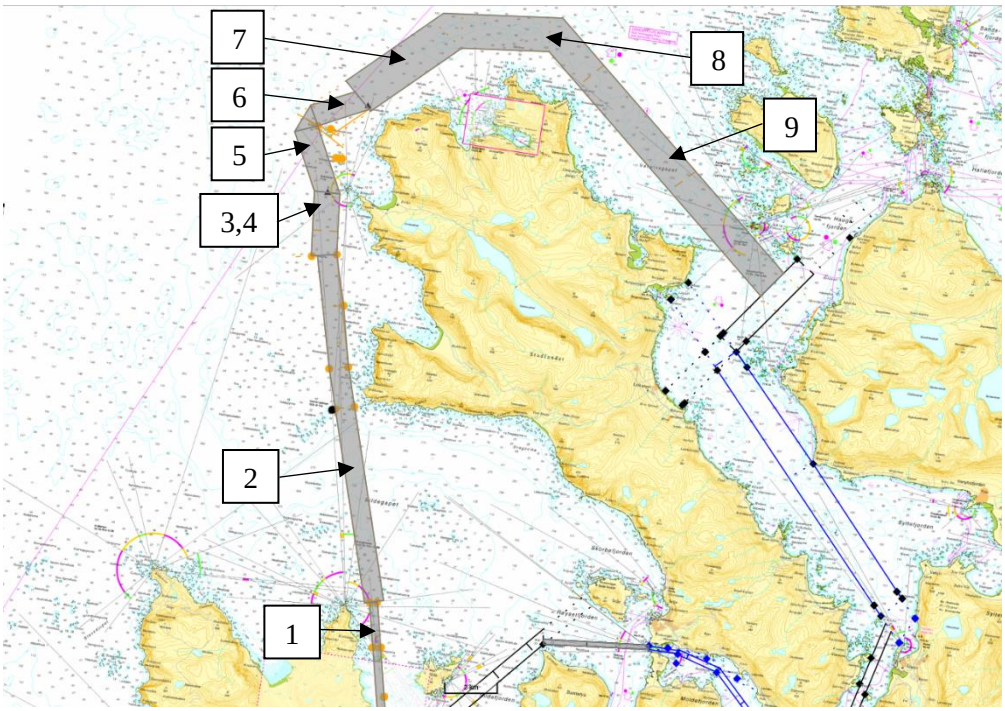

Figure 5.35 Stad sea route sections around obstacles, numbered from west to east

Table 5.5 Lane section parameters for Stad sea route round obstacles

Section	Length [m]	Width [m]	Southbound o_1, o_2 [m]	Northbound o_1, o_2 [m]	Southbound obstacle span after bend	Northbound obstacle span after bend
1	5060	300	790, 600	7260,7090	0,1	0,1
2	12950	710	N/A	N/A	0	0
3	3850	950	6500,5730	1300,1301	0,1	0.79,0.89
4	1	950	N/A	2340,2040	0	0.5,1
5	1500	950	6180,4810	N/A	0	0
6	2300	950	N/A	N/A	0	0
7	4250	1400	2170,1550	N/A	0.5,0.93	0
8	3815	1250	7300,6420	N/A	0,1	0
9	12185	1200	2130,1780	N/A	0,1	0

The method of modelling bends around the obstacles is assumed to be the most accurate option for modelling this part of the Stad sea route, and this method is therefore selected for further analysis. However, the effects of the methods employed to model complex navigational patterns will be discussed in further sections.

5.5 Collision and Grounding Frequencies

5.5.1 Computational Methodology

The methodology for calculating frequencies of collision and grounding is based on the IWRAP method and Pedersen/Simonsen's model as discussed in section 3.1. To

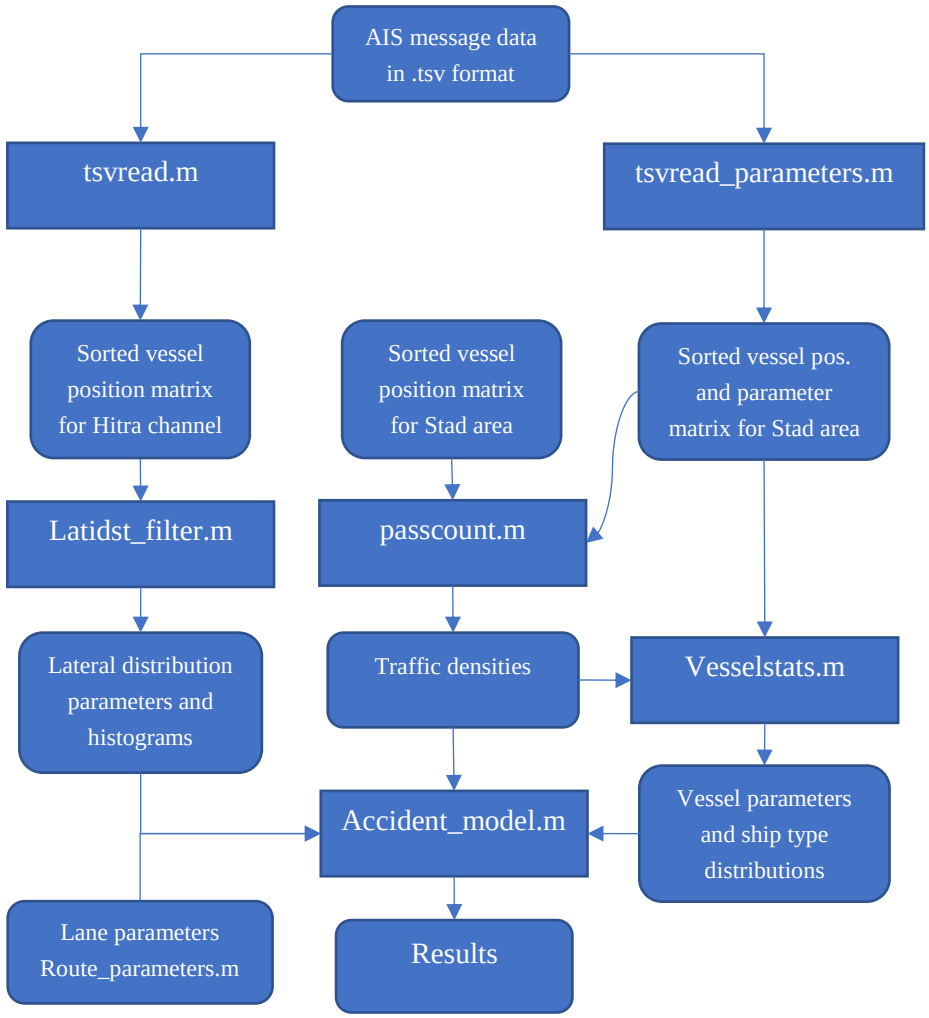

Figure 5.36 Flowchart describing the methodology of the Matlab program developed for this analysis

perform the calculations, a Matlab program is created which takes in traffic density, lateral distribution, and vessel and fairway parameters to calculate the number of accident candidates for each section individually. An overview of the programs used in this analysis, with corresponding inputs and outputs is shown in Figure 5.36. The programs are attached in the appendix. In the following sections, the calculations and assumptions are described in detail.

5.5.2 Collision frequencies

Frequencies are calculated for head-on and overtaking collisions according to the IWRAP methodology described in section 3.1.5. Calculations are carried out for every combination of vessel type encounters, for each lane section.

5.5.3 Grounding frequencies

Grounding frequencies of type I are calculated according to the IWRAP methodology described in section 3.1.5. For type II groundings, the IWRAP method is also used, but a refinement of the model is proposed.

Both Simonsen and IWRAP mention that the number of type II groundings is very sensitive to the mean distance between navigational checks a. To complicate matters, this value is likely to be highly dependent on navigational circumstances. In a test case for a 30m wide navigable channel near Esbjerg in Denmark, with average leg lengths of approximately 600m, Simonsen proposes a value of mean checking distance to be 0.75 ship lengths. For wider channel parts 1 ship length is proposed. At local ship speeds and lengths this corresponds to a mean time between checks at 8 seconds (Simonsen, 1997). This is a large difference to the value used by IWRAP, which is 180 seconds, and this shows that situational circumstances are an important factor in deciding the mean distance between checks.

As the Stad fairways contain many bends and a variety of lane widths and lengths, a flat rate in time between checks or in ship lengths between checks for the entire area will not accurately model individual navigational situations. For the purpose of this analysis, a mean distance between checks which is dependent on *leg length* is proposed. Thus, the mean distance between checks is independent of vessel speed, illustrating that navigators will be more vigilant at higher speeds.

The adapted expression for the number of type II grounding candidates for each section is then:

$$N_{II} = \sum_{i=1}^{n\,class} P_C Q_i * [\frac{1}{2}\exp(\frac{a^2\sigma^2 - 2btL_w}{2tL_w{}^2})\{2\Phi\left(\frac{ztL_w + a\sigma^2}{\sigma tL_w}\right) - 1\}]_{z_{min}}^{z_{max}}$$

Where t is the fraction of section length between navigational checks, and L_w is the section length.

For Simonsen's test case, mean distance between checks are assumed to be 1 ship length of 49.9m for wider sections of the waterway, which are more comparable to the Stad tunnel route lanes than the narrower lanes of only 30m. If leg lengths are approximately 600m long, this corresponds to 12 navigational checks during the leg, and a mean distance between navigational checks is approximately 8.3% of the leg length. For a general model that contains legs longer than 10 NM, it might be appropriate to cap the mean distance between navigational checks to prevent it from becoming unreasonably long, perhaps at the IWRAP value of 180 seconds times vessel speed. There are however no legs longer than this in the current model, and a value of 8.3% of leg length for mean distance between checks is implemented for analysing the waterways near Stad.

5.5.4 Causation probabilities

IWRAPS default causation probabilities are used in this analysis, for both sea and tunnel routes. The values are listed in Table 3.2:

6 Results

6.1 Estimated frequency of accidents

6.1.1 Tunnel Route

For head-on collisions, the total number of head-on collision candidates N_{hoc} is 1635.42. With a causation probability $P_c = 0.5 * 10^{-4}$, the expected annual number of head-on collisions is 0.0818.

For overtaking collisions, the total number of candidates N_{oc} is 34.23. With a causation probability $P_c = 1.1 * 10^{-4}$, the expected annual number of head-on collisions is 0.0038, bringing the total number of expected collisions to 0.0855.

For type I-groundings, or grounding on obstacles in the lane, only section 2 contains an obstacle, and the total number of candidates in both directions is 59.29 per year.

For type II-groundings, i.e. grounding due to striking an obstacle or waterway edges due to failing to turn at a bend, the total number of southbound accident candidates $N_{ii,south}$is 1087.58 vessels per year. Northbound accident candidates $N_{ii,north}$ tally 209.99. The sum of type II and type I groundings in both directions is therefore 1356.9, and with a $P_c = 1.6 * 10^{-4}$, the number of yearly expected groundings is 0.2171. The number of expected accidents is summarised in Table 6.1 and the number accident candidates for each section is displayed in Table 6.2.

Table 6.1 Expected yearly collisions and groundings for the tunnel route

Number of collisions per year	Number of groundings per year
0.0855	0.2171

Table 6.2 Accident candidates in each category for each section of the tunnel route

Section	1	2	3	4	5	6	7	8	9	10	Total
N_{hoc}	69.87	153.74	120.61	120.21	104.54	242.54	166.22	160.08	314.37	183.25	**1635.42**
N_{oc}	2.87	6.31	4.92	0.00	0.00	0.00	0.00	0.00	12.64	7.50	**34.23**
$N_{i,north}$	0.00	12.85	0.00	0.00	0.00	0.00	0.00	0.00	0.00	0.00	**12.85**
$N_{i,south}$	0.00	46.44	0.00	0.00	0.00	0.00	0.00	0.00	0.00	0.00	**46.44**
$N_{ii,north}$	0.00	85.18	0.00	0.00	2.84	103.58	6.23	0.00	0.00	12.17	**209.99**
$N_{ii,south}$	0.44	676.64	0.00	282.25	0.00	0.00	0.00	0.02	0.00	128.24	**1087.59**

6.1.2 Stad Sea Route

The total number of candidates is 814.12, and the number of collisions is thus 0.0407. Overtaking collision candidates are a total of 34.44 and the number of expected overtaking collisions is thus 0.038, giving a total amount of 0.0444 collisions.

There are no in-lane obstacles, but obstacles after bends account for a total of 683.80 grounding candidates due to failing to turn. The vast majority of candidates are found at either end of the route after long straight stretches of fairway. The expected number of groundings is 0.1094 per year. The total number of accidents are summarised in Table 6.3, and accident candidates for each section in Table 6.4.

Table 6.3 Expected yearly collisions and groundings for the sea route

Number of collisions per year	Number of groundings per year
0.0444	0.1094

Table 6.4 Accident candidates in each category for each section of the sea route

Section	1	2	3	4	5	6	7	8	9	Total
N_{hoc}	234.72	254.81	33.84	0.01	36.78	26.92	42.44	42.66	141.94	814.12
N_{oc}	9.57	10.45	1.39	0.00	1.51	1.10	1.74	1.75	5.83	33.35
$N_{il,north}$	0.00	0.00	0.00	0.01	0.00	0.00	0.00	0.00	0.00	**0.01**
$N_{il,south}$	377.28	0.00	0.00	0.00	0.00	0.00	0.00	0.00	306.51	**683.79**

The risk contribution from the approximately 4000 vessels that are considered to be offshore traffic (do not cross passline E), is found to be very low, and is equally present for tunnel and sea routes. It is therefore not included in the result.

6.2 Sensitivity analysis

6.2.1 Lane modelling alternatives

In section 5.4.2, alternative methods to model traffic navigation around a specific set of obstacles off the Stad headland were described. Results from the method of placing the lane over the obstacles will here be compared to the method used in the analysis, in which a bend around the obstacles was modelled. The amount of accident candidates in each section is summarised in Table 6.5

Table 6.5 Accident candidates in each category for each section of the sea route - over obstacles

Section	1	2	3	4	5	6	7	8	Total
N_{hoc}	234.72	254.81	36.78	0.01	22.07	42.29	42.66	141.94	**775.28**
N_{oc}	9.57	10.45	1.51	0.00	0.91	1.74	1.75	5.83	**31.76**
$N_{i,north}$	0.00	0.00	80.02	1149.47	0.00	0.00	0.00	0.00	**1229.49**
$N_{i,south}$	0.00	0.00	10.40	3354.83	0.00	0.00	0.00	0.00	**3365.23**
$N_{ii,north}$	0.00	0.00	0.00	0.00	0.00	0.00	0.00	0.00	**0.00**
$N_{ii,south}$	377.28	0.00	0.00	0.00	0.00	0.00	0.00	306.51	**683.79**

This method yields a significantly larger amount of collision candidates on the rocks off Stad, as can be seen in Table 6.5 for $N_{i,south}$ and $N_{i,north}$ for sections 3 and 4. This is reasonable as such a model would assume that no vessels have planned to navigate around the obstacles, and are dependent on observing the obstacles and making an evasive manoeuvre.

The total number of groundings is 0.8446 per year, which is roughly eight times as high as the method used in analysis, and four times for the estimated amount of groundings in the tunnel route. The values are compared in Table 6.6. If this method was utilised, one would conclude that the route around Stad entails a significantly higher frequency of groundings than the tunnel route, which shows that uncertainty in exact lane placement around these obstacles is an important factor to the accuracy of the model.

Table 6.6 Comparison of accident frequencies for sea route over obstacles vs round obstacles

	Number of collisions per year	Number of groundings per year
Over obstacles	0.0423	0.8446
Round obstacles	0.0444	0.1094

In reality, one might expect most navigators to have planned a bend in one direction or another around the obstacles. However, this might not be the case for every vessel, and perhaps lateral traffic distributions in the area may extend over obstacles to some degree. For future research, an extensive investigation of the lateral

distribution, composition of vessel types, potential weather dependent patterns, and quantity of vessels across the various approaches to round the obstacles is suggested.

6.2.2 Mean distance between positional checks

Simonsen notes that the number of groundings in his model, used in IWRAP and this analysis, is quite sensitive to the mean distance between positional checks a_i (Simonsen, 1997). In this analysis this value is expressed in terms of leg length.

$$a_i = t * L_w, t = 0.083$$

A sensitivity test is carried out for the value of t for the tunnel route and the Stad sea route. Increasing t to 0.10, or by approximately 120%, gives the following results for the tunnel route:

Table 6.7 Type II grounding candidates for t = 0.10, tunnel route

section	1	2	3	4	5	6	7	8	9	10	Total
$N_{ii,north}$	0.00	151.70	0.00	0.00	9.02	178.41	17.72	0.00	0.00	31.78	**388.63**
$N_{ii,south}$	1.93	847.21	0.00	409.97	0.00	0.00	0.00	0.12	0.00	213.70	**1472.94**

The resulting number of groundings is 0.3073 per year, an increase of approximately 142%. For the Stad sea route, the following accident candidates are calculated:

Table 6.8 Type II grounding candidates for t = 0.10, sea route

section	1	2	3	4	5	6	7	8	9	Total
$N_{ii,north}$	0.00	0.00	0.00	0.09	0.00	0.00	0.00	0.00	0.00	**0.09**
$N_{ii,south}$	521.68	0.00	0.00	0.00	0.00	0.00	0.00	0.00	439.08	**960.75**

The amount of groundings per year is 0.1537, which is an approximate increase of 140%.

Decreasing t to 0.05, a decrease of 40% gives the following results for the tunnel route:

Table 6.9Type II grounding candidates for t = 0.05, tunnel route

section	1	2	3	4	5	6	7	8	9	10	Total
$N_{ii,north}$	0.00	9.06	0.00	0.00	0.03	12.55	0.10	0.00	0.00	0.23	**21.98**
$N_{ii,south}$	0.00	282.81	0.00	66.32	0.00	0.00	0.00	0.00	0.00	17.43	**366.56**

The number of groundings per year is 0.0717, which is a decrease of 66%. For the Stad sea route the results are the following:

Table 6.10 Type II grounding candidates for t = 0.05, sea route

section	1	2	3	4	5	6	7	8	9	10	Total
$N_{ii,north}$	0.00	0.00	0.00	0.00	0.00	0.00	0.00	0.00	0.00	0.00	**0.00**
$N_{ii,south}$	107.28	0.00	0.00	0.00	0.00	0.00	0.00	0.00	75.97	183.25	**107.28**

Groundings per year are 0.0293, a 73% reduction. A comparison of the grounding frequencies for different t's is displayed below in Table 6.11.

Table 6.11 Comparison of total groundings for varying t, tunnel and sea route

	Number of groundings sea route	Number of groundings tunnel route
$\boldsymbol{t = 0.083}$	0.1094	0.2171
$\boldsymbol{t = 0.010}$	0.1537	0.3073
$\boldsymbol{t = 0.05}$	0.0293	0.0717

It is clear that the number of type II groundings is sensitive to changes in mean distance between navigational checks, as the number of groundings changes significantly more than the change in mean distance between checks. However, the number of groundings remain higher for the tunnel route than the sea route for both low and high mean distances between checks.

6.2.3 Vessel type distributions and traffic density

In the analysis, only vessels that pass both lines E and A are considered tunnel candidates. However, all vessels that make up the data for the area are narrow enough to fit the tunnel, and therefore all vessels that pass A may nominally be tunnel candidates. If one assumes that all vessels of sufficient beam will prefer the tunnel route, traffic through the tunnel route will increase by 4335 vessels per year, and the number of grounding candidates is then as shown in Table 6.12

Table 6.12 Accident candidates for increased traffic density case

Section	1	2	3	4	5	6	7	8	9	10	Total
N_{hoc}	142.19	312.89	245.45	244.65	212.76	493.61	338.29	325.78	639.79	372.94	**3328.34**
N_{oc}	5.83	12.84	10.01	0.00	0.00	0.00	0.00	0.00	25.72	15.27	**69.67**
$N_{i,north}$	0.00	18.33	0.00	0.00	0.00	0.00	0.00	0.00	0.00	0.00	**18.33**
$N_{i,south}$	0.00	66.25	0.00	0.00	0.00	0.00	0.00	0.00	0.00	0.00	**66.25**
$N_{ii,north}$	0.00	121.51	0.00	0.00	4.06	147.76	8.88	0.00	0.00	17.36	**299.57**
$N_{ii,south}$	0.63	965.29	0.00	402.66	0.00	0.00	0.00	0.02	0.00	182.94	**1551.54**

The number of collisions per year is then 0.1741, and the number of groundings per year is 0.3097.

There is also some uncertainty related to the distribution of vessel types that pass Stad, as data for this distribution has only been collected for one month. Additionally, there is the possibility that traffic will increase due to new opportunities presented by the tunnel. If, for instance, a regular high-speed passenger service from Bergen to Ålesund with departures twice a day is established, this will significantly increase the proportion of high-speed craft (HSC). Assuming the monthly proportion of HSCs increase by 120 (departures twice a day) yields the following results:

Table 6.13 Accident candidates for increased HSC proportion case

Section	1	2	3	4	5	6	7	8	9	10	Total
N_{hoc}	60.81	133.81	104.99	115.24	100.28	232.65	159.45	153.70	273.82	159.50	**1494.25**
N_{oc}	5.58	12.28	9.58	0.00	0.00	0.00	0.00	0.00	24.69	14.61	**66.74**
$N_{i,north}$	0.00	12.85	0.00	0.00	0.00	0.00	0.00	0.00	0.00	0.00	**12.85**
$N_{i,south}$	0.00	46.44	0.00	0.00	0.00	0.00	0.00	0.00	0.00	0.00	**46.44**
$N_{ii,north}$	0.00	85.18	0.00	0.00	2.84	103.58	6.23	0.00	0.00	12.17	**209.99**
$N_{ii,south}$	0.44	676.64	0.00	282.25	0.00	0.00	0.00	0.02	0.00	128.24	**1087.59**

The number of collisions per year is 0.0821, and the number of groundings per year is unchanged at 0.2171. The respective accident frequencies for the normal case Q_{AE}, increased trafficQ_A, and increased proportions of HSC traffic Q_{HSC} are compared below in Table 6.14

Table 6.14 Accident frequencies comparison for different traffic densities and compositions

	Collisions per year	Number of groundings per year
$\boldsymbol{Q_{AE} = 10167}$	0.0855	0.2171
$\boldsymbol{Q_{A} = 14497}$	0.1691	0.3097
$\boldsymbol{Q_{HSC} = 11076}$	0.0979	0.2479

The comparison show that increased traffic density has a large effect on accident frequencies in the tunnel route, especially for collision frequencies. Collisions double in frequency, and groundings increase by approximately 40%, for an increase of approximately 40% in traffic.

Accident frequencies are also somewhat sensitive to traffic compositions. Increasing the proportion of HSC from approximately 2% of total traffic to approximately 20% increases the collision and grounding frequency by approximately 14%.

The vessel type composition is also an important factor in quantifying accident consequences. Accidents in which passenger vessels are involved often entail a higher risk of fatalities (Det Norske Veritas, 2010), and therefore it will be important to investigate future changes in vessel type composition in order to establish a proper risk picture of the Stad tunnel waterway.

6.2.4 Traffic distribution

The standard deviations of the lateral traffic distributions are varied from approximately 0.10 to 0.15 and 0.05, which has a negligible effect on results. As all the traffic distributions which have been observed in this thesis have had standard deviations between 0.09 and 0.11 it is concluded that the model is not particularly sensitive to distribution parameters.

6.3 Discussion

6.3.1 Risk in tunnel route versus sea route

The results show an increase of 0.0411 yearly collisions and an increase of 0.1077 yearly groundings for the tunnel route compared to the sea route, approximately doubling both figures. From a purely geometrical point of view this is reasonable, as the Stad sea route is less constrained by obstacles or shorelines, reducing the risk of running into waterway edges and allowing vessels to spread further apart.

However, as has been mentioned earlier in the thesis, the Stad sea is notoriously challenging to navigate, due to severe weather conditions. Therefore, one might expect a higher accident frequency off Stad than the frequency found in this analysis, which is approximately half of the accident frequency for the tunnel route.

It should be noted that a lower accident frequency on the Stad sea route does not necessarily mean that the route carries lower risk. As mentioned earlier in the report, risk of an event can be perceived as the product of frequency and consequences. The consequences of an accident off Stad may in many cases be more severe than a corresponding accident in the tunnel fairways. Several factors contribute to this: the severe weather and wave conditions, and the geology and ruggedness of the ironbound coast of the headland. Severe weather conditions would exacerbate the danger for any accident and prevent efficient rescue or salvage, and striking the coast or rocks near the Stad headland might cause more structural damage to vessels than the inshore waterway edges.

Additionally, there are several known foundering incidents off Stad, in which vessels are lost solely due to weather conditions. In these situations, fatalities, and therefore consequences, are often high (Det Norske Veritas, 2010). Such accidents have not been included in this analysis and are therefore not included in the risk picture provided by the accident frequencies shown above.

A natural way to evaluate the risk picture provided by the accident frequencies is to compare them to accident frequencies found in the accident-statistics based approach of the previous risk assessment made by DNV.

6.3.2 DNV comparison

The results for the number of collisions and groundings in the tunnel route are quite comparable to the results obtained in the previous risk assessment by DNV. With the

traffic prognosis for 2025, DNV finds that there would be 0.07 collisions and 0.19 groundings in the tunnel route per year. The corresponding values of 0.09 and 0.21 found in this analysis are slightly higher, but this can be attributed to the increased traffic density found in this analysis: 28 vessels per day as opposed to the predicted 25.

For the sea route, the results differ. DNV found 0.05 collisions and 0.22 groundings per year for 2025. In this analysis, the results were 0.04 collisions per year, and only 0.11 groundings. As the results for the tunnel route were much more compatible, this might indicate that the developed method does not accurately model conditions in the Stad sea. There are several possible reasons for this. As discussed above, weather conditions may affect navigational ability. Therefore, it might be necessary for the causation factor P_c to be increased for the sea route compared to the tunnel route.

6.3.3 Uncertainty issues and simplifications

The largest cause of uncertainty uncovered in the sensitivity analysis is the lane modelling off Stad, where traffic patterns are complicated and dependant on unknown factors. Assuming that the traffic lane is continuous over the obstacles leads to a very high number of accidents, while assuming the lane bends around the obstacles leads to practically none. An accurate approximation might be found somewhere between these approaches.

It has been mentioned that vessels that approach Stad from pass line B defined in the DNV analysis (Figure 2.3) are assumed to be tunnel candidates. However, this stretch of water is not defined as a part of either the sea route or tunnel route in the DNV analysis and consequently it is assumed that vessels from this traffic component follow the defined route past Haugsholmen. Identifying the route this traffic component would take to enter the tunnel approaches is suggested to increase the accuracy of the model.

6.3.4 Risk acceptance criteria for tunnel route

As a significantly lower frequency of accidents than calculated in the DNV analysis has been found for the Stad sea route, it should be discussed whether the results found in this analysis might affect the decision to build a tunnel.

Figure 6.1 displays the expected number of fatalities per year for different tunnel alternatives from the DNV analysis, divided into 4 accident categories. It is clear that fatalities from foundering accidents massively outweigh the number of fatalities from other accident types, and that the risk of fatalities from foundering is non-existent for the wide tunnel alternative.

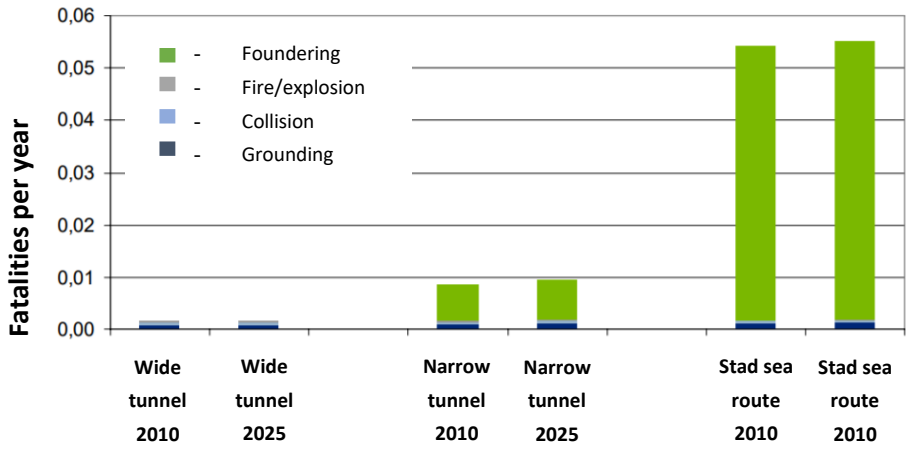

Figure 6.1Expected fatalities per year for various tunnel alternatives. Adapted from (Det Norske Veritas, 2010).

Therefore, calculating half as many collisions and groundings off Stad as expected is unlikely to greatly affect the risk perspective with regard to human lives. However, it might affect the extent to which safety measures are implemented in the tunnel route.

6.3.5 Model potential and flexibility

It has been seen that the model has found reasonable values for accident frequencies in the Stad tunnel fairways. It has also been shown that the model is flexible in regard to parameters such as lane positioning, lateral traffic distribution and density, vessel types composition and speed restrictions. Therefore, the potential for increasing the accuracy of the model is large.

An additional advantage of the developed model is that the most dangerous elements can be identified and analysed. For a historical-accident-statistics-based model such as the analysis carried out by the DNV, it is not possible, for example, to examine exactly how many vessels are expected to ground on a particular shoal. Having the

ability to pinpoint each contribution to risk is a great benefit in establishing the risk picture of both the Stad sea and tunnel route.

7 Conclusions

A geometric accident model has been developed to estimate the number of accident frequencies on the Stad sea route and the Stad tunnel route. The frequency of accidents on the sea route are found to be significantly lower than in the tunnel route. The values are compared to values estimated in a previous risk assessment carried out by DNV. The accident frequencies for the tunnel route are comparable, while the sea route accident frequencies are, again, significantly lower.

It is concluded that while the model appears to be suitable for calculating accident frequencies in enclosed waters, further research into the effect of local weather conditions on navigational abilities, and on the traffic pattern around obstacles off Stad will improve the accuracy of the values calculated for the Stad sea route.

In regard to the choice of methodology for this analysis, it is found that a geometrical model has both advantages and disadvantages compared to an analysis based on historical accident data. The main advantages are detailed overviews over specific contributions to risk, and the ability to model local geographical features in great detail which contributes to greater accuracy. However, this also means that a lot of detail is required to reach a satisfactory level of accuracy. For the Stad sea route, it is found that this level of accuracy has not been reached for this iteration, but further research is suggested to remedy this.

8 Further research

In this chapter suggestions for further research and development of the model are summarised:

- Possible causation probabilities for the Stad sea should be investigated. This can be done analytically, for example with a Bayesian network that takes meteorological effects into account, or by calibrating accident statistics off Stad to the amount of accident candidates found in this analysis.
- Effects of weather on traffic patterns between the obstacles off Stad should be investigated. Other factors that may influence the choice of route around the obstacles should be identified to model traffic behaviour around these obstacles.
- The accuracy of the model of the sea route can be increased by extending it to include tributary routes, such as the different routes past the obstacles off Stad or the various approaches towards Stad. Examining and identifying individual traffic distributions and possible merging patterns might also reveal merging situations that should be analysed.
- Drift models: If an accurate model of currents and wind can be established for the Stad sea, the risk of drifting ashore due to engine blackouts can also be considered, further increasing the accuracy of the mode.

References

Andreassen, T., 2017. *Rapport Stad skipstunnel* [Interview] (29 May 2017).

Andreassen, T., 2018. *Speed limits Stad ship tunnel* [Interview] (9 January 2018).

Åsheim, H., 2017. *Access to historical AIS data* [Interview] (9 September 2017).

Askheim, S., 2017. *Stad.* [Online]
Available at: https://snl.no/Stad
[Accessed 28 December 2017].

Asplan Viak, 2017. *Stad Skipstunnel-regulering.* [Online]
Available at:
http://asplanviak.maps.arcgis.com/apps/MapTools/index.html?appid=5d3bdecb39b14605adec5ede53a6ec6f
[Accessed 10 11 2017].

BE-AWARE, 2014. *Final Report of the BE-AWARE 1 project.* [Online]
Available at: http://www.bonnagreement.org/be-aware/i/final-report
[Accessed 12 April 2017].

Det Norske Veritas, 2010. *Analyse av AIS data og beregning av ventetid, Rapportnr 2010-1858,* Oslo: DNV.

Det Norske Veritas, 2010. *Risikoanalyse av Stad skipstunnel for to tunnellalternativer, Rapportnr 2010-1866,* Oslo: DNV.

Friis-Hansen, P., 2008. *IWRAP Mk II, Basic Modelling Principles for Prediction of Collision and Grounding Frequencies,* Lyngby: Technical University of Denmark.

IWRAP, 2014. *IWRAP - Theory.* [Online]
Available at: http://www.iala-aism.org/wiki/iwrap/index.php/Theory
[Accessed 22 December 2017].

Kristiansen, S., 2005. Traffic based models. In: *Maritime transportation: Safety Management and Risk Analysis.* Oxford: Elsevier Butterworth-Heinemann, p. Chapter 6.

Kystverket, 2015. *Stad Skipstunnel Brochure,* Ålesund: Kystverket.

Kystverket, 2016. *Track Server User Guide.* [Online]
Available at:
http://aisstat.kystverket.no/statistikk/auth/Track_Server_User_Guide.html#MapPage
[Accessed 10 December 2017].

Kystverket, 2017. *Stad Skipstunnel.* [Online]
Available at: http://www.kystverket.no/Maritim-infrastruktur/Utbygging-av-fiskerihavner-og-farleder/Stad_skipstunnel/
[Accessed 15 December 2017].

Kystverket, n.d. *Track Server.* [Online]
Available at: http://aisstat.kystverket.no/statistikk/#/login
[Accessed 28 November 2017].

Ladan, M. & Hänninen, M., 2012. *Data Sources for Quantitative Marine Traffic Accident Modelling,* Helsinki: Aalto University.

Mazaheri, A., 2009. *Probabilstic modeling of ship grounding - A review of the literature,* Espoo: Helsinki University of Technology, Department of Applied Mechanics.

Norwegian Ministry of Transportation, 2017. *Stad Skipstunnel blir en realitet.* [Online]
Available at: https://www.regjeringen.no/no/aktuelt/stad-skipstunnel-blir-ein-realitet/id2548488/
[Accessed 15 December 2017].

Pedersen, P. T., 2010. *Review and application of ship collision and grounding analysis procedures,* Lyngby: Technical University of Denmark.

Rausand, M., 2011. *Risk Assessment: Theory, methods and applications.* Trondheim: John Wiley & Sons, Inc..

Silveira, P., Teixeira, A. & Soares, C. G., 2013. *Use of AIS Data to Characterise Marine Traffic Patterns and Ship Collision Risk off the Coast of Portugal,* Lisbon: Technical University of Lisbon.

Simonsen, B. C., 1997. Estimation of Grounding Frequency. In: *Mechanics of ship grounding.* Kongens Lyngby: Technical University of Denmark, Department of Naval Architecture and Offshore Engineering, pp. 9-15.

University of Minnesota, 2001. *Carta Marina.* [Online]
Available at: https://www.lib.umn.edu/apps/bell/map/OLAUS/SEC/esect.html
[Accessed 26 December 2017].

Xiao, F., Ligteringen, H., Gulijk, C. v. & Ale, B., 2015. Comparison study on AIS data of ship traffic behavior. *Ocean Engineering,* Volume 95, pp. 84-93.

Appendix A: accident_model.m

```
% Calculates number of accidents for head-on and overtaking
collisions,
% type I and II groundings.

clear all
%-----------------------------------------------------------------
------
% Parameters
% route 1: Stad tunnel route
% route 2: Stad route - over obstacles
% route 3: Stad route - around obstacles
route = 1;
t = 0.083; % Fraction of leg distance between nav checks
[Bw,Lw,X,o1s,o2s,o1n,o2n,zn,zs] = route_parameters(route);
n_sections = length(Bw);

% Lateral distribution parameters:
load('Hitra_pos'); %Hitra channel area data Nov2016-Nov2017
[muS,muN,sigmaS,sigmaN] = latdist_filter(pos, ia);

% Traffic density data
load('Stad_pos') % Stad area traffic data, Oct2016-Oct2017
[A1,AE1,ki1,kae1] = passline_count(pos,ia);
Q = (AE1)/2; % n vessels each way [1/yr]
q = Q/(365*24*3600); %[1/s]

load('Stad_pos_dim') %Data for Stad area March2017 with Vessel
parameters
[A,AE,ki,kae] = passline_count(pos,ia);
[Vstats,Stats,vType] = vesselstats(vType,pos,ki,ia,kae);

%Vessel group parameters
n_groups = length(Stats); % Number of vessel types
f = Stats(:,1)/sum(Stats(:,1)); % Group fraction of traffic
Qi = f*Q; % Amount of vessels in group [1/yr]
qi = f*q; % [1/s]
v_g = zeros(n_groups,n_sections);
for i = 1:n_sections
    v_g(:,i) = Stats(:,5); %[knts]
end

if route == 1
    v_g(:,4:8) = 8; %Speed restriction in sections 4-8, 8 [knts]
end
```

```
v_g = v_g*0.5144;%[m/s]
b_g = Stats(:,2); %Avg beam [m]

sigmaSN = sqrt(sigmaN^2+sigmaS^2); %Standard deviation of both
distrib.
sigmaSN = Bw.*sigmaSN; %[m]
muSN = (muN-muS)*Bw; %[m]

%-------------------------------------------------------------------
------
%IWRAP method for calculating head-on collisions

Nghoc=zeros(n_groups,n_groups);

for k = 1:n_sections
    for i = 1:n_groups
        for j=1:n_groups
            Pgoc(i,j) = normcdf(((b_g(i)+b_g(j))/2-
muSN(k))/sigmaSN(k))...
                -normcdf((-((b_g(i)+b_g(j))/2+muSN(k)))/sigmaSN(k));
            Nghoc(i,j) = (Pgoc(i,j)*...
                (v_g(i,k)+v_g(j,k))/(v_g(i,k)*v_g(j,k))*qi(i)*qi(j));
        end
    end

    Nghoc = Nghoc*Lw(k); % Acc. candidates per vessel type and
section
    Nghoc = Nghoc*(365*24*3600);  %[1/yr]
    tNghoc(k) = sum(sum((Nghoc))); % Number of acc. candidates per
section
end

ttNghoc = sum(tNghoc); % Total number of accident candidates

%-------------------------------------------------------------------
------
% Overtaking collisions

for k = 1:n_sections
    for i = 1:n_groups
        for j=1:n_groups
            if v_g(i,k)>v_g(j,k)
            Pgoc(i,j)=normcdf(((b_g(i)+b_g(j))/2)/sigmaSN(k))...
                -normcdf((-((b_g(i)+b_g(j))/2))/sigmaSN(k));
            Ngoc(i,j)=(Pgoc(i,j)*...
```

```
                (v_g(i,k)-v_g(j,k))/(v_g(i,k)*v_g(j,k))*qi(i)*qi(j));
            else
                Pgoc(i,j)=0;
                Ngoc(i,j)=0;
            end
        end
    end
    Ngoc = Ngoc*Lw(k); % Acc. candidates per vessel type and section
    Ngoc = Ngoc*(365*24*3600); % [1/yr]
    tNgoc(k) = sum(sum((Ngoc))); % Number of acc. candidates per
section
end

ttNgoc = sum(tNgoc); % Total number of accident candidates

%--------------------------------------------------------------------
------
% Total number of collision accidents

PcHoc = 0.5*10^-4;
PcOc = 1.1*10^-4;
Nahoc = PcHoc*(ttNghoc);
Naoc = PcOc*(ttNgoc);
Nacol = Naoc+Nahoc;
disp('Collisions per yr =');
disp(Nacol);
%--------------------------------------------------------------------
------
% IWRAP type I grounding probabilty (hit obstacles in lane)

sigmaS = Bw*sigmaS;
sigmaN = Bw*sigmaN;
muS = Bw.*muS;
muN = Bw.*muN;

for i =1:n_sections
    X(i,:) = X(i,:)*Bw(i);
    Pg1s(i) = normcdf((X(i,2)-muS(i))/sigmaS(i))...
        -normcdf((X(i,1)-muS(i))/sigmaS(i));
    Ng1s(i) = Q*Pg1s(i);
    Pg1n(i) = normcdf((X(i,2)-muN(i))/sigmaN(i))...
        -normcdf((X(i,1)-muN(i))/sigmaN(i));
    Ng1n(i) = Q*Pg1n(i);
end

tNg1s = sum(Ng1s);
```

```
tNg1n = sum(Ng1n);
Ng1 = tNg1n+tNg1s;
%-------------------------------------------------------------------
------
%IWRAP type II grounding probability (failure to change course at
bend)

ai = t*Lw; % Mean distance between navigational checks

if route == 1 % Correction for "double" sections
    ai(4) = t*Lw(4)+t*Lw(3);
    ai(3) = t*Lw(4)+t*Lw(3);
else
    ai(3)=t*Lw(3)+t*Lw(4);
    ai(4)=t*Lw(3)+t*Lw(4);
end

% Obstacle function - describes obstacle orientation to lane
for i = 1:n_sections
    o2s(i,1) = o2s(i,1)*Bw(i);
    v(i,:) = [(o2s(i,2)-o1s(i,2)),(o2s(i,1)-o1s(i,1))];
    a(i) = v(i,1)/v(i,2);
    b(i) = -a(i)*(o1s(i,1))+o1s(i,2);
end

Ng2s = zeros(n_groups,n_sections);

for i = 1:n_sections
    zs(i,:) = zs(i,:)*Bw(i);
    for j = 1:n_groups
        p1(j,i) = (2*normcdf((zs(i,1)*ai(i)+a(i)^2*sigmaS(i)^2)/...
            (sigmaS(i)*ai(i)))-1);
        p2(j,i) = (2*normcdf((zs(i,2)*ai(i)+a(i)^2*sigmaS(i)^2)/...
            (sigmaS(i)*ai(i)))-1);
        Ng2s(j,i) = (0.5*exp((a(i)^2*sigmaS(i)^2-2*b(i)*ai(i))/...
            (2*ai(i)^2)))...
        *(p2(j,i)-p1(j,i));
        Ng2s(j,i) = Ng2s(j,i)*Qi(j);
    end
end

tNg2s = sum(Ng2s);
ttNg2s = sum(tNg2s);

for i = 1:n_sections
    o2n(i,1) = o2n(i,1)*Bw(i);
```

```
    v(i,:) = [(o2n(i,2)-o1n(i,2)),(o2n(i,1)-o1n(i,1))];
    a(i) = v(i,1)/v(i,2);
    b(i) = -a(i)*(o1n(i,1))+o1n(i,2);
end


for i = 1:n_sections
    zn(i,:) = zn(i,:)*Bw(i);
    for j = 1:n_groups
        p1(j,i) = (2*normcdf((zn(i,1)*ai(i)+a(i)^2*sigmaN(i)^2)/...
            (sigmaN(i)*ai(i)))-1);
        p2(j,i) = (2*normcdf((zn(i,2)*ai(i)+a(i)^2*sigmaN(i)^2)/...
            (sigmaN(i)*ai(i)))-1);
        Ng2n(j,i) = (0.5*exp((a(i)^2*sigmaN(i)^2-2*b(i)*ai(i))/...
            (2*ai(i)^2)))...
        *(p2(j,i)-p1(j,i));
        Ng2n(j,i) = Ng2n(j,i)*Qi(j);
    end
end

tNg2n = sum(Ng2n);
ttNg2n = sum(tNg2n);
Ng2 = ttNg2n+ttNg2s;

%-------------------------------------------------------------------
------
% Total number of grounding accidents
Pcg = 1.6*10^-4;
Naground = (Ng2+Ng1)*Pcg;
disp('groundings per yr =');
disp(Naground);

% Accident candidate matrix
Nmat = [tNghoc;tNgoc;Ng1n;Ng1s;tNg2n;tNg2s];
for i = 1:length(Nmat(:,1))
    Nmat(i,n_sections+1) = sum(Nmat(i,:));
end

xlswrite('Results.xls',Nmat);
```

```
Collisions per yr =

    0.0855
```

```
groundings per yr =

    0.2171
```

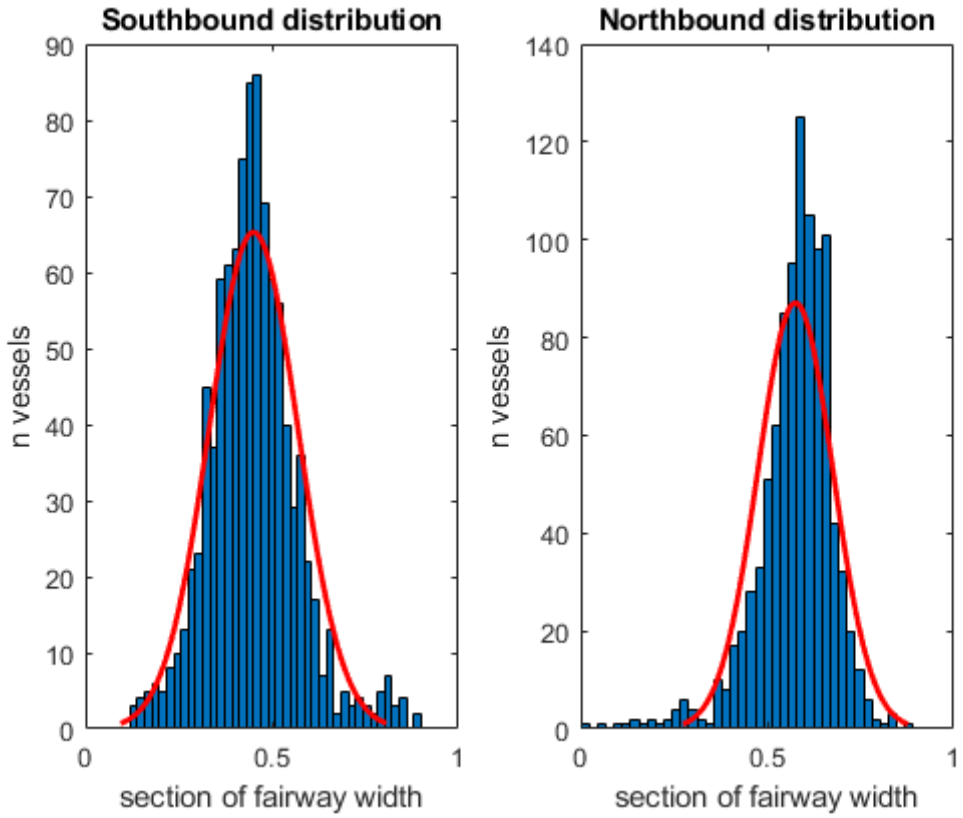

Published with MATLAB® R2017b

Appendix B: route_parameters.m

```
function [Bw,Lw,X,o1s,o2s,o1n,o2n,zn,zs] = route_parameters(route)
% ROUTE_PARAMETERS calculates fairway parameters for a given route
%
% Inputs:
%   route:  integer defining one of three routes
%
% Outputs:
%   Bw:     Section widths [m]
%   Lw:     Length of sections [m]
%   X:      Obstacle span in lane
%   o1s:    Southbound bend obstacle start coordinate
%   o2s:    Southbound bend obstacle end coordinate
%   o1n:    Northbound bend obstacle start coordinate
%   o2n:    Northbound bend obstacle end coordinate
%   zn:     Northbound bend obstacle transverse span
%   zs:     Southbound bend obstacle transverse span

if route == 1 % Tunnel
    Bw = [800,1000,300,300,180,180,180,130,170,450];
    Lw = [4000,11000,2600,1900,1000,2320,1590,1120,3880,5910];
    X = [0 0;0.397 0.4;0 0;0 0;0 0;0 0;0 0;0 0;0 0;0 0];
    o1s = [0 2870;0 1200;0 0;0 800;0 0;0 0;0 1650;0 1100;0 1600;0
1320];
    o2s = [1 2710;1 900 ;1 0;1 540;1 0;1 0;1 650 ;1 960 ;1 70  ;1 520
];
    zs = [0 1;0,1;0,0;0 1;0 0;0 0;0 1;0 1;0 1;0 1];
    o1n = [0 0;0 3100;0 3670;0 0;0 560;0 610;0 690;0 0;0 0;0 2040];
    o2n = [1 0;1 3100;1 1080;1 0;1 460;1 490;1 260 ;1 0;1 0;1 520];
    zn = [0 0;0 1;0 1;0 0;0 1;0 1;0 1;0 0;0 0; 0 1];

elseif route == 2 % Stad 1 over obstacles
    Bw = [300,710,950,950,950,1400,1250,1200 ];
    Lw = [5060,12950,2500,1,1500,4235,3815,12185];
    X = [0 0;0,0;0.79 0.89;0 0.5;0 0;0 0;0 0;0 0];
    o1s = [0 790;0 0;0 6500;0 0;0 0;0 0;0 7300;0 2130];
    o2s = [1 600;1 0;1 5730;1 0;1 0;1 0;1 6420;1 1780];
    zs = [0 1;0,0;0 1;0 0;0 0;0 0;0 1;0 1];
    o1n = [0 7260;0 0;0 0;0 0;0 0;0 0;0 0;0 0;0 0;];
    o2n = [1 7090;1 0;1 0;1 0;1 0;1 0;1 0;1 0];
    zn = [0 1;0 0;0 0;0 0;0 0;0 0;0 0;0 0;0 0;];

elseif route == 3 % Stad 2 bend before obstacles
```

```
    Bw = [300, 710, 950,950, 950, 950,1400,1250, 1200];
    Lw = [5060, 12950, 2300, 1, 2500, 1830, 4250, 3815, 12185];
    X = [0 0;0,0;0 0;0 0;0 0;0 0;0 0;0 0;0 0];
    o1s = [0 790;0 0;0 6500;0 0;0 6180;0 0;0 2170;0 7300;0 2130];
    o2s = [1 600;1 0;1 5730;1 0;1 4810;1 0;1 1550;1 6420;1 1780];
    zs = [0 1;0 0;0 1;0 0;0 0;0 0;0.5 .93;0 1;0 1];
    o1n =[0 0;0 0;0 1300;0 2340;0 0;0 0;0 0;0 0;0 0];
    o2n =[1 0;1 0;1 1301;1 2040;1 0;1 0;1 0;1 0;1 0];
    zn = [0 0;0 0;0.79 0.89;0 0.5 ;0 0;0 0;0 0;0 0;0 0];
end
```

Appendix C: latdist_filter.m

```
function [muS,muN,sigmaS,sigmaN] = latdist_filter(pos,ia)
% LATDIST_FILTER finds lateral distributions across defined cross-
sections
% and creates distribution histograms per vessel
%
% Inputs:
%   pos: Vessel position matrix
%   ia:  vessel indexes in position matrix
%
% Outputs:
%   muS:    Southbound mean position mu
%   muN:    Northbound mean position mu
%   sigmaS: Southbound standard deviation sigma
%   sigmaN: Northbound standard deviation sigma
%

ID = pos(:,1);  % Vessel ID
long = pos(:,2);% Longitude
lat = pos(:,3); % Latitude
n_v = length(ia); % n vessels
n_m = length(pos); % n messages

% Trondheimsleia, Hitra
% Snekkflua-Eiteraå
H1 = [8.7247,63.4524];
H2 = [8.7535,63.4246];

% Cross section line function
v = [(H2(2)-H1(2)),(H2(1)-H1(1))];
a = v(1)/v(2);
c = -a*(H1(1))+H1(2);


% Southbound vessels lateral distributions----------------------------
-------
for i = 1:n_v-1
    for j = ia(i):ia(i+1)-1
        if
ID(j)==ID(j+1)&&lat(j)>a*long(j)+c&&lat(j+1)<=a*long(j+1)+c&&...
                long(j+1)>=H1(1)&&long(j+1)<=H2(1)
            V1(i,:) = [long(j),lat(j)];
            V2(i,:) = [long(j+1),lat(j+1)];
            vV(i,:) = [(V2(i,2)-V1(i,2)),(V2(i,1)-V1(i,1))];
            b(i) = vV(i,1)/vV(i,2);
```

```
            d(i) = -b(i)*(V1(i,1))+V1(i,2);
            S(i,:)= [(d(i)-c)/(a-b(i)),(a*d(i)-b(i)*c)/(a-b(i))];
        end
    end
end

% Separate loop for last vessel
for j = ia(n_v):length(pos)-1
    if
ID(j)==ID(j+1)&&lat(j)>a*long(j)+c&&lat(j+1)<=a*long(j+1)+c&&...
            long(j+1)>=H1(1)&&long(j+1)<=H2(1)
        V1(n_v,:) = [long(j),lat(j)];
        V2(n_v,:) = [long(j+1),lat(j+1)];
        vV(n_v,:) = [(V2(n_v,2)-V1(n_v,2)),(V2(n_v,1)-V1(n_v,1))];
        b(n_v) = vV(n_v,1)/vV(n_v,2);
        d(n_v)=-b(n_v)*(V1(n_v,1))+V1(n_v,2);
        S(n_v,:)= [(d(n_v)-c)/(a-b(n_v)),(a*d(n_v)-b(n_v)*c)/(a-
b(n_v))];
    end
end


s1 = nonzeros(S(:,1));
s2 = nonzeros(S(:,2));
S1(:,1) = s1;
S1(:,2) = s2;

% Intersect distances from start point of histogram line.
% Start point is lowest longitude
VS = [S1(:,2)-H1(2),S1(:,1)-H1(1)];
VSabs = sqrt((VS(:,1)).^2+(VS(:,2).^2));
v_abs = sqrt((v(1)).^2+(v(2)).^2);
SRatio = VSabs/v_abs;

B = SRatio>1;
b = find(B);
SRatio(b) = [];


% Northbound vessels lateral distributions----------------------------
------
for i = 1:n_v-1
    for j = ia(i)+1:ia(i+1)-1
        if ID(j)==ID(j+1)&&lat(j-1)<a*long(j-
1)+c&&lat(j)>=a*long(j)+c&&...
                long(j)>=H1(1)&&long(j)<=H2(1)
```

```
            V1(i,:) = [long(j-1),lat(j-1)];
            V2(i,:) = [long(j),lat(j)];
            vV(i,:) = [(V2(i,2)-V1(i,2)),(V2(i,1)-V1(i,1))];
            b(i) = vV(i,1)/vV(i,2);
            d(i)=-b(i)*(V1(i,1))+V1(i,2);
            N(i,:)= [(d(i)-c)/(a-b(i)),(a*d(i)-b(i)*c)/(a-b(i))];
        end
    end
end

% Separate loop for last vessel
for j = ia(n_v)+1:length(pos)-1
    if ID(j)==ID(j+1)&&lat(j-1)>a*long(j-1)+c && lat(j)<=a*long(j)+c
&&...
            long(j)>=H1(1) && long(j)<=H2(1)
        V1(n_v,:) = [long(j-1),lat(j-1)];
        V2(n_v,:) = [long(j),lat(j)];
        vV(n_v,:) = [(V2(n_v,2)-V1(n_v,2)),(V2(n_v,1)-V1(n_v,1))];
        b(n_v) = vV(n_v,1)/vV(n_v,2);
        d(n_v) = -b(n_v)*(V1(n_v,1))+V1(n_v,2);
        N(n_v,:) = [(d(n_v)-c)/(a-b(n_v)),(a*d(n_v)-b(n_v)*c)/(a-
b(n_v))];
    end
end

n1 = nonzeros(N(:,1));
n2 = nonzeros(N(:,2));
N1(:,1) = n1;
N1(:,2) = n2;

% Intersect distances from start point of histogram line. Start point
is
% lowest longitude

VN = [N1(:,2)-H1(2),N1(:,1)-H1(1)];
VN_abs = sqrt((VN(:,1)).^2+(VN(:,2).^2));
v_abs = sqrt((v(1)).^2+(v(2)).^2);
NRatio = VN_abs/v_abs;

B = NRatio>1;
b = find(B);
NRatio(b) = [];

%-------------------------------------------------------------------
------
% Plot histograms of lateral distribution
```

```
pdN = fitdist(NRatio,'normal');
pdS = fitdist(SRatio,'normal');
muN = pdN.mu;
muS = pdS.mu;
sigmaN = pdN.sigma;
sigmaS = pdS.sigma;

figure(1)
subplot(1,2,1), histfit(SRatio,40,'normal');
xlim([0 1])
ylabel('n vessels')
xlabel('section of fairway width')
title('Southbound distribution')
subplot(1,2,2),histfit(NRatio,40,'normal')
xlim([0 1])
ylabel('n vessels')
xlabel('section of fairway width')
title('Northbound distribution')

end
```

Appendix D: passline_count.m

```
function [A,AE,ki,kae] = passline_count(pos,ia)
% PASSLINE_COUNT counts passages across passlines
%
% Inputs:
%   pos: Vessel position matrix
%   ia: vessel indexes in position matrix
%
% Outputs:
%   A:  Sum of passages across the passline A
%   AE: Sum of passages across both passlines A and E
%   ki: relevant vessel index in position matrix
%   kae: passline matrix

%Passline coordinates
A1 = [4.50000,62.39167];
A2 = [5.09843,62.19222];
E1 = [5.54584,62.33473];
E2 = [5.12622,62.02920];

ID = pos(:,1);  % Vessel ID
long = pos(:,2);% Longitude
lat = pos(:,3); % Latitude
n_v = length(ia); % n vessels
n_m = length(pos); % n messages

% Passline A function
vA = [(A2(2)-A1(2)),(A2(1)-A1(1))];
aA = vA(1)/vA(2);
bA = -aA*(A1(1))+A1(2);

% Passline E function
vE = [(E2(2)-E1(2)),(E2(1)-E1(1))];
aE = vE(1)/vE(2);
bE = -aE*(E1(1))+E1(2);

k = zeros(n_v,2);

for i = 1:n_v-1
    for j = ia(i)+1:ia(i+1)-1
        if lat(j-1)<aA*long(j-1)+bA && lat(j)>=aA*long(j)+bA &&...
                ID(j-1)==ID(j)
            k(i,1) = k(i,1)+1;
        elseif lat(j-1)>aA*long(j-1)+bA && lat(j)<=aA*long(j)+bA
&&...
```

```
                ID(j-1)==ID(j)
            k(i,1) = k(i,1)+1;
        elseif lat(j-1)<aE*long(j-1)+bE && lat(j)>=aE*long(j)+bE
&&...
                ID(j-1)==ID(j)
            k(i,2) = k(i,2)+1;
        elseif lat(j-1)>aE*long(j-1)+bE && lat(j)<=aE*long(j)+bE
&&...
                ID(j-1)==ID(j)
            k(i,2) = k(i,2)+1;
        end
    end
end

%Separate for loop for last vessel on list
for h = ia(n_v)+1:n_m
    if lat(h-1)< aA*long(h-1)+bA&&lat(h)>=aA*long(h)+bA&&...
            ID(h-1)==ID(h)
        k(n_v,1) = k(n_v,1)+1;
    elseif lat(h-1)>aA*long(h-1)+bA&&lat(h)<=aA*long(h)+bA&&...
            ID(h-1)==ID(h)
        k(n_v,1) = k(n_v,1)+1;
    elseif lat(h-1)< aE*long(h-1)+bE&&lat(h)>=aE*long(h)+bE&&...
            ID(h-1)==ID(h)
        k(n_v,2) = k(n_v,2)+1;
    elseif lat(h-1)>aE*long(h-1)+bE&&lat(h)<=aE*long(h)+bE&&...
            ID(h-1)==ID(h)
        k(n_v,2) = k(n_v,2)+1;
    end
end

% A and E-passages respectively:
A = sum(k(:,1));
E = sum(k(:,2));

% Passages across both A and E
kae = zeros(length(k),1);
for i = 1:length(k)
    if k(i,1)>k(i,2)
       kae(i,1) = k(i,2);
    else
        kae(i,1) = k(i,1);
    end
end
```

```
AE = sum(kae(:,1));
z=kae(:,1)==0;
kae(z)=[];
ki=find(kae);
end
```

Appendix E: vesselstats.m

```
%Ship type and dimension statistics
function [Vstats,Stats,vType]=vesselstats(vType,pos,ki,ia,kae)
% VESSELSTATS
%
% Inputs:
%   vType:List of observed vessel types
%   pos: Vessel position matrix
%   ki: index of relevant vessels
%   ia: index of relevant pos matrix entries
%   kae: Passline matrix
%
% Outputs:
%   Vstats:Vessel parameters for each vessel
%   Stats:Vessel parameters
%   vType:Reordered list of vessel types


ncats = size(vType); %Vessel categories
ncats = ncats(1);
Vstats = zeros(length(ki),5);
Typecount=zeros(ncats,1);

for i =1:length(kae)
    if kae(i,1)>0
        Vstats(i,1)=pos(ia(ki(i)),6); %Type
        Typecount(Vstats(i,1))=Typecount(Vstats(i,1))+kae(i,1);
        Vstats(i,2)=pos(ia(ki(i)),4); %Breadth
        Vstats(i,3)=pos(ia(ki(i)),5); %Length
        Vstats(i,4)=pos(ia(ki(i)),7); %Draught
        Vstats(i,5)=pos(ia(ki(i)),8); %SOG
    end
end


Bmat=zeros(length(Vstats),ncats);
Lmat=Bmat;
Dmat=Bmat;
Smat=Bmat;

for i = 1:length(Vstats)
    for j = 1:ncats
       if Vstats(i,1)==j
          Bmat(i,j)=Vstats(i,2);
          Lmat(i,j)=Vstats(i,3);
```

```
            Dmat(i,j)=Vstats(i,4);
            Smat(i,j)=Vstats(i,5);
        end
    end
end

%Average dimensions vectors
for i = 1:ncats
    Bavg(i,1)=sum(Bmat(:,i))/nnz(Bmat(:,i));
    Lavg(i,1)=sum(Lmat(:,i))/nnz(Lmat(:,i));
    Davg(i,1)=sum(Dmat(:,i))/nnz(Dmat(:,i));
    if nnz(Smat(:,i))>0
        Savg(i,1)=sum(Smat(:,i))/nnz(Smat(:,i));
    else
        Savg(i,1)=0;
    end
end

%avg vessel type parameters matrix
Stats(:,1) = Typecount;
Stats(:,2) = Bavg;
Stats(:,3) = Lavg;
Stats(:,4) = Davg;
Stats(:,5) = Savg;

%Filter out zero entries - vessels that don't cross specified lines
nrows=Stats(:,1)==0;
Stats(nrows,:)=[];
vType(nrows,:)=[];
nrows=Stats(:,5)==0;
Stats(nrows,:)=[];
vType(nrows,:)=[];
%Concentrate misc vessel types into 1 category
zrows=Stats(:,1)<=5;
Statsk=Stats;
Statsk(zrows,:)=[];
vType(zrows,:)=[];
if nnz(zrows)>1
    Statsk(length(Statsk)+1,:)=[sum(Stats(zrows,1))
mean(Stats(zrows,2:5))];
elseif nnz(zrows)==1
    Statsk(length(Statsk)+1,:)=[sum(Stats(zrows,1))
(Stats(zrows,2:5))];
end
Stats=Statsk;
```

```
vType(length(Statsk),:)='Misc
';

end
```

Appendix F: latdist_unfilter.m

```
function [muS,muN,sigmaS,sigmaN] = latdist_unfilter(pos,ia)
% LATDIST_UNFILTER finds lateral distributions across defined
% cross-sections and creates distribution histograms per vessel
%
%
% Inputs:
%   pos: Vessel position matrix
%   ia:  vessel indexes in position matrix
%
% Outputs:
%   muS:    Southbound mean position mu
%   muN:    Northbound mean position mu
%   sigmaS: Southbound standard deviation sigma
%   sigmaN: Northbound standard deviation sigma
%


ID = pos(:,1);  % Vessel ID
long = pos(:,2);% Longitude
lat = pos(:,3); % Latitude
n_v = length(ia); % n vessels
n_m = length(pos); % n messages


%Cross-section coordinates
%Vanylvsfjorden
%H1=[5.3880,62.093];
%H2=[5.4327,62.1112];
%Gamla lysbøye-Furuneset
H1=[5.092,62.0963];
H2=[5.109,62.0963];
%Passline A- 10 km
%H1=[4.9512533,62.24927];
%H2=[5.09843,62.19222];
%Passline A - short
%H1= [5.0804108,62.1992205];
%H2= [5.0965404,62.1930597];
%-Trondheimsleia, Hitra-
%Snekkflua-Eiteraå
%H1=[8.7247,63.4524];
%H2=[8.7535,63.4246];

%Cross section line function
v = [(H2(2)-H1(2)),(H2(1)-H1(1))];
```

```
a = v(1)/v(2);
c = -a*(H1(1))+H1(2);

%Southbound passage-------------------------------------------------
------
k=0; %n Crossings

for i = 1:n_v-1
    for j = ia(i):ia(i+1)-1
        if
lat(j)>a*long(j)+c&&lat(j+1)<=a*long(j+1)+c&&ID(j)==ID(j+1)&&...
                long(j+1)>=H1(1)&&long(j+1)<=H2(1)
            k = k+1;
            V1(k,:) = [long(j),lat(j)];
            V2(k,:) = [long(j+1),lat(j+1)];
            vV(k,:) = [(V2(k,2)-V1(k,2)),(V2(k,1)-V1(k,1))];
            b(k) = vV(k,1)/vV(k,2);
            d(k) = -b(k)*(V1(k,1))+V1(k,2);
            S(k,:) = [(d(k)-c)/(a-b(k)),(a*d(k)-b(k)*c)/(a-b(k))];
        end
    end
end

% Separate loop for last vessel
for j = ia(n_v):length(pos)-1
    if
lat(j)>a*long(j)+c&&lat(j+1)<=a*long(j+1)+c&&ID(j)==ID(j+1)&&...
            long(j+1)>=H1(1)&&long(j+1)<=H2(1)
        k=k+1;
        V1(k,:) = [long(j),lat(j)];
        V2(k,:) = [long(j+1),lat(j+1)];
        vV(k,:) = [(V2(k,2)-V1(k,2)),(V2(k,1)-V1(k,1))];
        b(k) = vV(k,1)/vV(i,2);
        d(k) = -b(k)*(V1(k,1))+V1(k,2);
        S(k,:) = [(d(k)-c)/(a-b(k)),(a*d(k)-b(k)*c)/(a-b(k))];
    end
end

s1 = nonzeros(S(:,1));
s2 = nonzeros(S(:,2));
S1(:,1) = s1;
S1(:,2) = s2;

% Intersect distances from start point of histogram line. Start
points is
% lowest longitude.
```

```
VS = [S1(:,2)-H1(2),S1(:,1)-H1(1)];
VSabs = sqrt((VS(:,1)).^2+(VS(:,2).^2));
vabs = sqrt((v(1)).^2+(v(2)).^2);
SRatio = VSabs/vabs;

B = SRatio>1;
b = find(B);
SRatio(b) = [];

% Northbound passages-----------------------------------------------
------
k2 = 0;
for i = 1:n_v-1
    for j = ia(i):ia(i+1)-1
        if
lat(j)<a*long(j)+c&&lat(j+1)>=a*long(j+1)+c&&ID(j)==ID(j+1)&&...
                long(j+1)>=H1(1)&&long(j+1)<=H2(1)
            k2 = k2+1;
            V1(k2,:) = [long(j),lat(j)];
            V2(k2,:) = [long(j+1),lat(j+1)];
            vV(k2,:) = [(V2(k2,2)-V1(k2,2)),(V2(k2,1)-V1(k2,1))];
            b(k2) = vV(k2,1)/vV(k2,2);
            d(k2) = -b(k2)*(V1(k2,1))+V1(k2,2);
            N(k2,:) = [(d(k2)-c)/(a-b(k2)),(a*d(k2)-b(k2)*c)/(a-
b(k2))];
        end
    end
end

% Separate loop for last vessel
for j = ia(n_v):length(pos)-1
    if
lat(j)<a*long(j)+c&&lat(j+1)>=a*long(j+1)+c&&ID(j)==ID(j+1)&&...
                long(j+1)>=H1(1)&&long(j+1)<=H2(1)
        k2=k2+1;
        V1(k2,:) = [long(j-1),lat(j-1)];
        V2(k2,:) = [long(j),lat(j)];
        vV(k2,:) = [(V2(k2,2)-V1(k2,2)),(V2(k2,1)-V1(k2,1))];
        b(k2) = vV(k2,1)/vV(k2,2);
        d(k2) = -b(k2)*(V1(k2,1))+V1(k2,2);
        N(k2,:) = [(d(k2)-c)/(a-b(k2)),(a*d(k2)-b(k2)*c)/(a-b(k2))];
    end
end

n1 = nonzeros(N(:,1));
```

```
n2 = nonzeros(N(:,2));
N1(:,1) = n1;
N1(:,2) = n2;

% Intersect distances from start point of histogram line. Start point
is
% lowest longitude

VN = [N1(:,2)-H1(2),N1(:,1)-H1(1)];
VNabs = sqrt((VN(:,1)).^2+(VN(:,2).^2));
vabs = sqrt((v(1)).^2+(v(2)).^2);
NRatio = VNabs/vabs;

B = NRatio>1;
b = find(B);
NRatio(b) = [];

% Plot histograms of lateral distribution----------------------------
------
pdN = fitdist(NRatio,'normal');
pdS = fitdist(SRatio,'normal');
muN = pdN.mu;
muS = pdS.mu;
sigmaN = pdN.sigma;
sigmaS = pdS.sigma;

figure(1)
subplot(1,2,1), histfit(SRatio,40,'normal');
xlim([0 1])
ylabel('n vessels')
xlabel('section of fairway width')
title('Southbound distribution')
subplot(1,2,2),histfit(NRatio,40,'normal')
xlim([0 1])
ylabel('n vessels')
xlabel('section of fairway width')
title('Northbound distribution')
end
```

Appendix G: tsvread.m

```
% TSVREAD
%Reads lat, long, and MMSI data from .tsv format
% Outputs:
%   pos:position matrix
%   ia: vessel index in position matrix
%   vType:List of observed vessel types
FileID=dir('*.tsv');%All .tsv files in directory

N = {FileID.name};
N1 = char(N);
n = length(N);

Data = tdfread(N1(1,:));
Struct(1).MMSI = Data.MMSI;
Struct(1).Lat = Data.Decimal_Latitude;
Struct(1).Long = Data.Decimal_Longitude;
Struct(1).Type = Data.Ship_type;
Struct(1).Breadth = Data.Breadth;
Struct(1).Length = Data.Length;

%The following code is for catenating several tsv data files into one
%matrix. Note that the  procedure causes first message of every TSV
file
%to be lost. This should be negligible.

if n>=2
   for i = 2:n
        Data = tdfread(N1(i,:));
        %Find and save imported field names
        oldFields = fieldnames(Data);
        Breadthfield = char(oldFields(1,:));
        Lengthfield = char(oldFields(2,:));
        MMSIfield = char(oldFields(3,:));
        Typefield = char(oldFields(4,:));
        Latfield = char(oldFields(5,:));
        Longfield = char(oldFields(6,:));
        %Create new fields with correct names
        [Data.Breadth] = Data.(Breadthfield);
        [Data.Length] = Data.(Lengthfield);
        [Data.MMSI] = Data.(MMSIfield);
        [Data.Type] = Data.(Typefield);
        [Data.Lat] = Data.(Latfield);
```

```
        [Data.Long] = Data.(Longfield);
        %Remove old fields
        Data = rmfield(Data,Breadthfield);
        Data = rmfield(Data,Lengthfield);
        Data = rmfield(Data,MMSIfield);
        Data = rmfield(Data,Typefield);
        Data = rmfield(Data,Latfield);
        Data = rmfield(Data,Longfield);
        %Create struct with correct field names
        Struct(i).Breadth = Data.Breadth;
        Struct(i).Length = Data.Length;
        Struct(i).MMSI = Data.MMSI;
        Struct(i).Type = Data.Type;
        Struct(i).Lat = Data.Lat;
        Struct(i).Long = Data.Long;
    end
end

% Create vectors for MMSI, lat and long from struct arrays
Breadth=[];
Length=[];
MMSI=[];
Type=[];
lat=[];
long=[];


for i = 1:n
    Breadth = [Breadth;Struct(i).Breadth];
    Length = [Length;Struct(i).Length];
    MMSI = [MMSI;Struct(i).MMSI];
    Type = [Type;Struct(i).Type];
    lat = [lat;Struct(i).Lat];
    long = [long;Struct(i).Long];

end

%Find index vector ic to number MMSIs in order of appearance
[vID,ia,ic] = unique(MMSI,'rows','stable');

pos=zeros(length(ic),6);
pos(:,1) = ic; %vessel ID number in order of appearance
pos(:,2) = long;
pos(:,3) = lat;
pos(:,4) = Breadth;
pos(:,5) = Length;
```

```
[vType,via,vic] = unique(Type,'rows','stable');
pos(:,6) = vic;
pos = sortrows(pos,1);

%Find indexes vector of first appearance of unique MMSI in sorted pos
%matrix, ia
[vIDn,ia,ic2] = unique(pos(:,1),'rows','stable');
```

Appendix H: tsvread_parameters.m

```
% tsvread_parameters
%Reads data including lat, long, MMSI,
%breadth, length, draught and SOG from .tsv format
% Outputs:
%   pos:position matrix
%   ia: vessel index in position matrix
%   vType:List of observed vessel types

FileID=dir('*.tsv');%All .tsv files in directory
N = {FileID.name};
N1=char(N);
n=length(N);

Data = tdfread(N1(1,:));
fields = fieldnames(Data);
Struct(1).MMSI = Data.MMSI;
Struct(1).Lat = Data.Decimal_Latitude;
Struct(1).Long = Data.Decimal_Longitude;
Struct(1).Type = Data.Ship_type;
Struct(1).Breadth = Data.Breadth;
Struct(1).Length = Data.Length;
Struct(1).Draught = Data.Maximum_actual_draught;
Struct(1).SOG=Data.SOG;

%The following code is for catenating several tsv data files into one
%matrix. Note that the  procedure causes first message of every TSV
file
%to be lost. This should be negligible.

if n>=2
   for i = 2:n
        Data = tdfread(N1(i,:));
        %Find and save imported field names
        oldFields = fieldnames(Data);
        Breadthfield = char(oldFields(1,:));
        Lengthfield = char(oldFields(2,:));
        MMSIfield = char(oldFields(3,:));
        Draughtfield = char(oldFields(4,:));
        Typefield = char(oldFields(5,:));
        Latfield = char(oldFields(6,:));
        Longfield = char(oldFields(7,:));
        sogfield = char(oldFields(8,:));
        %Create new fields with correct names
        [Data.Breadth] = Data.(Breadthfield);
```

```
        [Data.Length] = Data.(Lengthfield);
        [Data.MMSI] = Data.(MMSIfield);
        [Data.Draught]=Data.(Draughtfield);
        [Data.Type] = Data.(Typefield);
        [Data.Lat] = Data.(Latfield);
        [Data.Long] = Data.(Longfield);
        [Data.SOG] = Data.(sogfield);
        %Remove old fields
        Data = rmfield(Data,Breadthfield);
        Data = rmfield(Data,Lengthfield);
        Data = rmfield(Data,MMSIfield);
        Data = rmfield(Data,Typefield);
        Data = rmfield(Data,Latfield);
        Data = rmfield(Data,Longfield);
        Data = rmfield(Data,Draughtfield);
        Data = rmfield(Data,sogfield);
        %Create struct with correct field names
        Struct(i).Breadth = Data.Breadth;
        Struct(i).Length = Data.Length;
        Struct(i).MMSI = Data.MMSI;
        Struct(i).Draught = Data.Draught;
        Struct(i).Type = Data.Type;
        Struct(i).Lat = Data.Lat;
        Struct(i).Long = Data.Long;
        Struct(i).SOG = Data.SOG;
    end
end


%Create vectors for MMSI, latitude and long from struct arrays
Breadth=[];
Length=[];
MMSI=[];
Draught=[];
Type=[];
lat=[];
long=[];
SOG=[];

for i = 1:n
    Breadth = [Breadth;Struct(i).Breadth];
    Length = [Length;Struct(i).Length];
    MMSI = [MMSI;Struct(i).MMSI];
    Draught = [Draught;Struct(i).Draught];
    Type = [Type;Struct(i).Type];
    lat = [lat;Struct(i).Lat];
```

```
    long = [long;Struct(i).Long];
    SOG = [SOG;Struct(i).SOG];

end

%Find index vector ic to number MMSIs in order of appearance
[vID,ia,ic] = unique(MMSI,'rows','stable');

pos=zeros(length(ic),6);
pos(:,1) = ic; %ID number in order of appearance
pos(:,2) = long;
pos(:,3) = lat;
pos(:,4) = Breadth;
pos(:,5) = Length;
[vType,via,vic] = unique(Type,'rows','stable');
pos(:,6) = vic;
pos(:,7) = Draught;
pos(:,8) = SOG;
pos = sortrows(pos,1);

%Find indexes vector of first appeareance of unique MMSI in sorted
pos
%matrix, ia
[vIDn,ia,ic2] = unique(pos(:,1),'rows','stable');
```